

12-2010

## Tracking the Flow of Information through the Hippocampal Formation in the Rat

Joshua P. Neunuebel

Follow this and additional works at: [https://digitalcommons.library.tmc.edu/utgsbs\\_dissertations](https://digitalcommons.library.tmc.edu/utgsbs_dissertations)



Part of the [Behavioral Neurobiology Commons](#), [Cognitive Neuroscience Commons](#), and the [Systems Neuroscience Commons](#)

---

### Recommended Citation

Neunuebel, Joshua P., "Tracking the Flow of Information through the Hippocampal Formation in the Rat" (2010). *The University of Texas MD Anderson Cancer Center UTHealth Graduate School of Biomedical Sciences Dissertations and Theses (Open Access)*. 95.  
[https://digitalcommons.library.tmc.edu/utgsbs\\_dissertations/95](https://digitalcommons.library.tmc.edu/utgsbs_dissertations/95)

This Dissertation (PhD) is brought to you for free and open access by the The University of Texas MD Anderson Cancer Center UTHealth Graduate School of Biomedical Sciences at DigitalCommons@TMC. It has been accepted for inclusion in The University of Texas MD Anderson Cancer Center UTHealth Graduate School of Biomedical Sciences Dissertations and Theses (Open Access) by an authorized administrator of DigitalCommons@TMC. For more information, please contact [digitalcommons@library.tmc.edu](mailto:digitalcommons@library.tmc.edu).

**Tracking the Flow of Information through  
the Hippocampal Formation in the Rat**

by

Joshua P Neunuebel

**APPROVED:**

---

James J. Knierim, Ph.D. Supervisory Professor

---

Valentin Dragoi, Ph.D.

---

William Dubinsky, Ph.D.

---

Harel Shouval, Ph.D.

---

Neal Waxham, Ph.D.

**APPROVED:**

---

Dean, The University of Texas

Health Science Center at Houston

Graduate School of Biomedical Sciences

**Tracking the Flow of Information through  
the Hippocampal Formation in the Rat**

**A  
DISSERTATION**

Presented to the Faculty of  
The University of Texas  
Health Science Center at Houston  
and  
The University of Texas  
M. D. Anderson Cancer Center  
Graduate School of Biomedical Sciences  
in Partial Fulfillment  
of the Requirements  
for the Degree of

DOCTOR OF PHILOSOPHY

by

Joshua Paul Neunuebel  
Houston, Texas

December, 2010

*This work is dedicated to my loving family and the memory of my cousin...*

“Keep your dreams alive. Understand to achieve anything requires faith and belief in yourself, vision, hard work, determination, and dedication. Remember all things are possible for those who believe.”

- Gail Devers



## **ACKNOWLEDGMENTS**

As I fly back to Virginia from the 2010 Society for Neuroscience conference, where I both presented a poster and completed writing my dissertation, I finally have a moment to reflect upon my experiences as a doctoral student. The past six and a half years have been anything but simple. This journey has been filled with many obstacles, which I've been able to overcome with support and guidance from my friends, family, and colleagues.

To name all my friends that have impacted my life and allowed me to drone on and on about the hippocampus would exceed the life of my laptop's battery. You know who you are and I thank you for being there during all the great times as well as the difficult times. To my lab mates, you fall into the above category. So, you've been thanked. To all the faculty members that have served on my committees, thank you for helping me overcome my nerves and sharing your wisdom. To my family, thank you for your patience, blessings, and love. Your wish is almost true. I will soon retire from my career as a professional student. A special thanks needs to be given to Jim and Geeta. I feel as if you have adopted me and cared for me as your own son. You were tolerant when I learned through the mistakes I made as a stubborn graduate student and you praised me for my achievements, both small and large. Thank you for the wonderful times we've had during the past years. You will forever be in my heart!

None of this would have been possible without my loving wife and son! Ramona and Christopher, thank you for your love and unwavering support.

## ABSTRACT

The hippocampus receives input from upper levels of the association cortex and is implicated in many mnemonic processes, but the exact mechanisms by which it codes and stores information is an unresolved topic. This work examines the flow of information through the hippocampal formation while attempting to determine the computations that each of the hippocampal subfields performs in learning and memory. The formation, storage, and recall of hippocampal-dependent memories theoretically utilize an autoassociative attractor network that functions by implementing two competitive, yet complementary, processes. Pattern separation, hypothesized to occur in the dentate gyrus (DG), refers to the ability to decrease the similarity among incoming information by producing output patterns that overlap less than the inputs. In contrast, pattern completion, hypothesized to occur in the CA3 region, refers to the ability to reproduce a previously stored output pattern from a partial or degraded input pattern.

Prior to addressing the functional role of the DG and CA3 subfields, the spatial firing properties of neurons in the dentate gyrus were examined. The principal cell of the dentate gyrus, the granule cell, has spatially selective place fields; however, the behavioral correlates of another excitatory cell, the mossy cell of the dentate polymorphic layer, are unknown. This report shows that putative mossy cells have spatially selective firing that consists of multiple fields similar to previously reported properties of granule cells. Other cells recorded from the DG had single place fields. Compared to cells with multiple fields, cells with single fields fired at a lower rate during sleep, were less likely to burst, and were more likely to be recorded simultaneously with a large population of neurons that were active during sleep and silent during behavior. These data suggest that single-field and multiple-field cells constitute at least two distinct cell classes in the DG. Based on these characteristics, we propose that putative mossy cells tend to fire in multiple, distinct locations in an environment, whereas putative granule cells tend to fire in single locations, similar to place fields of the CA1 and CA3 regions.

Experimental evidence supporting the theories of pattern separation and pattern completion comes from both behavioral and electrophysiological tests. These studies specifically focused on the function of each subregion and made implicit assumptions about how environmental manipulations changed the representations encoded by the hippocampal inputs. However, the cell populations that provided these inputs were in most cases not directly examined. We conducted a series of studies to investigate the neural activity in the entorhinal cortex, dentate gyrus, and CA3 in the same experimental conditions, which allowed a direct comparison between the input and output representations. The results show that the dentate gyrus representation changes between the familiar and cue altered environments more than its input representations, whereas the CA3 representation changes less than its input representations. These findings are consistent with longstanding computational models proposing that (1) CA3 is an associative memory system performing pattern completion in order to recall previous memories from partial inputs, and (2) the dentate gyrus performs pattern separation to help store different memories in ways that reduce interference when the memories are subsequently recalled.

# CONTENTS

ACKNOWLEDGMENTS .....	iv
ABSTRACT.....	v
CONTENTS .....	vii
LIST OF FIGURES .....	ix
LIST OF TABLES .....	xiii
1. GENERAL INTRODUCTION.....	1
1.1 Historical Perspective of Memory and the Hippocampus .....	1
1.2 Influential Theories of Hippocampal Function .....	5
1.2a Declarative Memory Theory.....	5
1.2b Relational Processing Theory .....	8
1.2c Configural Association Theory.....	11
1.2d Cognitive Map Theory.....	13
1.2e Episodic Memory Theory .....	19
1.3 Hippocampal Memory Mechanisms .....	24
1.3a Theoretical Concepts.....	24
1.3b Anatomical Evidence for Pattern Separation and Pattern Completion.....	25
1.3b Physiological Evidence for Pattern Separation and Pattern Completion.....	30
2. CHARACTERIZING THE SPATIAL FIRING PROPERTIES OF NEURONS FROM THE DENTATE GYRUS.....	34
2.1 Introduction .....	34
2.2 Results.....	36
2.3 Conclusion .....	65
2.4 Experimental Procedure .....	69
2.4a Subjects and Surgery .....	69

2.4b	Training and Recording .....	69
2.4c	Electrophysiological Recordings .....	70
2.4d	Unit Isolation .....	71
2.4e	Data Analysis .....	71
2.4f	Histological Procedures .....	73
3.	QUANTITATIVE EVIDENCE FOR PATTERN COMPLETION AND PATTERN SEPARATION PROCESSES IN CA3 AND DG .....	74
3.1	Introduction .....	74
3.2	Results .....	76
3.3	Conclusion .....	101
3.4	Experimental Procedure .....	103
3.4a	Subjects and Surgery .....	103
3.4b	Training and Recording .....	104
3.4c	Electrophysiological Recordings .....	106
3.4d	Unit Isolation .....	108
3.4e	Data Analysis .....	108
3.4f	Histological Procedures .....	110
4.	GENERAL DISCUSSION .....	112
4.1	Recap of Findings .....	112
4.2	Hippocampal Circuitry .....	112
4.3	Theories of Hippocampal Function .....	113
4.4	Potential Mechanism for Memory Recall in CA3 .....	114
4.5	Characterizing the Spatial Firing of Cells from the Dentate Gyrus .....	121
4.6	Mechanism for Memory Storage in the Dentate Gyrus .....	125
4.7	Dissociation of Input Streams .....	129
4.8	Overview Summary .....	130
	BIBLIOGRAPHY .....	133
	VITA .....	181

# LIST OF FIGURES

## **Chapter 1**

Figure 1.1. Simplified wiring diagram of the hippocampal formation. ....	26
--	----

## **Chapter 2**

Figure 2.1. Histology Localizing Tetrodes Targeting DG.....	38
Figure 2.2. Unit Isolation for Two Example Tetrodes Targeting DG.....	39
Figure 2.3. Full Tetrode Projections Used to Isolate Cells on Tetrode Localized to the Transition Between the Granule and Polymorphic Cell Layers.....	40
Figure 2.4. Full Tetrode Projections Used to Isolate Cells on Tetrode Localized to Polymorphic Cell Layer.. ....	41
Figure 2.5. Distribution of Mean Firing Rates During Sleep... ..	43
Figure 2.6. Negative Relationship Between Sleep and Behavior Clusters Recorded in DG.....	44
Figure 2.7. Spatial Firing Rate Maps of Cells from the Hilus.....	46
Figure 2.8. Unit Isolation for Cells Localized to Polymorphic Cell Layer.. ....	47
Figure 2.9. Different Spatial Firing Patterns for Cells Recorded in DG... ..	51
Figure 2.10. Ratemaps for All Active Cells Recorded In DG.. ....	52
Figure 2.11. Significantly More Sleep Clusters Detected on Tetrodes Recording Cells with Single Fields than Multiple Fields.. ....	53
Figure 2.12. Sparseness Ratios.. ....	54

Figure 2.13. Analyses with Velocity Filtered Data..	56
Figure 2.14. Subfield Size for DG Cells.....	57
Figure 2.15. Combined Field Size for DG Cells.....	57
Figure 2.16. In-Field Firing Rates for DG Cells..	58
Figure 2.17. Peak Firing Rate for DG Cells.....	58
Figure 2.18. Spatial Information for DG Cells.....	60
Figure 2.19. Burst Index for DG Cells Recorded During Behavior..	62
Figure 2.20. Burst Index of DG Cells Recorded During Sleep .....	62
Figure 2.21. Mean Firing Rates for DG Cells Recorded During Sleep..	64
Figure 2.22. Normalized Voltage Index for DG Cells Recorded During Sleep.	64
Figure 2.23. Example Waveforms Recorded During Sleep.....	66
Figure 2.24. Action Potential Duration for DG Cells Recorded During Sleep..	66
Figure 2.25. Action Potential Voltage for DG Cells Recorded During Sleep..	67

### **Chapter 3**

Figure 3.1. Histology Localizing Tetrodes to CA3, DG, LEC, and MEC. ....	77
Figure 3.2. Schematic illustrating one day of recording.....	77
Figure 3.3. Categorization of Putative Excitatory and Inhibitory Neurons. ....	79
Figure 3.4. Distribution of Spatial Information Scores on Circular Track.....	80
Figure 3.5. Example Ratemaps for Four Recorded Regions Showing Variety of Cellular Responses After Rotating the Local and Global Cues.....	81

Figure 3.6. Correlation Matrices Between Vectors of Positional Firing Rates for Population of Recorded Cells.....	82
Figure 3.7. Spatial Population Correlation Matrices for DG Layers.....	84
Figure 3.8. Spatial Population Correlation Matrices for Superficial Layers of the Entorhinal Cortex. ....	86
Figure 3.9. Schematic of Method for Calculating Mean Correlations for Diagonals of Correlation Matrix.....	86
Figure 3.10. Mean Correlations for Diagonals of Correlation Matrices.....	87
Figure 3.11. Cue Control Over Population. ....	88
Figure 3.12. Rotation Analysis Showing Responses of Individual Cells to Manipulations .....	91
Figure 3.13. Comparison between individual subjects. ....	93
Figure 3.14. Comparison between the first four days and subsequent days of recording. ....	94
Figure 3.15. Examples of Simultaneously Recorded Cells in Each Region. ....	95
Figure 3.16. Secondary Statistics on Responds of Ensembles in Each Region. ....	96
Figure 3.17. Secondary Statistics on Responds of Ensembles Concurrently Recorded from DG and CA3. ....	98
Figure 3.18. Ensemble Coherence.....	99
Figure 3.19. Categorical Response of Individual Cells to Mismatch Session..	102
Figure 3.20. Photograph of Double Rotation Recording Enviroment. ....	105



## **Chapter 4**

Figure 4.1. Potential Method for a Counterclockwise Rotation in a CA3 Cell.. 119

Figure 4.2. Model of Hippocampal Local Circuitry ..... 126

Figure 4.3. Summary of Mechanisms for Storing and Recalling Memories..... 132

## LIST OF TABLES

### **Chapter 2**

Table 2.1. Statistics for Additional Analyses with Data Not Shown. ....	61
---	----

“Memory is the treasure house of the mind wherein the monuments thereof are kept and preserved.” ”

- Thomas Fuller

# **1. GENERAL INTRODUCTION**

## **1.1 Historical Perspective of Memory and the Hippocampus**

The conception of many theories pertaining to memory and the development of protocols used to test memory flourished during the late nineteenth and early twentieth centuries. This work originated from notable scientists such as James Williams, Richard Semon, Hermann Ebbinghaus, and Frederic Bartlett and laid the foundation for current research. In (William, 1890), James Williams described memory as an association between a set of items (i.e., numbers, months, years, events) that could be retrieved or recalled when a triggering cue was presented. Recall was thought to be dependent on the “brain-paths” or neural circuits that connected the experience with a series of items. Williams separated memory into two types: primary and secondary memory. Primary memory, which is equivalent to short-term memory, was described as a transient stream of consciousness that held recently experienced stimuli. In contrast, secondary memory, which resembled long-term memory, was a longer-lasting phenomenon that was more difficult to retrieve than a primary memory. Following in the footsteps of Williams, Richard Semon proposed a separate, yet overlapping theory of memory that was based on two postulates (described in (Schacter, 2001)). Semon claimed that a stimulus caused a change in the “irritable substance” or “mind” that allowed the memory to persist for an extended period of time. This process, referred to as the law of engraphy, places an emphasis on individual events, each of which can produce a single memory trace that is stored separately from other memory traces. The second postulate, referred to as the law of ecphony, is based on the premise that recalling the entire memory trace can be achieved with only a partial set of cues or stimuli that were originally present during the initial storage. This process bares a strong resemblance to pattern completion, which is a current theory explaining a potential mechanism for recollecting a memory. Not only do the contemporary

memory theories gain insight from past theories, but many of the current methods used to probe memory show a marked resemblance to some of the original methods used to test mnemonic function.

The first rigorous experiments testing the mnemonic process in a laboratory setting were conducted by Hermann Ebbinghaus in the 1880's. These studies consisted of constructing various permutations of nonsense syllables and then Ebbinghaus attempted to memorize the list (Ebbinghaus, 1885). He measured the length of time required to learn the list and forget components. These observations were then used to plot the first reported learning and forgetting curves, which are still commonly used to show the rate of acquisition and extinction (Daum et al., 1989; Aigner et al., 1991; Sandi et al., 1997; Sikstrom, 2002; Nakazawa et al., 2003). Ebbinghaus used the learning and forgetting curves to illustrate two fundamental properties of memory. First, Ebbinghaus used the learning curve to show that the greatest increase in learning occurred during the initial stages and gradually decreased after each repetition. This process, referred to as a primacy effect, is believed to occur because the memories of the words learned earlier in the sequence are interfering with the words that occur later in the sequence. Furthermore, Ebbinghaus used the forgetting curve to show that after learning a list, one forgets the words learned prior to the most recently learned words more frequently than the last words in a sequence. This would explain the "u" shaped learning curve with the greatest probability of remembering the initial and later words in the sequence. Ebbinghaus's experimental method, which required subjects to memorize lists of nonsense syllables, was commonly used to investigate the properties of memory for nearly five decades after its conception until Frederic Bartlett broached the study of memory using a different strategy. The first approach was based on memorizing a more natural or familiar situation. After having subjects examine and memorize a picture or story, he asked them to describe the item from memory several times over several weeks to a scribe, who dictated the subject's response. A second approach involved subjects memorizing the same natural scenes, but instead of describing their memory of the scene to one scribe, it was

relayed to a series of subjects. For both approaches, Bartlett was interested in the changes that were detected over time between one's description of the memory and the original content. He referred to the first approach as repeated reproduction and the second approach as serial reproduction. Bartlett observed that recall tended to be biased by the feelings, desires, and cultural influences of the participants causing the stories to be recreated in ways that reflected their prior experiences (Bartlett, 1932). Consequently, he concluded that memories are reconstructed based on one's previous experiences. These innovative studies on human memory set a standard for probing mnemonic function that still influences current research.

The progress made on the methodologies to test memory and the numerous speculations on the mechanisms for encoding memories prompted considerable advances towards understanding the brain. Contrary to previous beliefs, accumulating evidence suggested that different parts of the brain perform different functions. John Hughlings Jackson noticed that memory loss was a malignant side effect of brain damage (Jackson, 1865). He also suggested that motor function could be localized to areas of the cortex. This theory was soon thereafter supported by work from David Ferrier (1876), who showed that stimulating the cortices of both dogs and monkeys could elicit a specific motor response. Furthermore, lesions to the same cortical areas caused a loss of function that could not be restored by stimulation (Ferrier, 1876). Similar to Jackson, Theodule-Armand Ribot, a French psychologist, reported that progressive brain disease caused impairments in memory and proposed that memory storage resulted from the altered activity of cortical neurons (Ribot, 1881). Additional support for the localization of function was provided by Carl Wernicke (Wernicke, 1881), which was translated by (Thomson et al., 2008), and Sergei Korsakov (1889), which was described in (Andersen et al., 2006); in particular, they showed that parts of the hippocampal system were associated with memory function. Both doctors observed patients that suffered from paralysis of eye movements, ataxia, and memory deficits. Upon necropsy, hemorrhaging was detected in the gray matter near the thalamus and

hypothalamus. Wernicke-Korsakoff syndrome, as the disease was later known, was caused from a deficiency of thiamine (<http://emedicine.medscape.com/article/288379-overview>) and shown by Johann Bernhard Aloys von Gudden (Von Gudden JBA, 1896) localized to damage to the mamillary bodies and mediodorsal nucleus of the thalamus. These regions were later reported to send efferent projections to the hippocampus (Witter and Amaral, 2004). Even stronger evidence connecting the hippocampus to memory came from the clinical studies of Bekhterev (1900), described in (Dickerson and Eichenbaum, 2010), who found brain damage localized to the hippocampus of amnesic patients suffering from severe memory deficits.

A momentous discovery was reported in (1957) when Scoville and Milner described the deleterious side effect of bilaterally removing the medial temporal lobe, which resulted in the patients losing their memory. The extent of the memory impairments showed a significant correlation with the amount of hippocampal damage caused by the operations. In the ten observed cases, it was noted that the memory capacity was not compromised in two of the patients; however, the medial temporal lobe was unscathed in their surgical procedure. Interestingly, the hypothalamic region of one of the patients was accidentally damaged during surgery and for a short period of time the clinical evaluation resembled the symptoms associated with Wernicke-Korsakoff syndrome. Three of the most severe memory deficits seen in patients H.M., D.C. and M.B. prevented the formation of memories following the surgery (anterograde amnesia) and to a lesser degree impaired the patient's ability to recall memories prior to the surgery (retrograde amnesia). Scoville and Milner believed, but never rigorously tested, that the retrograde amnesia only extended a few years prior to the operation because the patients could recall earlier childhood memories. Furthermore, the technical skills of the patients did not deteriorate. When describing the difficulties these patients encountered, it was common to see the patients struggling to remember dates, conversations, people, locations of where objects were placed, paths from their room to the bathroom, events of the day, and series of recently eaten items. Despite suffering from memory problems, the

intelligence quotient, perception, abstract thinking, reasoning, and motivation of the patients were not obviously impaired. This landmark discovery showed that the hippocampus was critical for memory, which pushed the hippocampus into the forefront of memory research and intensified the search to determine the exact nature of hippocampal mnemonic function.

## **1.2 Influential Theories of Hippocampal Function**

The number of theories attempting to explain hippocampal function exceeded twenty in the 1980's (Schmajuk and Segura, 1981) and the count continued to grow over the next three decades. These theories to some extent addressed how the hippocampus could inhibit responses (Sainsbury, 1998), filter the information being stored (Hsu, 2007), or store varying types of memory traces (Marr, 1971;Hirsh, 1974;O'Reilly and McClelland, 1994;McClelland et al., 1995;Bontempi et al., 1999;Nadel et al., 2000;Morris et al., 2003;Olson et al., 2006). The most influential hippocampal theories claimed that the hippocampus was instrumental for forming declarative memories (Cohen and Squire, 1980), processing the relationships between stimuli (Cohen and Eichenbaum, 1993), constructing stimulus configurations (Rudy and Sutherland, 1989), creating cognitive maps (O'Keefe and Nadel, 1978), and forming episodic memories (Tulving, 1983). These theories proposed significantly different functions, yet had a number of overlapping attributes.

### **1.2a Declarative Memory Theory**

The medial temporal lobe, which is the region of the brain where the hippocampus is located, has been suggested to play a central role in forming declarative memories (i.e., memories of facts and events) as opposed to nondeclarative memories, which are associated with skills, habits, and priming (Squire, 2004). Declarative memories require conscious recollection, whereas nondeclarative memories are performance-based operations. Cohen and Squire (1980) provided evidence supporting this claim by showing that amnesic patients and control subjects were capable of learning a novel task requiring the subjects



to use a mirror in order to read reversely printed words. The amnesic patients retained the skill, but had no recollection of the training, whereas the control group could remember both the new skill and the training. Similarly, Knowlton and Squire (1993) showed that both amnesic patients and control subjects could group new sets of patterns with recently learned patterns; however, the amnesic patients could not recall the training events. Considerable emphasis was placed on how amnesic patients with pathology to the medial temporal lobe showed deficits in recalling events and facts despite the patients showing some forms of learning. Other research has shown that amnesic patients could enhance their performance in a motor skills task (Milner, 1962), recall words or images that were primed (Gold et al., 2006;Haist et al., 1992;Musen and Squire, 1992;Cave and Squire, 1992;Conroy et al., 2005), and learn new habits, which is commonly referred to as probabilistic category learning (Knowlton et al., 1994;Hopkins et al., 2004).

Great strides were made following the development of protocols used to test amnesia in nonhuman primates. Results showed that monkeys with hippocampal lesions performed poorly in tasks that were believed to test declarative, but not nondeclarative memories when using pattern (Squire and Zola-Morgan, 1983), spatial (Gaffan, 1994), and object (Barefoot et al., 2003) discrimination tasks. Squire and Zola-Morgan (Squire and Zola-Morgan, 1983) used a pattern discrimination task to show that hippocampal lesioned monkeys could differentiate between two gradually learned patterns. These patterns were unequally rewarded such that only one was associated with reinforcement. Similar to the pattern discrimination task, the spatial and object discrimination task require monkeys to make a choice between two options, but either the spatial location or object identity of two cues influences the decision. Further distinctions were made in hippocampal function when comparing lesioned and control monkeys in delayed response (Zola-Morgan and Squire, 1985) and delayed nonmatching-to-sample (Alvarez et al., 1995). These authors showed that monkeys with a damaged hippocampus performed worse than control monkeys, and they suggested that the hippocampus is involved in declarative

memory. These tasks have been suggested to resemble the task used to test declarative memory in amnesic patients (Andersen et al., 2006).

The evidence accumulated over the years suggests that the hippocampus is critical for declarative memory. However, there are points of contention based on how the data were interpreted or the methodology used to obtain the results, thus leading to the debate that the delayed nonmatching-to-sample and other similar tasks were not hippocampal dependent, but instead were dependent on the perirhinal cortex. One of the points of contention leading to the perirhinal vs. hippocampal debate pertained to the relationship between hippocampal damage and the severity of the memory impairment. Zola-Morgan et al., (1994) claimed that subjects with greater damage to the medial temporal lobe showed more severe memory impairments when testing with a delayed nonmatching-to-sample task, whereas Murray and Mishkin (1998) and Baxter and Murray (2001) provided conflicting evidence that showed an inverse relationship (i.e., monkeys with extensive damage to the medial temporal lobe showed a reduced memory impairment using the nonmatching-to-sample task than monkeys with less damage). Murray and Mishkin (1998) showed that the monkeys with the most severe memory deficits had damage that was localized to perirhinal cortex. Squire and colleagues (2001) argued that disparities in surgical or training procedures might account for the difference seen between the two studies. A second criticism was based on the interpretation of the Zola-Morgan et al. (1994) results, where the authors reported that hippocampal lesioned monkeys showed a deficit in delayed nonmatching-to-sample tasks when the delays exceeded ten minutes. Interestingly, there was a procedural difference between trials with shorter delays and longer delays. In the trials with longer delays, animals were returned to their cages during the delay period. Nadel (1995) suggested this caveat introduced a spatial contextual change that may have affected the hippocampal damaged monkeys and caused the deficit seen during the longer retention intervals, whereas the control monkeys might have been able to deal with the spatial contextual change and still solved the behavioral task.

Most of the data from experiments using animals as a model system implicating the hippocampus in declarative memory was collected in monkeys. In the middle of 1980's, however, techniques were developed to test rats on a modified delayed nonmatching-to-sample task (1986). Over the next fifteen years, many groups made slight variations to the original rodent delayed nonmatching-to-sample task in order to test the effects of hippocampal damage in rats; rarely were behavioral deficits observed as the rodents performed these tasks (Aggleton et al., 1986; Rothblat and Kromer, 1991; Jackson-Smith et al., 1993; Duva et al., 1997). However, in one example, Clark et al. (2001) observed rodent memory deficits during a delayed nonmatching-to-sample task for retention periods lasting a minute or longer. The differences reported in Clark et al. (2001) mirrored the previously mentioned results from Zola-Morgan et al. (1994) and suggests that context may play an important role in hippocampal function. The declarative memory theory does not exclude the possible role of context in recalling events and facts, but it does not specifically account for exploration of novelty, spatial memory, or the relationship between items.

### **1.2b Relational Processing Theory**

The declarative memory theory emphasizes that the hippocampus plays a significant role in storing events and facts, but refrains from explaining how learning and memory might be applied to animals. Much of the animal literature about hippocampal-dependent memory deficits in rodents was not incorporated into the declarative memory theory, since rats cannot directly tell the experimenter about their experiences. Thus, Eichenbaum and Cohen proposed the theory of relational processing to bridge the gap between human and rodent studies (Cohen and Eichenbaum, 1993; Eichenbaum, 2001; Eichenbaum, 2004). This theory suggests that the hippocampal network creates a framework for storing and linking associations between sequences of events with common features and the network properties allow the stored information to be retrieved easily in order to solve impending problems. Similar to one of the postulates of the declarative memory theory, the relational processing theory suggests that the

hippocampus is only temporarily involved in storing memory traces, whereas the cortex is the site for permanent storage (Ross and Eichenbaum, 2006;Squire et al., 2004). However, the precise cortical region where memories are permanently stored is still debated, but it is believed that the consolidation of memories occurs in a cortical region conveying the sensory modalities associated with the memory (Squire, 1992;Herry et al., 2010;Diekelmann and Born, 2010).

Evidence from humans supporting the relational processing theory was provided using a variety of imaging techniques. Binder et al. (2005) examined human hippocampal activation using functional magnetic resonance imaging (fMRI) as volunteers were shown scrambled and unscrambled scenes. They reported that the anterior hippocampal activity (measured by the blood oxygen level dependence or the BOLD signal) increased when showing the recognizable images and suggested the activity was a result of processing associations. Furthermore, Hannula and Ranganath (2008) used fMRI to measure human hippocampal activity during a behavioral task that examined the relationships between objects in a picture. The procedure required the subjects to compare two images. After viewing the first image and waiting eleven seconds during a retention phase, subjects saw a second image. The second image was the original image rotated by 90°, and then the image components were either slightly altered or they remained the same as the first image. Hannula and Ranganath (2008) showed that the BOLD signal in the posterior hippocampus was greater when the relationships were maintained. Another study by Giovanello et al. (2009) showed increases in activity for both the anterior and posterior hippocampus during a word relationship task; however, the activity in the posterior hippocampus was uncorrelated with how accurately the subjects recalled the word pairs. A positron emission tomography (PET) experiment was designed to test the role of the hippocampus in encoding single or associated items (Henke et al., 1997). Briefly, a picture was presented to the subjects; one side of the picture showed a house and the other half showed a person. The subjects needed to decide whether the person in the picture was visiting or living

in the house. A second part of the experiment required subjects to distinguish two separate features of the split photo (i.e., the gender of the person and from which perspective the house was being viewed). Henke et al. (1997) reported that the hippocampus was active only while learning the associations and claimed this evidence supported the relational processing theory. In (2005), Kumaran and Maguire published a conflicting report arguing that spatial, but not social relationships activated the hippocampus. This evidence suggests that relationships are important for activating the hippocampus, but emphasizes the importance of space.

Animal model systems have been useful for promoting the role of the hippocampus in processing relationships. Work from Dusek and Eichenbaum (1997) used a transitive inference task to examine the role of the hippocampus in learning the relationship between sequences of items. Initially, rats learned to identify one odor associated with a reward in four sets of paired odors. In the sets, each odor was assigned a salience reward value (i.e., set 1:  $A > B$ ; set 2:  $B > C$ ; set 3:  $C > D$ ; and set 4:  $D > E$ ). On probe tests, rats were forced to choose between two novel sets of pairings (A or E and B or D) in order to evaluate whether their decisions were based on the previous rewarding history or whether the rats learned the sequence. Dusek and Eichenbaum (1997) found that rats with their hippocampi disconnected from either cortical or subcortical input were impaired in the transitive inference task compared to controls. This idea was further developed in the Eichenbaum lab, when a rodent model of the serial reaction time task, which is commonly used to test the ability of humans to learn higher-order sequences, was developed (Ergorul and Eichenbaum, 2006). The task required rats to use cues that predicted the reward by multiple steps; in essence, the preceding cues could be used to predict the future reward. The authors showed that rats with functional hippocampi learned to use the preceding cues in order to pick the correct reward locations (based on second-order sequences) compared to hippocampal lesioned rats. In addition, Manns et al. (2007) showed that the temporal firing pattern of a recorded population of hippocampal cells gradually changed during a sequence of odors and they

suggested the change in activity served as a context for remembering the order of events. The role of the hippocampus in processing relationships or associations is not specific just to rodents, but seen across multiple species such as monkey (Saunders and Weiskrantz, 1989;Wirth et al., 2003;Buckmaster et al., 2004;Wirth et al., 2009) and rabbits (Disterhoft et al., 1986;Geinisman et al., 2001).

### **1.2c Configural Association Theory**

Another compelling hippocampal theory is the configural association theory, which was originally proposed by Rudy and Sutherland (1989). This theory claimed that animals use the hippocampus to solve associative problems based on the configuration of stimuli in the environment in conjunction with a conditioned stimulus. This theory was directly tested with a battery of behavioral tasks (negative patterning, feature-neutral discriminations, transverse patterning, and biconditional discriminations) and indirectly with context-specific conditioning and contextual fear conditioning. These tests provided a mixture of evidence that in some circumstances supported the theory and other times forced the original theory to be modified.

In the negative patterning discrimination task, the reward depends on the configuration of two stimuli. For example, stimulus A or B is rewarded when either stimulus is presented in isolation; however, when both stimuli (A and B) are presented together the reward is omitted (Woodberry, 1943;Rescorla, 1972;Whitlow and Wagner, 1972). Several studies showed that rats with hippocampal damage caused from injecting either a cocktail of kainic acid and colchicine or just ibotenic acid performed the negative patterning discrimination task significantly worse than controls (Rudy and Sutherland, 1989;Sutherland et al., 1989;Sutherland and McDonald, 1990;Alvarado and Rudy, 1995a). However, Davidson et al., (1993) could not replicate the results that hippocampal damage impaired configural learning in rats and the authors suggested that the rats were responding to contextual cues such as the number or intensity of the stimuli

instead of the configurations. Further evidence supporting the theory came from the transverse patterning paradigm. This task incorporates three stimuli, two of which are simultaneously presented to the subject, that are rewarded differentially depending on the pairings (i.e., if the choices consist of 1 and 2, 2 and 3, or 3 and 1, then choice 1 over 2, choice 2 over 3, and choice 3 over 1 elicit a reward). Alvarado and Rudy (1995b) reported damage to the hippocampal formation caused a significant defect when rats were required to learn all three conditions. It was reported that rats with hippocampal damage were impaired in a Pavlovian contextual discrimination task (i.e., a stimulus starts evoking a response after repeated pairings with another stimulus that does evoke a response), whereas controls did not show a deficit in representing stimulus configurations that were necessary for the task (Good and Honey, 1991). Numerous studies have reported rodents with a hippocampal lesion do not exhibit contextual fear conditioning, whereas healthy animals freeze when placed in contexts where shocks were previously delivered (Kim and Fanselow, 1992; Phillips and LeDoux, 1992; Kim et al., 1993; Maren and Fanselow, 1997; Maren et al., 1997; Anagnostaras et al., 1999). It was suggested by Fanselow (1990) that the configuration of the context is associated with the unpleasant unconditioned stimulus (US). In the hippocampal damaged animals, the configuration might not have been stored in the hippocampus; therefore, the configuration might never have been associated with the US (Rudy and Sutherland, 1995).

Two tasks, the feature-neutral and biconditional discrimination tasks, provided evidence that contradicted the original theory. First, the feature-neutral task, similar to transverse patterning, involves three stimuli with different reward conditions. Rats are rewarded when stimuli 1 and 2 are paired or stimulus 3 is in isolation, whereas a pairing of stimuli 1 and 3 or stimulus 2 in isolation produces no reward. The other task, biconditional discrimination, employs a combination of four stimuli that are rewarded as follows, with a plus representing a reward and a minus indicating the absence of reward: 1&2 (+), 3&4 (+), 1&3 (-), and 2&4 (-). In both paradigms, animals with damage to the hippocampus gradually learned

to perform the task (Saunders and Weiskrantz, 1989;Gallagher and Holland, 1992;Alvarado and Rudy, 1995b). Since the rats learned the associations between the different configurations, Rudy and Sutherland modified their initial theory. Instead of the hippocampus creating and storing the conjunctive representations, Rudy and Sutherland (1995) suggested that the cortex performs these operations and the hippocampus increases the salience of the new configurations by strengthening the association between the configurations and the unconditioned stimulus. Rudy and Sutherland (1995) proposed that increasing the salience of these representations decreased the similarity between the simultaneous occurrence of cues and the individual cues. Furthermore, they thought that increasing the salience of the representations associated with the reward would expedite the rate of learning.

### **1.2e Cognitive Map Theory**

The hippocampus has been suggested to be the core of a neural memory system that provides a spatial frame work for binding events and items (O'Keefe and Nadel, 1978). The events, items, and spatial features that create these memories are believed to be stored as cognitive maps and as animals explore novel environments or places, new information might be incorporated into the spatial representations (Nadel, 1995). Many authors have suggested these cognitive maps (stored in the hippocampus) might provide a substrate for the striatum and/or other regions of the brain to use in order to help guide navigational behavior (Jones and Wilson, 2005;Johnson and Redish, 2007;van der Meer et al., 2010). Much of the pioneering work on the cognitive map theory was conducted by Edward Tolman, who provided the behavioral ground work for many of the labs currently studying the hippocampus. Tolman (1948) argued that rats learned to solve complex mazes using a set of cognitive maps, with each map selectively incorporating salient stimuli, rather than the theory proposed by Hull (1934b;1934a) suggesting that rats used a stimulus-response tactic requiring a series of behavioral responses to reach a goal. To demonstrate this idea, Tolman et al. (1946a) initially trained rats to navigate a maze consisting



of a sequence of 90 degree turns in order to reach a goal box. After the rats learned to run to the goal without hesitation, the apparatus was modified such that the sequence of 90 degree turns was removed and replaced with a series of radial arms paths (18 total paths), but the starting path, circular table, and first linear segment remained. On the new apparatus, the initial linear segment exiting the table was open and allowed the rats to enter; however the end was blocked. Furthermore, six of the new radial arms were shorter than the other new additions. Tolman et al. (1946a) reported that when the rats finally circumnavigated through the new apparatus, the rats typically choose the path that ended near the front of the original reward location, suggesting that rats used a cognitive map to solve the task. In a companion study, evidence showed that rats learned to solve a t-maze using a strategy that emphasized place learning faster than one depending on stimulus responses (Tolman et al., 1946b). The authors concluded from these reports that the rats might be solving the new tasks with a cognitive map acquired from the previous training.

Over the last forty years, three landmark discoveries were made that provided strong evidence indicating that the hippocampus was involved in spatial memory and forming a cognitive map. Initially, O'Keefe and Dostrovsky (1971) recorded single units in the dorsal hippocampus of freely moving rats and reported that approximately 11% the units responded maximally at particular locations in the environment. The number of cells in the hippocampus that fired in spatial locations, or place fields, was later to be shown as high as 52% (O'Keefe, 1976). These hippocampal units that had place fields were classified as place cells and O'Keefe and Dostrovsky proposed that the hippocampus might function as a spatial map. Another crucial component for a map based navigation system is the ability to determine direction. In (1990a), Taube and colleagues recorded cells in the postsubiculum, which is an important input into the hippocampus, and reported that 26% of the cells had a peak firing rate in a particular direction regardless of the rat's behavior, location, or trunk position. This input to the hippocampus is thought to set the orientation of the spatial representation in relation to the external environment (McNaughton et al.,

1996;Muller et al., 1996;O'Keefe and Burgess, 1996;Yoganarasimha and Knierim, 2005;Knierim et al., 1995). Nearly fifteen years later, Hafting et al. {Hafting, 2005 26 /id /d} reported that the inputs into the hippocampus from the medial entorhinal cortex provide a spatial signal by showing that individual cells fire in a repeating grid-like pattern, with each point of the grid representing a vertex of an equilateral triangle, which covers the entire environment. The combination of these three discoveries has provided strong support for the theory that the hippocampus functions as a cognitive map.

The majority of work supporting the cognitive map theory comes from rodent studies, with numerous reports pertaining to hippocampal place cell firing. The firing properties of place cells are observed during a rat's initial exposure to an environment {Hill, 1978 199 /id} and then stabilize after continued exposure to an environment (Frank et al., 2004;Wilson and McNaughton, 1993). Place fields tend to be located along the periphery of an open enclosure; however, the entire environment is represented when a large enough hippocampal ensemble is recorded (Hetherington and Shapiro, 1997;Muller et al., 1987;Wilson and McNaughton, 1993). Unlike the visual (Hughes, 1971), motor (Asanuma and Rosen, 1972), auditory (Middlebrooks et al., 1980), and gustatory (Finger, 1976) systems, the hippocampus lacks a topographic relationship between function (i.e. spatial firing) and anatomical location (Redish et al., 2001). Furthermore, location-specific firing of a place cell can be stable for days (Muller et al., 1987) and even months (Thompson and Best, 1990) when the environment remains unaltered. In contrast, a number of paradigms such as the morph box (flexible walls permit the environment to gradually change shapes), double rotation (local and distal cue sets are rotated in equal, but opposite directions), and rate remapping protocols (change the colors, but maintain the location of the environment) have been used to show that the hippocampal cells can alter their firing depending on the context (Wills et al., 2005;Leutgeb et al., 2005b;Leutgeb et al., 2005a;Knierim, 2002). Furthermore, both visual landmarks and local surface cues have been shown to exert control over place cells (Knierim, 2002;Knierim et al., 1998;Knierim et al., 1996b;Knierim et al., 1995;Muller and

Kubie, 1987;Shapiro et al., 1997;O'Keefe and Conway, 1978;Knierim and Van, 1992) as well as the shape of the environment (Muller and Kubie, 1987;O'Keefe and Burgess, 1996;Thompson and Best, 1990). These studies place an emphasis on the electrophysiological properties of hippocampal principal cells, showing that they play an important role representing space, and are nicely complemented with many behavioral experiments showing the importance that the hippocampus has in spatial learning.

Behavioral studies linking the rodent hippocampus to spatial learning and the arsenal of experimental paradigms used to test the theory such as the Y, circular, radial, arena, water, and T mazes have been extensively reviewed (see reviews from (O'Keefe and Nadel, 1978;Paul et al., 2009). One study providing support for the cognitive map theory was performed by Save et al. (1992). Save and colleagues allowed rats to forage in an open cylindrical arena with a glass floor for a five-minute interval. During the second and third sessions, a second rat was placed in a chamber below the transparent floor of the environment while the subject foraged for five minutes. Immediately before starting the last session, the stimulus rat was removed. Save and colleagues observed that the percent of time reinvestigating the area with the missing stimulus was significantly less for rats with hippocampal damage compared to controls. Consequently, the authors concluded that the hippocampus was important for spatial memory. This could also be interpreted as a deficit in detecting contextual changes. Work from Jarrard (1978) showed that rats receiving hippocampal lesions prior to the initial exposure to an eight-arm radial maze were impaired in the acquisition and performance of place learning and reference memory. Furthermore, Morris et al. (1982) found that hippocampal lesioned rats, caused by aspiration, solved the Morris water maze slower than healthy rats. Therefore, Morris and associates suggested that spatial navigation was dependent on the hippocampus.

One of the strongest arguments that the hippocampus is involved in creating cognitive maps comes from the discovery that rodent hippocampal pyramidal cells represent space. It is more difficult to expand the theory across

species, since the evidence of place cells in primates is both scarce and questionable. To date, the technical challenges of recording from freely-moving non-human primates and humans have limited the amount of data. However, some evidence from both species does support the theory. For example, Fried and coworkers (2003) implanted depth electrodes targeting the hippocampus of patients suffering from epilepsy and showed that 11% of the hippocampal units had place selectivity as the subjects navigated around a virtual town. Individual cells fired at different locations in the virtual town as subjects viewed particular locations; however, the patients did not physically pass through a place field to activate the cells, which is a property affiliated with rodent place cells (Markus et al., 1995; Gothard et al., 1996b; Terrazas et al., 2005). Nonetheless, numerous reports show that the human hippocampus is active during spatial navigation tasks and thus connects the human hippocampus to other physiological data in rodents (Maguire et al., 1998; Thomas et al., 2001; Parslow et al., 2004). In (2000), Maguire and colleagues published a report on taxi cab drivers, which supported the theory that the hippocampus plays a central role in spatial memory. They showed that taxi drivers had larger posterior hippocampi than controls. Furthermore, there was a positive correlation seen in the volume of the posterior hippocampi and duration of time that drivers worked (i.e., the longer on the job force the larger the posterior hippocampus), suggesting that the posterior hippocampus is involved in storing spatial representations, especially for taxi cab drivers that depend on navigating through cities to make a living.

Similar to humans, data from non-human primates supporting the theory is considerably less than that reported for rodents. In most monkey studies, the head is restrained, which prevents the animal from moving freely and complicates the process of recording place cells. Recordings from monkey hippocampi have revealed that cells fire in response to the location that the monkey is looking, which is also referred to as one's spatial view (Rolls et al., 1989; Rolls et al., 1997; Rolls et al., 1998; Rolls, 1999; Robertson et al., 1998; Georges-Francois et al., 1999; Tamura et al., 1992). In a few studies from the Ono lab, head fixation that typically hinders place cell recordings in monkeys

was circumvented by allowing the monkeys to maneuver a cart around the environment (Ono et al., 1993a; Ono et al., 1993b; Matsumura et al., 1999; Eifuku et al., 1995). These reports all described hippocampal cells with place-related activity as monkeys drove the cart through each cell's place field. One report by Ludvig et al. (2004) showed that hippocampal units recorded from freely moving monkeys had place activity similar to place cells recorded in rats; thus, this evidence provided the strongest support for cognitive maps seen across species.

The theory that the hippocampus functions as a cognitive map is not ironclad and, consequently, has encountered resistance over the years. Critics of the theory suggest that all of space should be represented equally and the cells mapping one's trajectory through the environment should be topographically distributed in the hippocampus (Eichenbaum et al., 1999). Evidence shows that a higher proportion of place fields are distributed along the periphery of an open environment (Muller et al., 1987) and cells with neighboring place fields are not juxtaposed in the hippocampus (Redish et al., 2001), which has been used as an argument against spatial maps. Furthermore, Hetherington and Shapiro (1997) reported that place fields tended to concentrate near the local cues in a square recording chamber, suggesting that the relationship between the stimulus and place field was an essential component of spatial firing. Consequently, opponents of the cognitive map theory argued that the Hetherington and Shapiro finding supported the criticism that space was not equally represented and the hippocampus was not creating a cognitive map (Eichenbaum et al., 1999). Moreover, the hippocampus has been shown to represent nonspatial information in addition to spatial information (O'Keefe and Dostrovsky, 1971; O'Keefe, 1976; Ranck, Jr., 1973; Wible et al., 1986; Wood et al., 1999; Young et al., 1994), which critics of the cognitive map theory, such as Eichenbaum, have used to argue against the theory. However, Manns and Eichenbaum (2009) recorded hippocampal pyramidal cells during an object recognition memory task and reported that information pertaining to the spatial location of an object was represented more than the object identity. They suggested that hippocampal spatial representations could incorporate objects and these maps were used to

recall the specific object and spatial encounter, which is similar to the theory proposed by O'Keefe and Nadel (O'Keefe and Nadel, 1978).

### **1.2e Episodic Memory Theory**

The hippocampus has also been suggested to play a central role in forming episodic memories. These memories involve recalling a particular event that happened at a specific time and in a distinct place. Conceptually, episodic memories represent the what, when, and where of the past. In (1972), Endel Tulving first made the distinction between episodic and semantic memories. He described episodic memory as the automatic binding of events, places, and time, whereas semantic memory was a structured knowledge regarding words, other verbal symbols, and the relationships between the words and symbols (Tulving, 1972). He insisted that in order for a brain system to process episodes, the system needed to be downstream of fibers that modulated attention and receive highly processed sensory information. The hippocampus is innervated with fibers from cholinergic centers such as medial septal nucleus, which have been implicated in behaviors that require attention (Voytko, 1996;Everitt and Robbins, 1997;Baxter and Chiba, 1999;Chudasama et al., 2004;Cobb and Davies, 2005). The MEC, which is one of the primary inputs into the hippocampus, receives input from neurons that are sensitive to visuospatial information (primary, lateral, and medial visual cortical areas) as well as cells from the dorsal presubiculum and retrosplenial cortex that are directionally and spatially tuned (Taube et al., 1990b;Taube et al., 1990a;Chen et al., 1994;Cacucci et al., 2004;Bucci et al., 2000;Norman and Eacott, 2005). Moreover, the LEC, another primary input to the hippocampus, receives input from unimodal sensory areas such as perirhinal cortex (Norman and Eacott, 2005).

The concept of episodic memory has been difficult to experimentally test in nonhuman animals, prompting Tulving to claim that it is a process exclusive to humans (Tulving, 2002). The foundation for this argument is based on one being “autonoetic” (self-reasoning) and consciously aware of “mentally time traveling” through their past in order to recall the experience and verbally express the

memory (Tulving and Markowitsch, 1998; Tulving, 2001; Tulving, 2002). The linguistic clause makes demonstrating episodic memory in animals unattainable; therefore, experimentalists using animals to test mnemonic processes have adopted the term “episodic-like” memory to include all the behavioral criteria, while excluding the dependence on expressing one’s self reasoning consciousness (Clayton et al., 2001; Clayton et al., 2003). After removing the inclusion criteria of “autonoetic” consciousness, the importance of the hippocampus for episodic-like memory has been reported across species such as humans, nonhuman primates, birds, and rats.

Vargha-Khadem and colleagues (1997) published a seminal paper that dissociated episodic and semantic memory in humans and showed that the hippocampus was essential for episodic memory. The authors used magnetic resonance techniques on three subjects, who all started suffering from anterograde amnesia prior to adolescence, and found damage to the hippocampus on both hemispheres of the brain. None of these patients could recall prior experiences, but they learned to speak, read, and acquired facts as they progressed through grade school; thus, the subjects showed a deficit in episodic memory, but not semantic memory. Additional support for the human hippocampus functioning in episodic memory was shown when Weiler et al., (2010) used functional magnetic resonance imaging to examine hippocampal activity while subjects were asked to recall previous Christmas experiences after being prompted with a word related to the holiday, such as *Christmas tree*. The authors found that the activity of the right posterior hippocampus increased when subjects recollected previous events. The hippocampal formation’s role in recalling experiences is believed to be a phenomenon observed across primates. In (1994), Gaffan reported that monkeys with damage to one of the major output pathways of the hippocampus, the fornix, showed significant deficits in object-in-place tasks; thus, Gaffan suggested that the impairments were similar to the deficits experienced in humans suffering from amnesia.

Strong evidence for episodic-like memory was shown in food-caching birds. Clayton and colleagues exploited the ethology of scrub jays and showed a striking example of episodic-like memory. In the wild, scrub jays collect and store perishable and nonperishable food in order to consume it at a later point in time. Clayton and Dickinson (1998) took advantage of this natural behavior by devising a task that required the birds to cache wax worms and peanuts. The wax worms were the birds' preferred choice of food, but were only available for a short duration of time because the worms quickly decomposed, whereas the peanuts could be recovered after being buried for a longer period of time. When the scrub jays were allowed to search for either cached item, the birds chose the location of the worm or peanut depending on whether the intervals between caches were shorter or longer in duration, respectively. Clayton and Dickinson proposed that the evidenced behavior satisfied the what, when, and where criteria for episodic-like memory. Clayton and coworkers (2007) even showed that scrub jays could plan for the future, which Tulving argued was dependent on episodic memories and unique to humans (Tulving, 2002).

Wood et al., (2000) recorded hippocampal pyramidal cell activity as rats circumnavigated a modified T maze alternating between left and right turn loops. The data showed that the majority of the cells with firing on the central common arm of the maze showed a disparity in firing patterns (i.e., some cells had a higher firing rate on the left turn trails and others had a higher firing rate on the right turn trials) and the authors interpreted this as evidence for hippocampus encoding episodic-like memories. However, the results from Wood et al. (2000) could not be replicated under conditions that one would expect to produce the differential firing pattern (Lenck-Santini et al., 2001; Bower et al., 2005; Griffin et al., 2007). Poucet and coworkers (2001) reported that eighteen place cells with fields in the central stem of a Y-maze did not alternate their firing patterns between left and right turns and they suggested this might result from a difference in the two protocols. Rats used in Wood et al. (2000) only traversed the central stem in one direction, whereas the rodents from Lenck-Santini et al. (2001) approached the central stem of the maze from two directions (inward and



outward paths). Bower et al (2005) used a series of tasks to examine the sequential firing patterns of place cells on behavioral apparatus with repeated sequences. In one complicated task, consisting of eight segments with two links that were repeated, no differential activity was observed in CA1 pyramidal cells. However, the differential firing pattern was replicated when using a modified T-maze, like Wood et al. (2000), and either training the rats with wooden blocks to shape the behavior or alternating the laps that a reward was received. McNaughton and coworkers suggested that the differential firing pattern reported in Wood et al. (2000) and (2005) was a mechanism that the hippocampus used to either encode sequences or different contexts (i.e., left or right turns). Griffin et al. (2007) examined the firing pattern of CA1 neurons during the encoding (sample) and retrieval (choice) phases of a discrete trial delayed-nonmatch-to-place task and observed that neurons were selective for either the sample or choice phase of the task and fewer neurons showed the differential firing between right and left trials than previously reported. The authors proposed that the differences might have been caused by the different memory demands of the tasks. The results from Lenck-Santini et al. (2001), Bower et al. (2005), and Griffin et al. (2007) do not exclude the possibility that the hippocampus is encoding episodic memories. Eichenbaum and coworkers (2002) continued to accumulate evidence supporting a role for the hippocampus in forming memories about events when they observed that rats with hippocampal lesions were worse at remembering sequences of events compared to controls. A subsequent study found that the firing pattern of hippocampal ensembles was influenced by recent and present events as well as predictive signals that forecasted future events (Ferbinteanu and Shapiro, 2003). Taken together, the data provides support for the hippocampus playing a pivotal role in forming episodic memories; however, the data showing when the experience occurred is still questionable.

Some critics have questioned whether memory should be partitioned into functionally different types or whether the hippocampus is specifically involved in one type of memory. The work of Vargha-Khadem et al. (1997) and many others (Thompson and Kim, 1996; Nobre et al., 1997; Sommer et al., 1997; Reinvang et

al., 1998) have provided strong support for distinct types of memory that can be localized to different regions of the brain. Furthermore, Kennedy and Shapiro (2004) and Moita et al. (2003) have provided evidence showing that the hippocampus encodes spatial (where) and nonspatial (what) information. An emerging consensus among the hippocampal field is that the hippocampus encodes an episodic memory by combining information from two parallel input streams, a spatial signal carried in the medial entorhinal cortex and a nonspatial signal carried in the lateral entorhinal cortex (Knierim et al., 2006; Manns and Eichenbaum, 2006). However, the mechanisms underlying this process are still being investigated.

Despite the controversy regarding the specific type of memory, it appears that the hippocampus plays a pivotal role in mnemonic function (Scoville and Milner, 1957; Vargha-Khadem et al., 1997; Squire et al., 2004; Squire, 2004; Leutgeb et al., 2005b; Thompson, 2005; Andersen et al., 2006; Moscovitch et al., 2006; Gilboa et al., 2006). Many of the most influential theories of hippocampal function pertaining to memory share a common feature, which is the encoding of space; however, whether encoding space is the primary function or merely a consequence of the information processing occurring in the hippocampus remains debatable. The hippocampal formation receives input from the upper levels of the association cortex and this information is integrated into new memories that are stored until a recollection process is initiated. The exact mechanisms by which the hippocampus stores and recalls this information remain unresolved. It has been suggested that the theoretical concepts of pattern separation and pattern completion might be instrumental for storing and recollecting memory traces in the hippocampal formation, which will be discussed in the next section (Marr, 1971; McNaughton and Nadel, 1990; McNaughton and Morris, 1987; Guzowski et al., 2004; Rolls and Kesner, 2006).

## **1.3 Hippocampal Memory Mechanisms**

### **1.3a Theoretical Concepts**

The formation, storage, and recollection of hippocampal dependent memories theoretically utilize an autoassociative attractor network (Hopfield, 1982;Marr, 1971;Tsodyks, 2005). An attractor network encodes memories by storing them in recurrent neural networks as specific stable patterns of activity that are imprinted by long-lasting modifications, enabling the retrieval of these patterns with the input of a partial cue (Tsodyks, 2005). These stable patterns of neural network activity are referred to as attractor states, which link together coactive neurons forming a basin of attraction. Afferent information will perturb the stability of the network to different degrees. Small alterations in input will change the network activity, but not enough for it to leave the basin of attraction and the system will eventually return to the original state (i.e., same set of active neurons). This attribute of attractor networks would be a mechanism for pattern completion, which is the ability to reproduce a previously stored output pattern from a partial or degraded input pattern (Marr, 1971;Guzowski et al., 2004;McNaughton and Morris, 1987). To facilitate the formation of new memories and prevent interference from previously stored memory traces, a preprocessing state may be necessary prior to information entering the attractor network. This preprocessor stage, theorized to occur in the DG, might orthogonalize inputs to create new attractor basins, so the system could distinguish small input changes and prevent interference between similar experiences when desired. This feature of attractor networks would be a mechanism for pattern separation, which is the capacity to decrease redundancy amongst incoming information and then output patterns that overlap less than the inputs (McNaughton and Nadel, 1990;Rolls and Kesner, 2006;Guzowski et al., 2004). Large changes in sensory input may cause the network activity to leave the basin of attraction and fall into a different state.

### **1.3b Anatomical Evidence for Pattern Separation and Pattern Completion**

The neural architecture of the hippocampal formation is well suited for information storage and recall. This region is composed of five subregions (subiculum, CA1, CA2, CA3, and the dentate gyrus) and a simplified wiring diagram is illustrated in Figure 1.1. The entorhinal cortex sends projections from layer 3 to both CA1 and the subiculum via the perforant pathway (Witter and Amaral, 2004; Witter, 1993). In contrast, layer 2 of the entorhinal cortex projects to the dentate gyrus and CA3. The entorhinal input into the dentate gyrus is highly structured such that the fibers of the perforant pathway are confined to the superficial 2/3 of the molecular layer, with the MEC input restricted to the middle third of the layer and the fibers from LEC targeting the most superficial portion (Steward and Scoville, 1976; Steward, 1976; Witter et al., 1989; Wyss, 1981). The projection pattern from the entorhinal cortex to CA3 resembles the laminar entorhinal input into DG except that the fibers enter the stratum lacunosum-moleculare, which like the molecular layer of the dentate gyrus is superficial to the principal cell layer. Tamamaki and Nojyo (1993) showed that the collaterals of neurobiotin-filled stellate cells in layer 2 of the entorhinal cortex reach both the DG and CA3 fields, suggesting both fields receive similar cortical input. The entorhinal fibers form excitatory (glutamatergic) asymmetric synapses with both granule, pyramidal, and less frequently inhibitory interneurons (Nafstad, 1967; Desmond et al., 1994; Witter et al., 1992).

In addition to cortical input, the dentate gyrus also receives subcortical input from the septal, supramammillary, and pontine nuclei. The septal projection innervates all fields of the hippocampus, but cholinergic staining in the dentate gyrus is predominant (Witter and Amaral, 2004). The axons from cells in the medial septal nucleus and the nucleus of the diagonal band of Broca innervate the hippocampus through four pathways (i.e., fimbria, dorsal fornix, supracallosal stria, and a more indirect route passing near the amygdala). The input from the cells that surround the mammillary nuclei is glutamatergic (Kiss et al., 2000) and has been shown to project to the molecular layer of dentate gyrus.

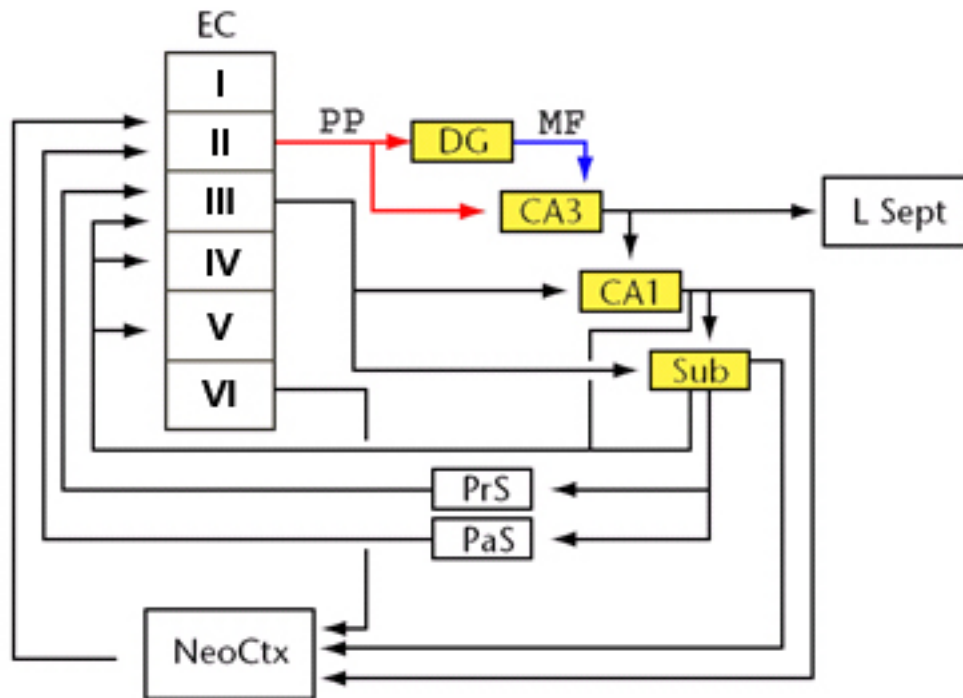


**Figure 1.1. Simplified Wiring Diagram of the Hippocampal Formation.** The anatomical regions of the hippocampus (highlighted in yellow) include the dentate gyrus (DG), hippocampus proper (CA1, CA2, CA3), and the subiculum (Sub). For simplicity, CA2 is not included in the diagram. The dentate gyrus and CA3 are innervated by the perforant path (PP; red arrows), which projects from layer II of the entorhinal cortex. CA3 is also innervated by the mossy fiber pathway (MF; blue arrow), which is the sole extrinsic dentate projection. CA1 and the lateral septum (L Sept) receive efferent information from CA3. The subicular output is carried to presubiculum (PrS), parasubiculum (PaS), and the neocortex (NeoCtx).

The dentate gyrus also receives noradrenergic input from the pontine nucleus locus coeruleus, which typically terminate in the hilus.

The dentate gyrus, one of the hippocampal subfields associated with the “classic trisynaptic pathway”, has a complicated local circuitry that is oversimplified in the classic trisynaptic loop. Similar to CA1 and CA3, this region consists of three layers; however, unlike the CA regions, the dentate gyrus has more than one putative excitatory cell type (i.e., granule and mossy cells). Granule cells, which in rat surpass a million neurons (West et al., 1991; Rapp and Gallagher, 1996; Amaral and Witter, 1989), constitute the majority of cells in the granule cell layer. In contrast, the mossy cells, which are the principal cells of the polymorphic cell layer, number approximately 10,000 - 50,000 (West et al., 1991; Buckmaster and Jongen-Relo, 1999; Henze and Buzsaki, 2007). The granule cells are the only cells in the dentate gyrus that project to a different hippocampal subfield (i.e. sole output of the dentate gyrus), but the mossy cells have been reported to project to the dentate gyrus on the contralateral hemisphere (Fricke and Cowan, 1978; Witter and Amaral, 2004). Granule cell axons (i.e., mossy fibers) make strong, detonator-like synapses with CA3 pyramidal cells. The majority of mossy fibers terminate on the dendrites of pyramidal cells; however, the most proximal portion of CA3 (i.e. region located between the upper and lower blades of the granule cell layer) also receives input from the infrapyramidal and intrapyramidal bundles (Blackstad et al., 1970; Gaarskjaer, 1978a; Gaarskjaer, 1978b; Swanson et al., 1978). In route, the mossy fibers sprout smaller collaterals in the polymorphic cell layer that also make strong, *en passant* synapses with mossy cells. Not only do mossy cells receive input from granule cells, but they also receive input from CA3 cells (Scharfman, 1994); therefore, they likely play a central role in the only excitatory feedback pathway in the “trisynaptic loop”. The local circuitry of the polymorphic layer is an integral component of the recurrent circuitry within the dentate gyrus. Directly excited by input from granule cells, mossy cells excite inhibitory basket cells and other distantly located granule cells (Witter and Amaral,

2004;Buckmaster et al., 1996;Wenzel et al., 1997). The local circuitry of the dentate may play a pivotal role regulating the flow of information through the hippocampus.

Cells in the entorhinal cortex (300,000) make contact with an expanded number of granule cells (1,000,000) in the dentate (Amaral et al., 1990;Witter and Amaral, 2004), which might permit neuronal activity patterns to be differentiated by redistributing overlapping neural activity from a smaller population of cortical cells into nonoverlapping activity in a much larger granule cell population (Marr, 1971;McNaughton and Morris, 1987;Rolls and Treves, 1998). This expansion recoding might allow the dentate gyrus to perform pattern separation and prevent spurious recall by producing nonoverlapping, sparse representations from entorhinal cortex input (McNaughton and Morris, 1987;McNaughton and Nadel, 1990); however, recent experimental data suggest that under some conditions, the dentate gyrus disambiguates similar inputs, or makes the inputs less similar, by changing the spatial firing patterns of a constant active population of cells instead of the theorized mechanism of expansion recoding (Leutgeb et al., 2007).

A unique attribute of the adult dentate gyrus and currently one other region, the olfactory bulb, is the continuous incorporation of newborn cells into the existing neural circuitry (Kaplan and Hinds, 1977;Bayer, 1983). This renewed growth of the dentate gyrus originates from a layer of stem cells that reside at the transition between the granule and polymorphic cell layers (Li et al., 2009). Over the course of approximately a month, the stem cells specifically develop into granule cells and become functional units in the hippocampal circuit (Overstreet-Wadiche and Westbrook, 2006). Developing granule cells undergo dramatic changes in cellular morphology and electrophysiological properties throughout the first four weeks of life (Overstreet-Wadiche and Westbrook, 2006). During the first week, the cell body is typically located in the granule cell layer in close proximity to the hilus, but occasionally cells can migrate further into the layer (Overstreet-Wadiche and Westbrook, 2006). At this point in time, the developing granule cells do not receive synaptic input despite having dendrites that extend

through the granule cell layer (Li et al., 2009). The lack of input rapidly changes, since GABAergic current is detected on day eight, which has been shown to depolarize the newborn cells (Li et al., 2009). The depolarizing GABAergic current diminishes after two weeks, after which the typical inhibitory GABAergic and excitatory glutamatergic currents are recorded in the newborn cells (Li et al., 2009). Furthermore, as the excitatory GABAergic current decreases, the threshold for inducing long-term potentiation is lowered (Ge et al., 2006; Schmidt-Hieber et al., 2004; Wang et al., 2000; Li et al., 2009). In conjunction with the electrophysiological changes, the morphology develops to resemble a mature granule cell with extensive processes that project from the small round cell body, which has migrated into the granule cell layer, and an axon projecting to the CA3 region of the hippocampus (Li et al., 2009). After twenty-eight days, the newborn granule cell resembles a fully mature granule cell and has been incorporated into the hippocampal circuit (Li et al., 2009). The survival rate of newborn granule cells has been reported to be affected by environment, exercise, aging and stress (Aimone et al., 2010). Aimone et al. (2006) proposed that the newborn cells might timestamp memories that are encoded as the neurons differentiate and become incorporated into the hippocampal circuitry; thus, performing temporal pattern separation.

After transforming perforant path input, the dentate mossy fiber projections are in a position to influence the activity of CA3 pyramidal cells (Witter and Amaral, 2004). It is estimated that a granule cell can influence 14-28 pyramidal cells, yet each pyramidal cell receives contact from 50 granule cells (Witter and Amaral, 2004). CA3 has extrinsic connections with the amygdaloid complex that primarily come from the basal nucleus (Pikkarainen et al., 1999; Pitkanen et al., 2000). CA3 also receives serotonergic and noradrenergic input from the brainstem. Like the dentate, pontine nucleus locus coeruleus projects to CA3, but terminates in stratum lacunosum-moleculare at synaptic junctions that connect the fibers to pyramidal cells (Pickel et al., 1974; Loy et al., 1980). Unlike the noradrenergic input, direct synapses onto the pyramidal cells from the



serotonergic input of the midbrain raphe nuclei are absent (Jacobs et al., 1978); but see (Moore et al., 1978). The diffuse and sparse fibers appear to release neurotransmitter into the extracellular space (Andersen et al., 2006). The primary output from CA3 is the Schaffer collaterals, which project to the ipsilateral CA1 subfield of the hippocampus. The CA3 pyramidal cells located closest to the dentate gyrus (proximal CA3) project to more distal parts of CA1, whereas the neurons closer to CA1 project to more proximal parts of CA1. Like the mossy cell in the dentate gyrus hilar region, the CA3 pyramidal cells form a cross commissural projection to all CA fields of the contralateral hemisphere (Blackstad, 1956;Fricke and Cowan, 1978). The perforant path, mossy fibers, and subcortical input innervate CA3, but the largest number of synapses results from recurrent collaterals of pyramidal cells themselves (Ishizuka et al., 1990;Li et al., 1994). Due to the Hebbian plasticity that couples coactive elements of a neuronal population, this circuitry theoretically permits the completion of the whole representation when a few neurons of the original set are activated (McNaughton and Morris, 1987). Therefore, many models hypothesize that the CA3 region of the hippocampus is responsible for pattern completion via its recurrent collaterals (Marr, 1971;McNaughton and Morris, 1987;Rolls and Treves, 1994).

### **1.3c Physiological Evidence for Pattern Separation and Pattern Completion**

The anatomical connections of the hippocampus support the computational models of pattern separation and pattern completion, but until recently experimental evidence for pattern separation was scarce. McNaughton and colleagues (McNaughton et al., 1989) showed that dentate lesions result in severe spatial learning defects and alter the temporal, but not spatial, firing properties of CA3 pyramidal cells. Moreover, novel environments enhanced the induction and maintenance of long-term potentiation in the dentate gyrus (Davis et al., 2004). These results imply that this subfield of the hippocampal formation might be required for learning that a new experience is different from a similar prior experience. Gilbert et al. (2001) used a delayed-match-to-sample for

spatial location task to assess pattern separation and found that rats with ablated granule cells performed worse when spatial similarity was increased compared to vehicle injected controls. In addition, granule cells were recorded as rats navigated an eight-arm radial maze and were shown to have small receptive fields that coincided with low rate, sparse firing (Jung and McNaughton, 1993). Furthermore, putative granule cells have been reported to fire in multiple locations in the environment (Leutgeb et al., 2007;McNaughton et al., 1983;Chawla et al., 2005) (but see chapter 2) and data from Leutgeb et al. (2007) showed that different firing fields of putative granule cells change their firing rates when the shape of the environment was altered. The variation in granule cell firing rates in different environments has been suggested as a mechanism to express pattern separation (Leutgeb et al., 2007). The idea that granule, hilar, and CA3c cells act as a functional unit to facilitate the pattern separation process was suggested by Hunsaker et al. (2008) in a report showing that lesions to both the dentate and to a lesser extent CA3c impaired an animal's ability to detect subtle changes in the distance between two objects in an environment. Myers and Scharfman (2009) proposed a model suggesting that increasing the firing rate of mossy cells can facilitate pattern separation because of the negative disynaptic feedback from mossy cells (+) → basket cells (-) → granule cells. The necessity of the granule cells to differentiate between objects that are spatially similar, the cellular firing characteristics, and the proliferation of new neurons suggest that the dentate may perform pattern separation to decrease interference between old and new memories (Aimone et al., 2006). Additional experiments should be conducted that directly examine neural activity in the dentate gyrus while sensory input is slightly altered.

Brain systems implemented in memory need to store information and recall the previously stored information. It has been suggested that the hippocampal formation recalls information via CA3 performing pattern completion. Behavioral evidence supporting the hypothesis that CA3 is necessary for pattern completion came from Gold and Kesner (2005) in a study that showed that chemically ablating CA3 decreased the ability of rats to find a

reward location after reducing the number of available cues. Complementing the evidence provided from the Gold and Kesner investigation, Nakazawa and colleagues (2002) found that removing most extramaze cues during a spatial memory task caused mice with a CA3 NMDA-receptor knockout to perform worse in the task than wild-type mice. In addition, they showed that CA1 place cells of a CA3 NMDA-receptor knockout mouse had a reduction in firing rate and place field size (Nakazawa et al., 2002). However, this study is not conclusive because no direct recordings from CA3 were conducted. In addition, other apparently conflicting results have been obtained regarding computations performed in CA3. One experiment performed by Lee et al. (2004b) involved rotating distal and local cues in opposite directions, which created a mismatch at each point on a track between the sensory input provided from the distal and proximal cues, and found that location-specific firing of CA3 cells maintained similar patterns of activity in both conditions (i.e., CA3 performed pattern completion). In contrast, data from Leutgeb et al. (2004) showed that completely different CA3 ensembles were active when rats foraged in identical enclosures located in different rooms, which suggests that CA3 performs pattern separation. A study that examined CA3 immediate early gene activity showed that ensemble activity overlapped when local and distal room cues were manipulated and overlapped less in two different environments (Vazdarjanova and Guzowski, 2004). Collectively, these data suggest that CA3 performs pattern completion or pattern separation depending on whether changes in the input are either small or large, respectively (Guzowski et al., 2004), which is in agreement with computational models (McClelland and Goddard, 1996; O'Reilly and McClelland, 1994). Alternatively, the dentate gyrus may actively perform either pattern separation or pattern completion, and CA3 may passively relay the results of information processing from a region located upstream. Consequently, it is necessary to examine the information sent from structures projecting into CA3 (i.e., dentate gyrus and entorhinal cortex), in order to directly compare input and output representations.

The first part of the research reported in this dissertation focuses on the under-characterized local circuitry of the dentate gyrus. Strong evidence is provided suggesting that cells localized to the polymorphic layer fire in multiple locations throughout an enclosure; this finding represents the first characterization of the spatial firing characteristics of hilar neurons in behaving rats. Moreover, it casts doubt on the previous reports claiming that granule cells typically have multiple firing fields distributed throughout an environment, but instead provides evidence suggesting that these cells typically fire in single locations in an environment. The second part of this dissertation focuses on the flow of information through the hippocampus and the computations occurring in the dentate gyrus and CA3 hippocampal subfields. This report compares the response of the CA3 subfield with all three of its primary inputs (LEC, MEC, and dentate gyrus). The results show that the dentate gyrus representation changes compared to its input representations, whereas the CA3 representation changes less than its input representations. Furthermore, even though individual LEC cells showed poor spatial tuning, a weak local-cue-related signal was observed at the population level that contrasted with the global-cue-related signal represented by the MEC. These results elaborate the previously reported dissociation between MEC and LEC representations (Hargreaves et al., 2005; Yoganarasimha et al., 2010). These findings are consistent with longstanding computational models proposing that (1) CA3 is an associative memory system performing pattern completion in order to recall previous memories from partial inputs and (2) the dentate gyrus performs pattern separation to help store different memories in ways that reduce interference when the memories are subsequently recalled.

## **CHAPTER 2 CHARACTERIZING THE SPATIAL FIRING PROPERTIES OF NEURONS FROM THE DENTATE GYRUS**

### **2.1 Introduction**

The dentate gyrus, one of the hippocampal subfields associated with the “classic trisynaptic pathway”, is essential in mnemonic function (McNaughton et al., 1989). Similar to CA1 and CA3, this region consists of three layers; however, unlike the CA regions, the dentate gyrus has more than one putative excitatory cell type (i.e., granule and mossy cells). Granule cells, which in rat surpass a million neurons (West et al., 1991; Rapp and Gallagher, 1996; Witter and Amaral, 2004) with their cell bodies composing the granule cell layer, receive multiple sources of input, one of which is from layer two of the entorhinal cortex (Witter and Amaral, 2004) and project via the mossy fibers to CA3. In contrast, mossy cells of the polymorphic cell layer number approximately 10,000 - 50,000 (West et al., 1991; Buckmaster and Jongen-Relo, 1999; Henze and Buzsaki, 2007). Mossy cells play a central role in the only excitatory feedback pathway in the “trisynaptic loop” receiving input from CA3c cells (Scharfman, 1994) and then projecting back to granule cells (Jackson and Scharfman, 1996). The local circuitry of the polymorphic layer is further complicated by the recurrent circuitry within the dentate gyrus. Directly excited by input from granule cells, mossy cells excite other distantly located granule cells and feedback to inhibitory basket neurons (Witter and Amaral, 2004; Buckmaster et al., 1996; Wenzel et al., 1997). Since the polymorphic layer plays a pivotal role in the flow of information through the hippocampus it is important to know whether cells in this layer show spatially selective firing.

Only a few studies have reported the spatial firing characteristics of excitatory cells in the dentate gyrus; however, interpreting the data has been difficult because of the ambiguity in identifying recordings of either granule or hilar cells. The previous reports showed that putative granule cells had multi-punctate firing fields that were distributed irregularly across the environment,

while occasionally cells only had a single field (Jung and McNaughton, 1993;Leutgeb et al., 2007). Gothard et al. (2001) reported similar findings except they claimed that the recordings were from cells in both the granule and polymorphic cell layers, but with the majority coming from the granule cell layer. Skaggs et al. (1996) observed that the majority of putative granule cells detected during sleep were silent during behavior; however, the few active cells were strongly theta-modulated, but the spatial firing patterns were not described. Currently, there have been no reports describing the spatial firing characteristics of cells in the polymorphic cell layer.

The electrophysiological properties of principle cells from the granule and hilar layers are distinctively different. The resting membrane potential of granule cells is extremely hyperpolarized both *in vivo* (Ylinen et al., 1995;Penttonen et al., 1997) and *in vitro* (Lambert and Jones, 1990;Spruston and Johnston, 1992;Staley et al., 1992;Soltesz and Mody, 1994), which contributes to the previously reported sparse spontaneous firing rates (Scharfman and Schwartzkroin, 1988;Penttonen et al., 1997). In contrast, the resting membrane potential of mossy cells is less polarized than granule cells both *in vivo* (Henze and Buzsaki, 2007) and *in vitro* (Scharfman and Schwartzkroin, 1988;Scharfman, 1992;Scharfman, 1994;Lubke et al., 1998). Since the resting membrane potential is closer to the threshold for spiking, mossy cells have the propensity to spontaneously fire (Scharfman and Schwartzkroin, 1988;Stowbridge et al., 1992;Buckmaster et al., 1993). Furthermore, granule cells have higher input resistances and shorter time constants than reported for mossy cells (Scharfman, 1992). Scharfman (1992) reported that granule cells recorded intracellularly in slice fire action potentials with shorter durations compared to mossy cells. Comparably, Henze and Buzsaki (2007) showed that mossy cells recorded in anesthetized rats have long, broad waveforms. The most striking disparity between granule cells and mossy cells is the capacity to fire in burst. Mossy cells recorded in slice have a higher propensity to fire trains of spikes either in response to a pulse of current or spontaneously than granule cells recorded in vitro (Scharfman and Schwartzkroin, 1988;Stowbridge et al., 1992;Scharfman,

1992;Buckmaster et al., 1993). These electrophysiological differences might help clarify the ambiguity associated with *in vivo* dentate gyrus recordings from freely moving animals.

The present study examines the spatial firing characteristics of cells from the dentate gyrus polymorphic layer. This is the first reported evidence from freely moving animals showing that hilar cells fire in multiple locations in a single enclosure. After partitioning dentate gyrus recordings into two groups (i.e., recordings from tetrodes detecting behaviorally active cells with spatial firing in either single or multiple locations), differences were observed when examining the firing properties during sleep and foraging. One group of cells had a significantly higher percentage of active cells recorded on a tetrode and fired in multiple locations in the environment, whereas a second group fired sparsely and the few cells that were active only fired in single locations in the environment. The group of cells recorded on tetrodes detecting at least one unit with multiple fields had fewer cells recorded during sleep with a higher mean firing and bursting rate compared to cells recorded on tetrodes detecting units with only single fields. These differences are consistent with previous reports of electrophysiological properties seen in slice and anesthetized animals for the excitatory cells in the dentate gyrus; consequently, we propose that cells from the polymorphic layer tend to have multi-punctate firing fields and granule cells-when active-fire in single locations.

## **2.2 Results**

Recordings of the dentate gyrus were obtained from seven rats implanted with independently movable multi-tetrode arrays as they quietly laid on a pedestal prior to and following an active foraging behavior. Tetrodes were advanced daily until gamma activity and dentate spikes were detected in the EEG (Bragin et al., 1995b;Bragin et al., 1995a), which occur ~300  $\mu\text{m}$  past the CA1 subregion of the hippocampus and indicated that the tetrodes were approaching the dentate gyrus. After observing the gamma activity and dentate spikes, the neural activity observed on the tetrodes was patiently monitored

during sleep for at least thirty minutes in order to determine if cells were present. If no cells were detected, then tetrodes were subsequently advanced 20  $\mu\text{m}$  or less a day.

Figure 2.1, shows coronal sections of a crystal violet stained rat hippocampus with tetrode tracks that were localized to the ambiguous region (Figure 2.1.A) and the polymorphic cell layer (Figure 2.1.B). The red boxes in A and B indicate regions of interest that were shown in the magnified (10X) image with arrows indicating the tip of the tetrode track. The data plotted in Figure 2.2.A was recorded on the tetrode identified in Figure 2.1.A, whereas the data in Figure 2.2.D was recorded on the tetrode identified in Figure 2.1.B. As tetrodes entered the dentate gyrus, numerous patterns of activity were detected on the four channels of the tetrode and visualized on scatter plots. For example, some tetrodes had multiple clusters of spikes that were only apparent when the animal was “sleeping” (see Figure 2.2.A sleep), whereas others detected a few clusters only during sleep. There were other tetrodes that only detected a few clusters (see Figure 2.2.A sleep) regardless of the animal’s sleep state. These observations in conjunction with previous reports suggesting that cells from the dentate gyrus only fire when the animal was asleep (Skaggs et al., 1996) provided precedence for us to collect multiple periods of sleep, each lasting 30 to 60 minutes, prior to and following the experiments to increase the likelihood of detecting a sparse firing population of granule cells.

In addition to observing differences in the patterns of activity on the tetrodes during sleep, it appeared that there were also differences during active behavior. The tetrodes with numerous clusters during sleep were relatively silent during behavior (Figure 2.2.A forage), whereas the tetrodes detecting only a few clusters during sleep were more active during behavior (Figure 2.2.B forage). Note in Figure 2.2.A the difference in the number of spikes for the six clusters well isolated clusters in both sleep sessions compared to the forage session. For the spikes on the tetrode plotted in figure 2.1.B, the one well isolated cluster showed robust patterns of firing in both sleep and behavior. For full tetrode projections used to isolate the cells on tetrodes see Figure 2.3 and



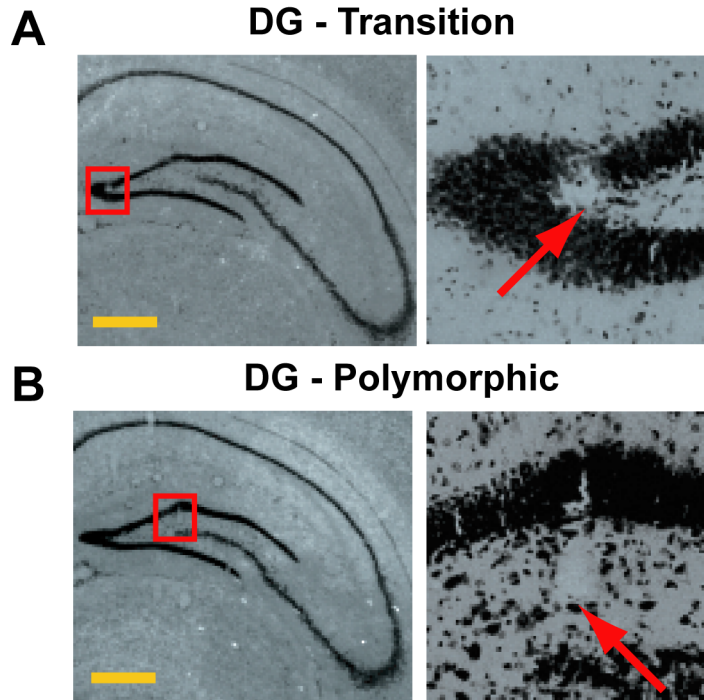


**Figure 2.1. Histology Localizing Tetrodes Targeting DG.** Histology from rat 153 showing tetrodes targeting the dentate gyrus subfield of the hippocampus localized to a region near the transition between the granule (A) and polymorphic cell layers (B). The regions of interest (red boxes) are magnified (10X) to show the tips of the tracks (arrows). Scale bar equals 600  $\mu\text{m}$ .

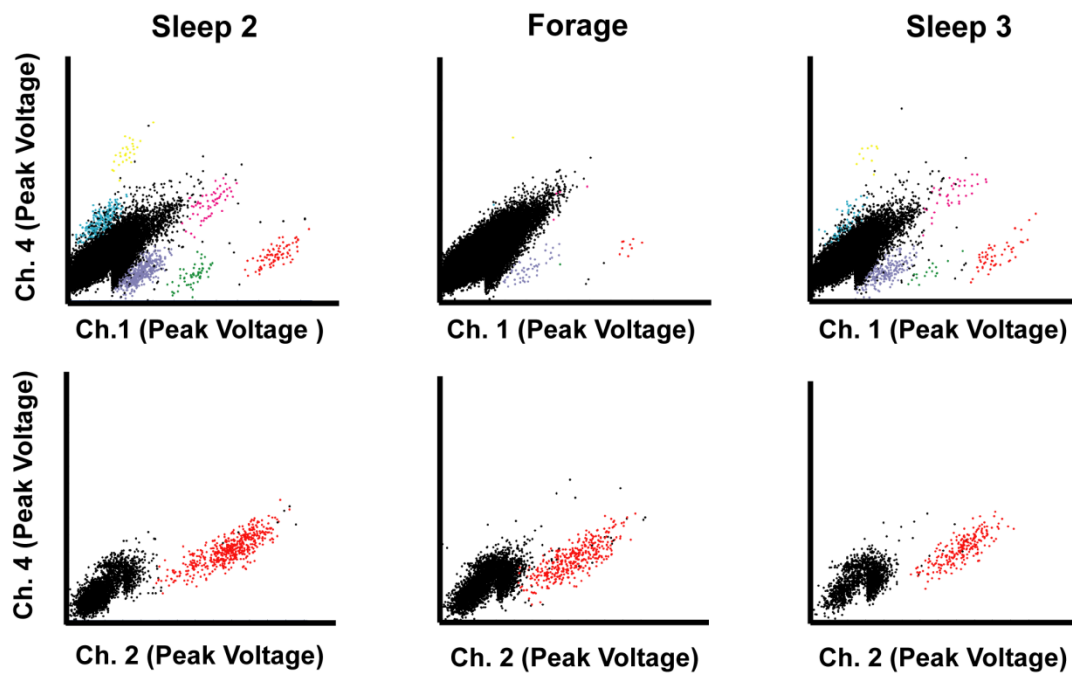
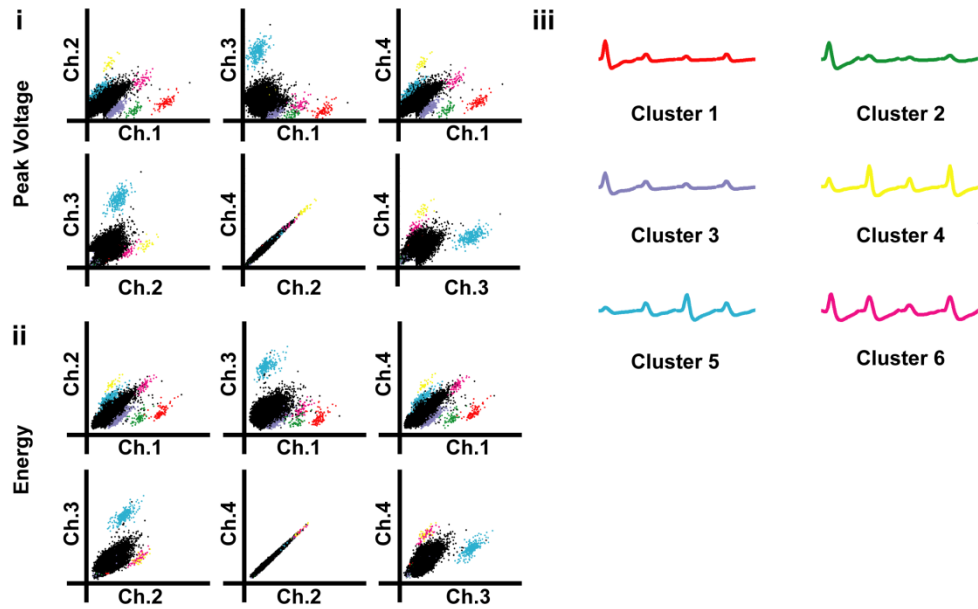
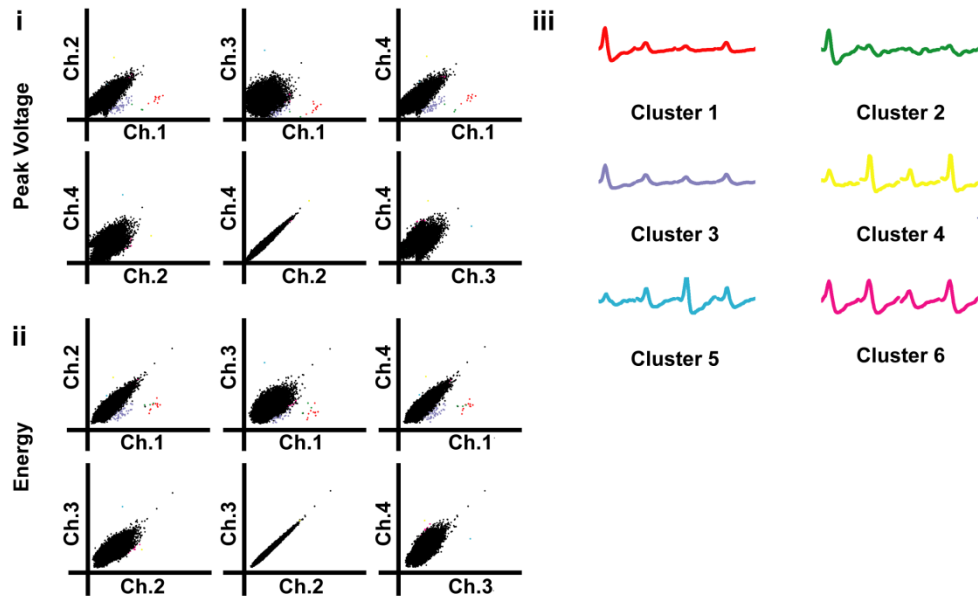


**Figure 2.2. Unit Isolation for Two Example Tetrodes Targeting DG.** Scatter plots showing the maximum height of triggered action potentials on two channels of a tetrode during two sleep sessions and a foraging session that each lasted 30 minutes. The data plotted in A were recorded on the tetrode classified as ambiguous (Fig 2.1.A), whereas the data in B were recorded on the tetrode localized to the polymorphic cell layer (Fig 2.1.B). Each set of colored points represents a different cluster. (See Figure 2.3 and 2.4 for all projections of these tetrodes.)

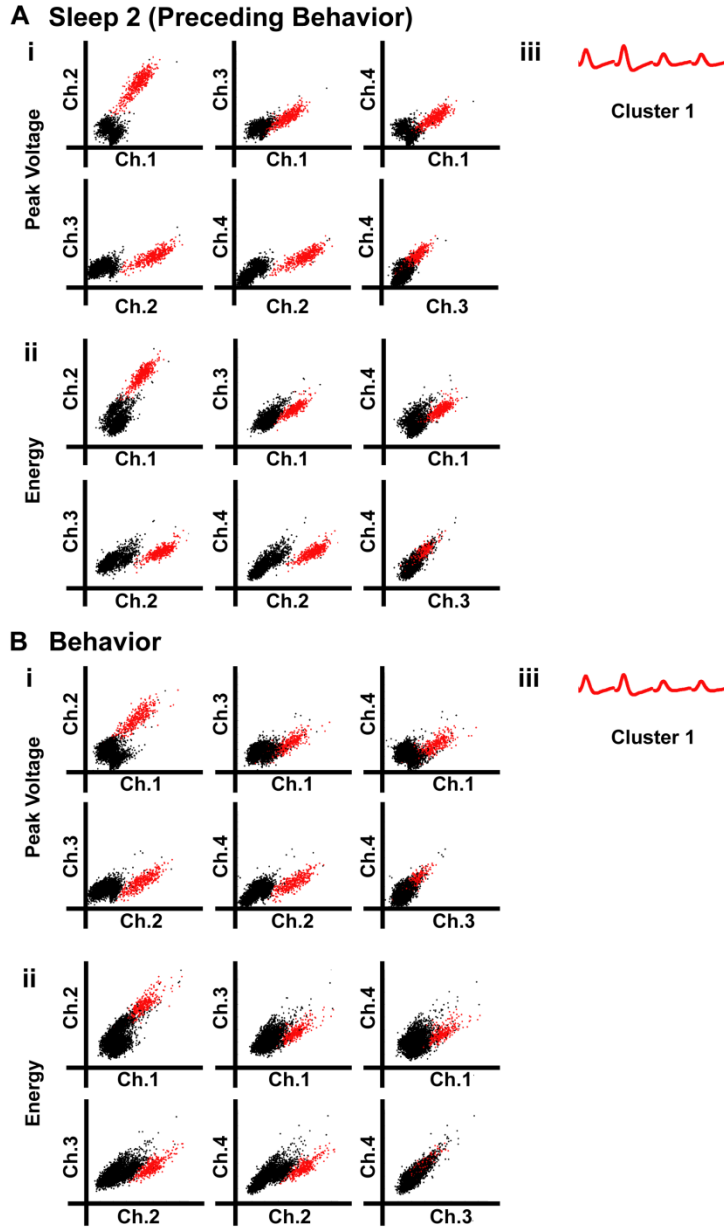
### A Sleep 2 (Preceding Behavior)



### B Behavior



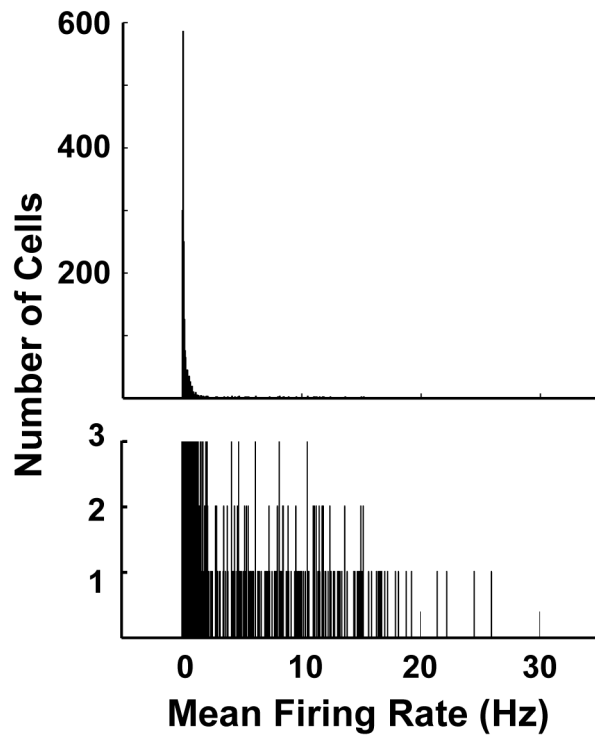
**Figure 2.3. Full Tetrode Projections Used to Isolate Cells on Tetrode Localized to the Transition Between the Granule and Polymorphic Cell Layers.** Full tetrode projections used to isolate the clusters from the tetrode in Figure 2.2A during pre-forage sleep (A) and open-field foraging (B). (A,B) Peak voltage (i) and energy (ii) were used to separate clusters. Six well-isolated clusters are shown in red, green, blue, yellow, cyan, and purple. Black points represent noise and clusters that were not clearly isolatable. Channels 2 and 4 were shorted together, resulting in the points falling on the 45° diagonal. The average waveforms (iii), detected on the four channels of the tetrode, are shown for each cluster.



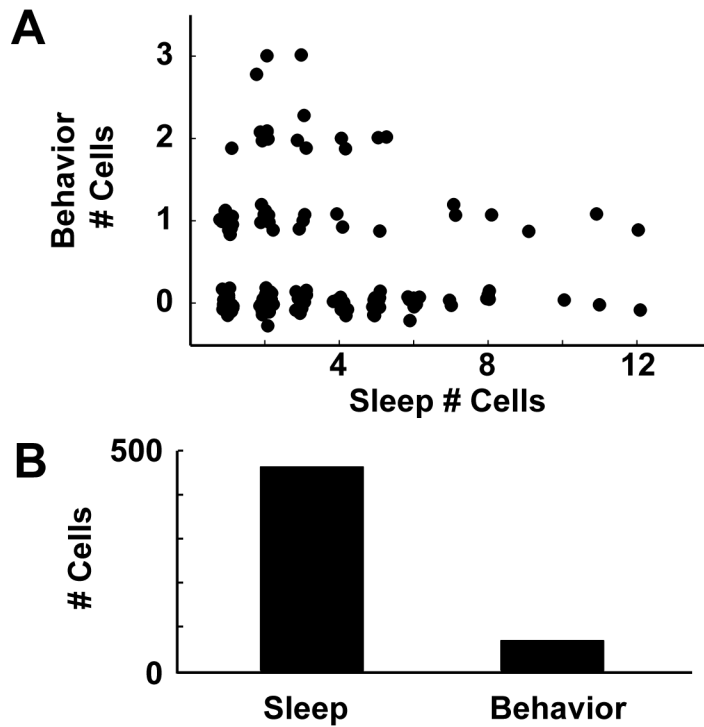
**Figure 2.4. Full Tetrode Projections Used to Isolate Cells on Tetrode Localized to Polymorphic Cell Layer.** Full tetrode projections used to isolate the clusters from the tetrode in Figure 2.2B during sleep 2 (A) and open-field foraging (B). (A,B) Peak voltage (i) and energy (ii) were used to separate the one well-isolated cluster shown in red. Black points represent noise and clusters that were not clearly isolatable. The waveforms (iii) from each spike, detected on the four channels of the tetrode, are shown for the lone cluster.

Figure 2.4. When postmortem histology was performed on the implanted rats, the tetrode tracks ended in all three layers of the dentate gyrus (i.e., the molecular, granule, and polymorphic cell layers). Furthermore, many of the tetrode tracks were localized to the transition between granule cell layer and hilus, which was considered ambiguous. Histology was performed two weeks after the initial recordings were started, which confounded identifying the recording sites because the tetrodes could have shifted overtime; consequently, many parameters were examined to facilitate the identification of recording from specific cell types.

In an attempt to disambiguate the dentate gyrus recordings, we examined the mean firing rate during sleep for all the well isolated clusters and determined that the majority (91%) of recorded cells from the seven rats had a firing rate less than 2 Hz and 61% of the total population had a mean firing rate less than 0.15 Hz; however, there was no obvious way of differentiating the multiple types of cells in the dentate gyrus based solely on firing rate (Figure 2.5). To examine any potential relationship between the number of active cells, which were defined as having a statistically significantly ( $p \leq 0.01$ ; Monte-Carlo statistics) spatial information score that exceeded 0.5 bits/spike and fired more than 75 spikes while the rat foraged in square enclosure, and sleep clusters in rats that actively foraged ( $n = 4$ ; one rat was excluded because no cells were active and two rats were excluded because of inadequate spatial sampling), we plotted the number of cells active and sleep clusters detected on each tetrode for data pooled from 41 tetrodes and across 23 foraging sessions; thus, samples were repeated in the data set (i.e., the same cell recorded for multiple sessions) and statistical test were not conducted (Figure 2.6A). Several patterns emerged when comparing the number of sleep clusters and active cells recorded on a tetrode. First, all tetrodes that detected six or more clusters during sleep had at most one active cell; 6 tetrodes had one active cell, whereas the remaining 17 tetrodes had no active cells during sleep. Second, tetrodes that detected five or



**Figure 2.5. Distribution of Mean Firing Rates During Sleep.** Histogram of the mean firing rates during sleep for all cells detected on tetrodes localized to the dentate gyrus of seven rats (top). The bottom graph magnifies the bins showing the cell counts ranging from 1 to 3 in order to visualize the range of firing rate bins (0.05-35 Hz).



**Figure 2.6. Negative Relationship Between Sleep and Behavior Clusters Recorded in DG.** (A) Scatter plot of the number of cells active during behavior vs. the number of cells detected during sleep. To aid in visualization of the overlapping data points, jitter was added to the points. (B) Summary of data in panel A showing the number of cells firing during sleep and behavior. Samples were repeated in the data set (i.e., the same cell recorded for multiple sessions) and statistical test were not conducted.

fewer sleep clusters had as many as three active cells during behavior. There were three examples of a tetrode detecting more cells during behavior than sleep. Figure 2.6.B summarizes the data plotted in Figure 2.6.A and shows that sixty-eight cells were considered active compared to 463 putative excitatory sleep clusters. Furthermore, only a minority of tetrodes recorded active cells (24 out of 41). Interestingly, there was an inverse relationship noticed between the number of active and sleep cells suggesting that the population of recorded cells might consist of different cell types from the dentate gyrus. Since only a minority of tetrodes detected active cells and there was an inverse relationship detected between sleep and behavior, we decided to examine the spatial firing properties of the active cells.

There was a subset of active cells from the last day that 2 rats foraged in an open enclosure that were unambiguously localized to the polymorphic layer based on histological reconstruction of tetrode tracks (Figure 2.7). The active cells were restricted to 5 recording sites. During sleep, 12 different units fired less than 2 Hz from these 5 tetrodes. During foraging, 8 units showed robust spatial firing based on the previously mentioned criteria (see Figure 2.8 for the best projections used to isolate clusters). The mean spatial information of these 8 units was  $1.1 \text{ bits/spike} \pm 0.2 \text{ S.D.}$  The ratio of spatially selective cells to sleep clusters at the 5 recording sites was slightly variable (2/5, 1/1, 2/2, 2/3, 1/1), but all showed a relatively high ratio. The cells fired in multiple locations throughout the enclosure, similar to previously reports from putative granule cells (Jung and McNaughton, 1993;Leutgeb et al., 2007). To quantify the number of fields per cell, a field was defined as 10 contiguous pixels of the rate map, each of which had a firing rate that exceeded 20% of the peak firing in the rate map. The black place-field maps in Figure 2.7 show that the majority of the 8 spatially selective cells fired in multiple locations (quadruple fields: 1; triple fields: 3; double fields: 3; single fields: 1). Note that even the cell classified as having a single field



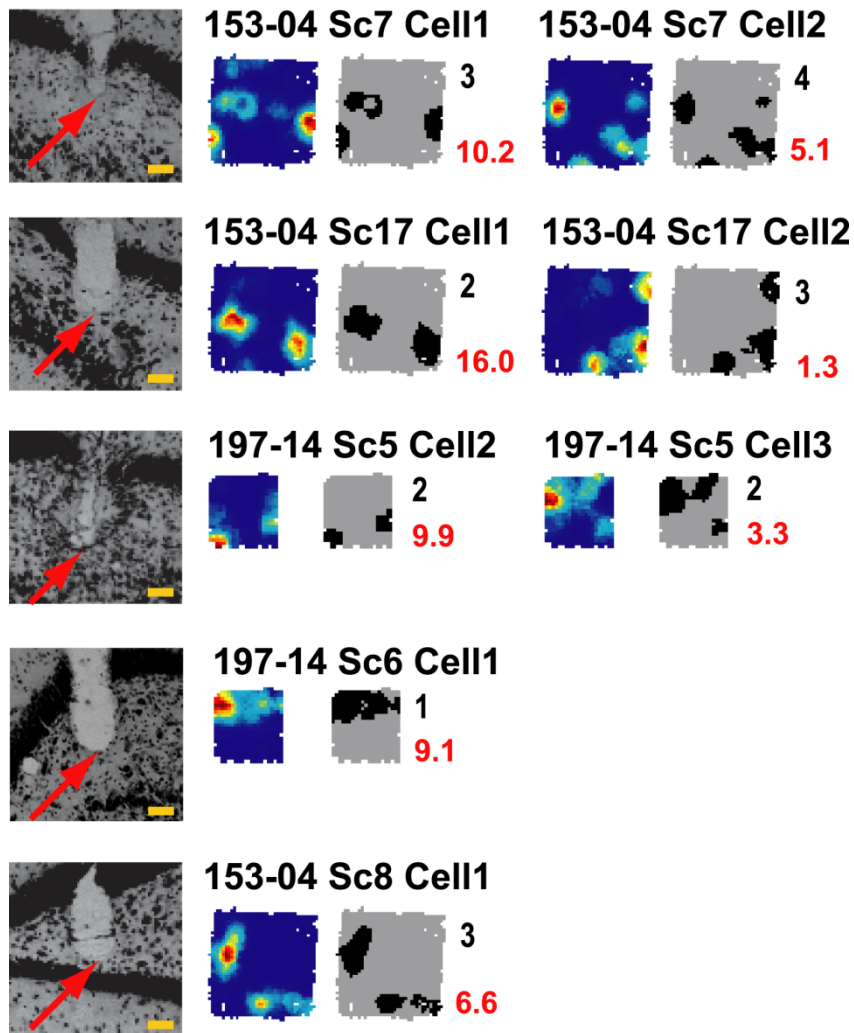
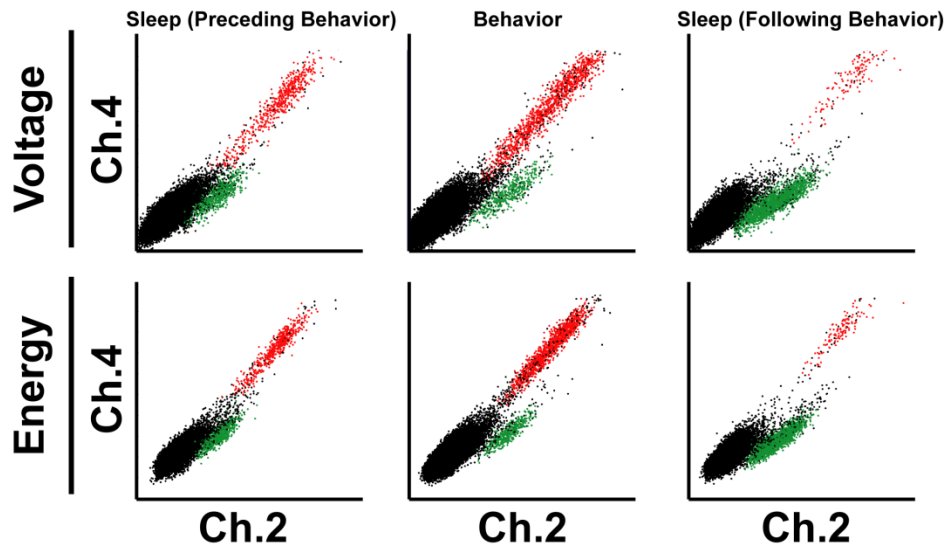
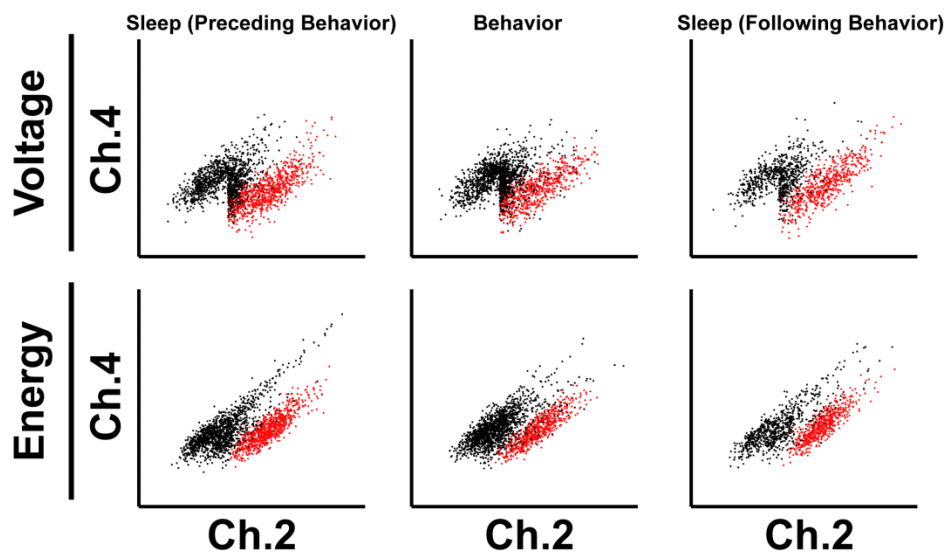


**Figure 2.7. Spatial Firing Rate Maps of Cells from the Hilus.** Rate maps and place-field count plots of cells that were localized to the polymorphic layer based on histological reconstruction of tetrad tracks. For the rate maps, blue represents no firing and red represents peak firing, which is labeled in red to the right of the field count plots. In the field count plots, black represents the regions that were included in each spatially selective subfield (see Experimental Procedures). The number of fields is labeled in black to the right of the field count plot. Rate maps and field count plots are for the day that the last open field session was recorded. Brain sections indicate the location of the tetrad track after the last day of experiments. Scale bars equal 60  $\mu\text{m}$ . All of these examples were recorded on tetrodes that were not adjusted between the time of recordings and the perfusion of the animal. Figure 2.8 shows the best projections used to isolate the clusters recorded on these tetrodes.

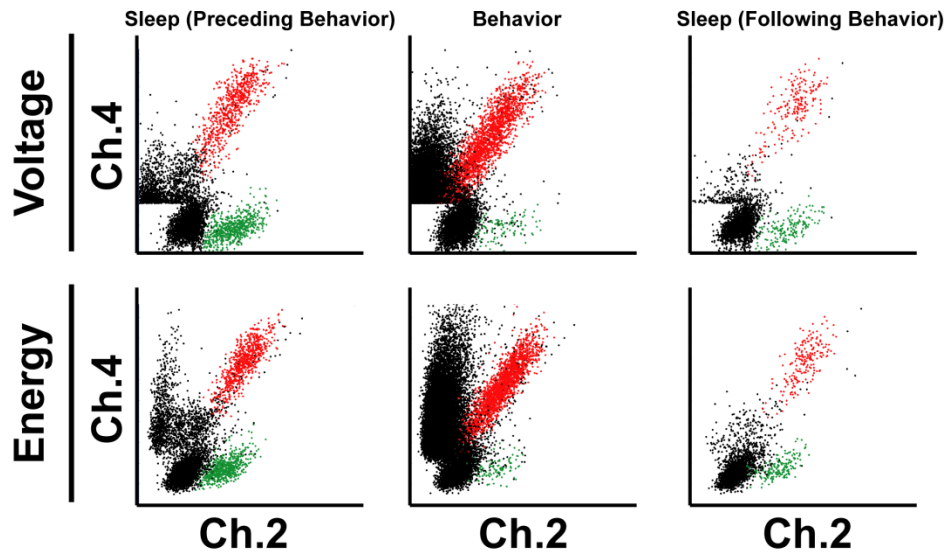
### 153-04 Sc7 Cell 1 (red) & Cell 2 (green)



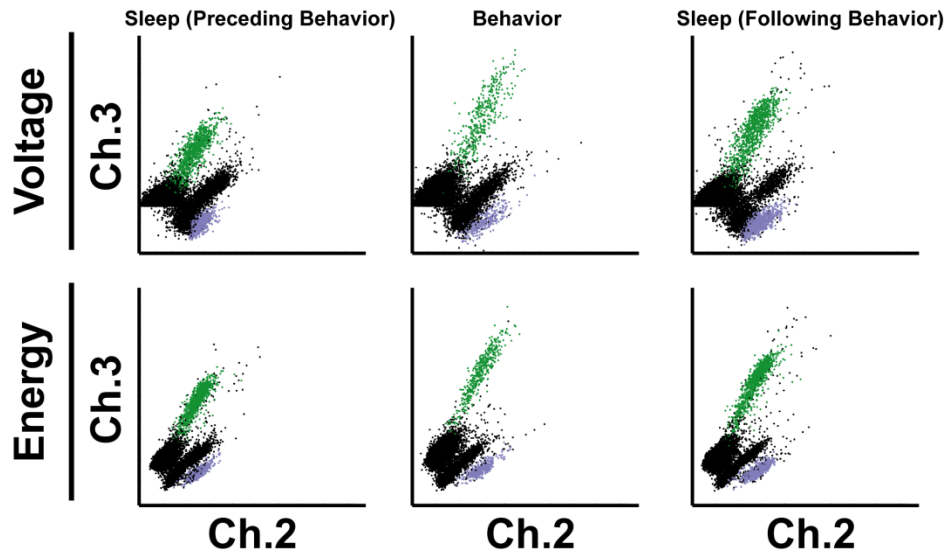
### 153-04 Sc8 Cell 1



### 153-04 Sc17 Cell 1 (red) Cell 2 (green)



### 197-14 Sc5 Cell 2 (green) Cell 3 (blue)



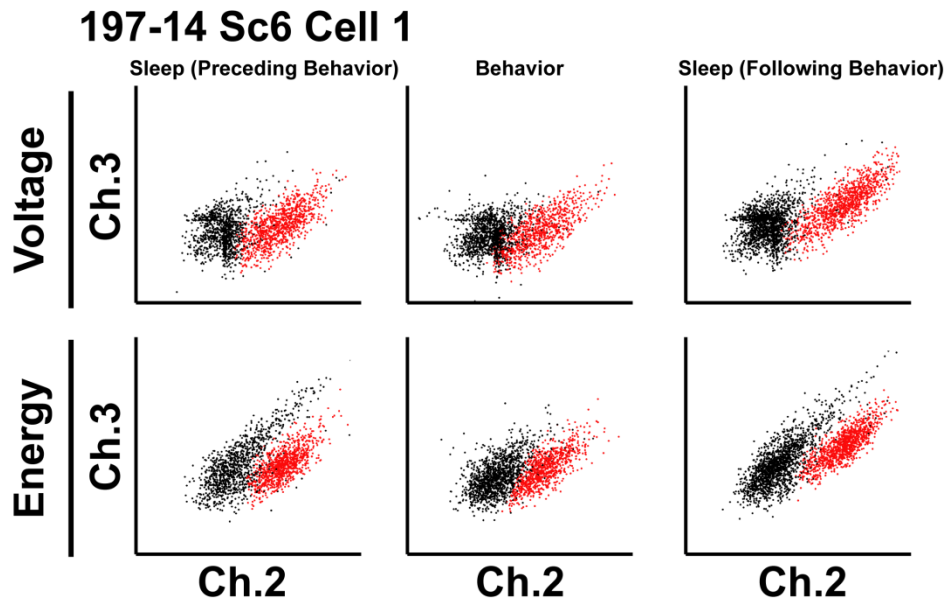


**Figure 2.8. Unit Isolation for Cells Localized to Polymorphic Cell Layer.** Best tetrode projections that were used to isolate the clusters localized to the polymorphic cell layer. Scatter plots show the peak voltage (top) and corresponding energy (bottom). All plots show data recorded during preceding sleep, open-field foraging, and final sleep sessions. Note, there is a similar pattern of firing (dense clusters) in all three sessions. During experiments 1-4 for rat 153, there was an additional hour of sleep recorded prior to the second and third sleep sessions that is not shown. The colored points represent the well-isolated cluster(s) of interest. Black points show all spikes recorded on the tetrode.

showed 2-3 peaks in the color-coded rate map. The non-spatially selective cells showed a variety of firing patterns (data not shown). One cell was silent, two fired diffusely with no clear spatial selectivity (mean rates 0.07 and 5.98 Hz), and one appeared to fire in multiple fields, but it did not reach criteria to be considered a spatially selective cell. In contrast to the recording sites localized to the polymorphic layer, of the 26 tetrodes localized to the granule layer or to the transition between the granule and polymorphic layers, only 1 tetrode recorded a cell with multiple place fields, 5 tetrodes recorded cells with single fields, 13 tetrodes did not record any cells that were active during behavior (although cells were active on these tetrodes during sleep), and 7 tetrodes did not record any cells in either sleep or behavior (perhaps due to poor electrode quality).

After observing cells in the polymorphic layer with multi-punctate firing and since we could not unambiguously identify the recording sites because the histology was performed two weeks after the initial recordings, we decided to partition the tetrode recordings into two groups; those that only recorded a cell with a single field (Figure 2.9.A) and ones that recorded at least one cell with multiple fields (Figure 2.9.B). For all analyses reported in the results, we included recordings from a tetrode with active cells only on the day that the most sleep clusters were detected to exclude repeated samples (see methods for details). There were 25 spatially active cells and the majority of these cells fired in multiple locations (pentuple or more fields: 5; quadruple fields: 2; triple fields: 3; double fields: 3; single fields: 12). The ratemaps and field counts for all spatial active cells are shown in the Figure 2.10. Of the tetrodes recording a cell with multiple fields, only 1 of the spatially active cells detected had a single field and this was included in the group recording multiple cells. When comparing the distribution of sleep clusters, the tetrodes detecting cells with single fields had significantly more sleep clusters than the tetrodes detecting at least one cell with multiple fields (Figure 2.11; Mann-Whitney *U*-test;  $p < 0.05$ ). To quantify the difference in activity between sleep and behavior, we calculated a sparseness index (number of putative excitatory cells active during behavior divided by

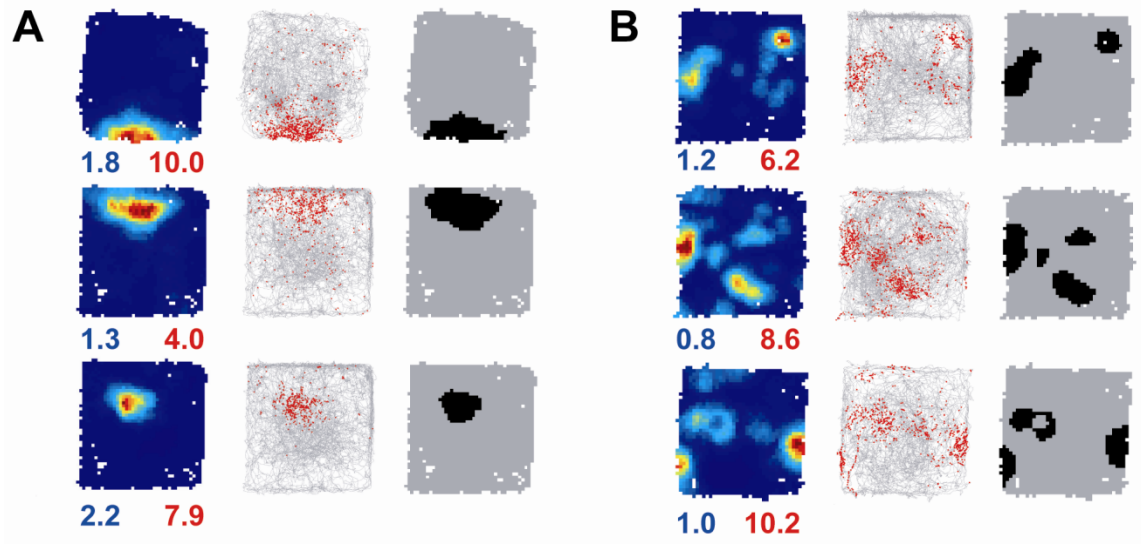


**Figure 2.9. Different Spatial Firing Patterns for Cells Recorded in DG.** Examples of cells with single (A) and multiple (B) fields. Rate maps, plots showing spikes (red) from the cell superimposed on the rat's trajectory (gray), and plots showing all fields are shown in the first, second, and third columns, respectively. For the rate maps, the peak firing rates (Hz; red) and spatial information scores (bits/spike; blue) were labeled below the lower right and left corners, respectively.

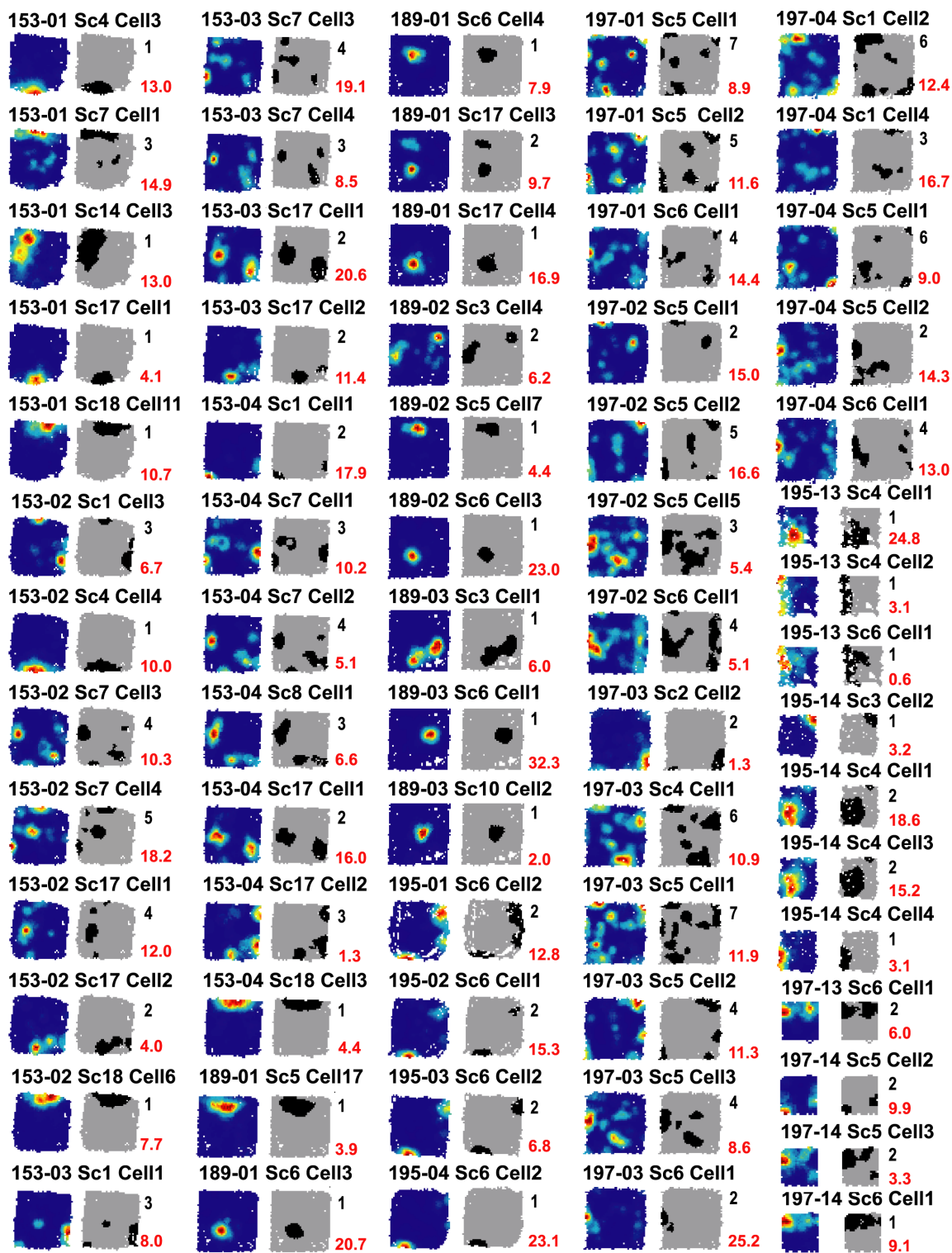


**Figure 2.10. Ratemaps for All Active Cells Recorded In DG.** Rate maps and place-field plots for all active cells recorded while animals foraged. Data from animals that actively foraged and had cells that were considered active (see Experimental Procedures) were included. In the rate maps, red represents peak firing and blue represents no firing. To the right of the field count plots, the peak firing rate (Hz) and number of fields are labeled in red and black, respectively. Cells were considered active when the cell had a statistically significantly ( $p \leq 0.01$ ) spatial information score that was greater than 0.5 bits/spike and fired more than 75 spikes. Cells were grouped by the day (i.e., experiment number) of each recording for individual rats (e.g., 153-01 Sc4 Cell3 refers to rat 153, day 01 of recording, tetrode 4, cell number 3). Note that the spatial firing pattern for some cells recorded on the same tetrode of a rat was similar across days, suggesting the recordings were stable and the same cell was recorded on multiple days; consequently, repeated samples were excluded by looking at data from the day that had the most sleep clusters recorded or from the first day that active cells were recorded on a given tetrode. For rat195-14, cells 1 and 3 have similar fields, but were clearly non-overlapping clusters in the tetrode projections. Both cells have waveforms with two humps suggesting that these two simultaneously recorded cells might be coupled by gap junctions.

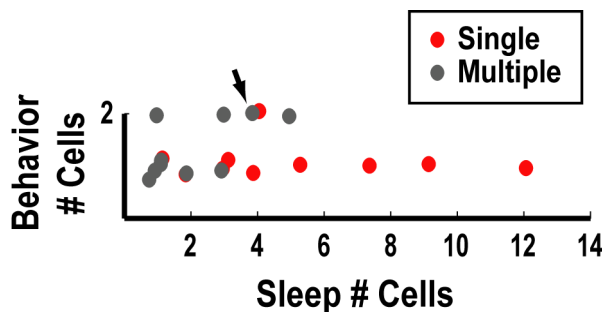


**Figure 2.11. Significantly More Sleep Clusters Detected on Tetrodes Recording Cells with Single Fields than Multiple Fields.** Single Fields Distribution of Sleep vs. Active Cell Recorded Scatter plot showing the number of active cells during behavior vs. the number of cells detected during sleep. Each point represents data from one tetrode (red represents tetrodes detecting cells with only single fields, whereas gray represents tetrodes detecting a cell with multiple fields). The arrow indicates the one ambiguous tetrode that detected a cell with multiple fields and a cell with a single field. Tetrodes recording cells with only single fields had significantly more sleep clusters than tetrodes recording at least one cell with multiple fields ( $p < 0.05$ ). To aid in visualization of overlapping points, jitter was added to the points.



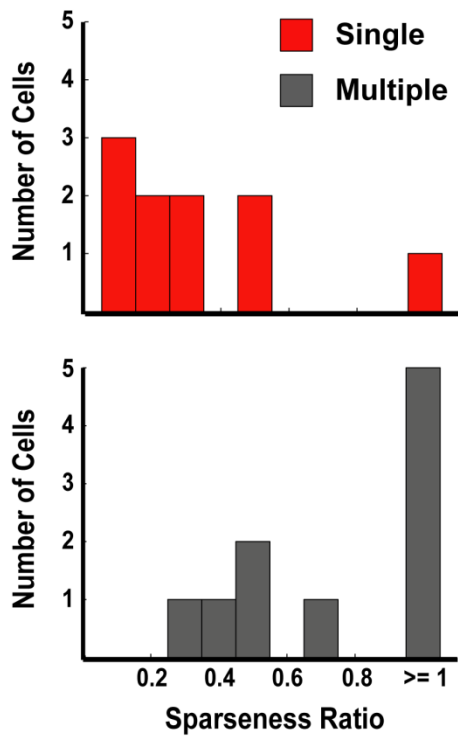


**Figure 2.12. Sparseness Ratios.** Histograms show sparseness ratios (number of active cells / number of sleep clusters) for tetrodes recording cells with only single fields (top panel; red bars) and tetrodes recording at least one cell with multiple fields (bottom panel; gray bars).

number of putative excitatory cells active during sleep) for each tetrode. Figure 2.12 shows that tetrodes recording a cell with only a single field had a significantly lower sparseness index than tetrodes recording cells with multiple fields (single median 0.29, IQR<sub>25to75</sub> 0.14-0.5; multiple median 0.83, IQR<sub>25to75</sub> 0.5-1; Mann-Whitney *U*-test;  $p < 0.01$ ). To remove any spikes occurring when the rats were stationary, which might contaminate the spatial signal, the data were velocity filtered. Similar to the non-velocity filtered data, tetrodes recording a cell with only a single field had a significantly lower sparseness index than tetrodes recording cells with multiple fields (Figure 2.13). When the one tetrode that simultaneously detected cells with single and multiple fields was excluded from the analysis, the results again showed that cells with single fields fired more sparsely and had more sleep clusters than cells with multiple fields (data not shown). The lower percentage of active cells on the tetrodes detecting cells with single fields resembles the previously reported sparse firing of granule cells (Barnes, 1990;Chawla et al., 2005), which contrast to the higher sparseness values seen on tetrodes recording cells with multiple fields.

The firing characteristics of active cells were further classified by comparing the size of each field. Fields were determined by the previously mentioned method and then the pixels were converted to cm<sup>2</sup>. The area of each field for the two groups were significantly different (Figure 2.14; single median 42.1 cm<sup>2</sup>, IQR<sub>25to75</sub> 29.0-72.8; multiple median 13.3 cm<sup>2</sup>, IQR<sub>25to75</sub> 7.1-21.0; Mann-Whitney *U*-test;  $p < 0.0001$ ). However, there was no significant difference between the two groups when looking at the total area of the environment that each cell was active (Figure 2.15; single median 42.1 cm<sup>2</sup>, IQR<sub>25to75</sub> 29.0-72.8; multiple median 53.2 cm<sup>2</sup>, IQR<sub>25to75</sub> 36.7-69.3; Mann-Whitney *U*-test;  $p = 0.5$ ). The mean in-field firing rates were not different between either group (Figure 2.16; single median 2.94 Hz, IQR<sub>25to75</sub> 1.83-6.06; multiple median 3.77 Hz, IQR<sub>25to75</sub> 3.01-4.72; Mann-Whitney *U*-test;  $p = 0.68$ ). Figure 2.17 shows that there was no difference in peak firing rates (single median 6.0 Hz, IQR<sub>25to75</sub> 3.45-13.0; multiple median 11.2 Hz, IQR<sub>25to75</sub> 8.87-15.3; Mann-Whitney *U*-test;  $p =$

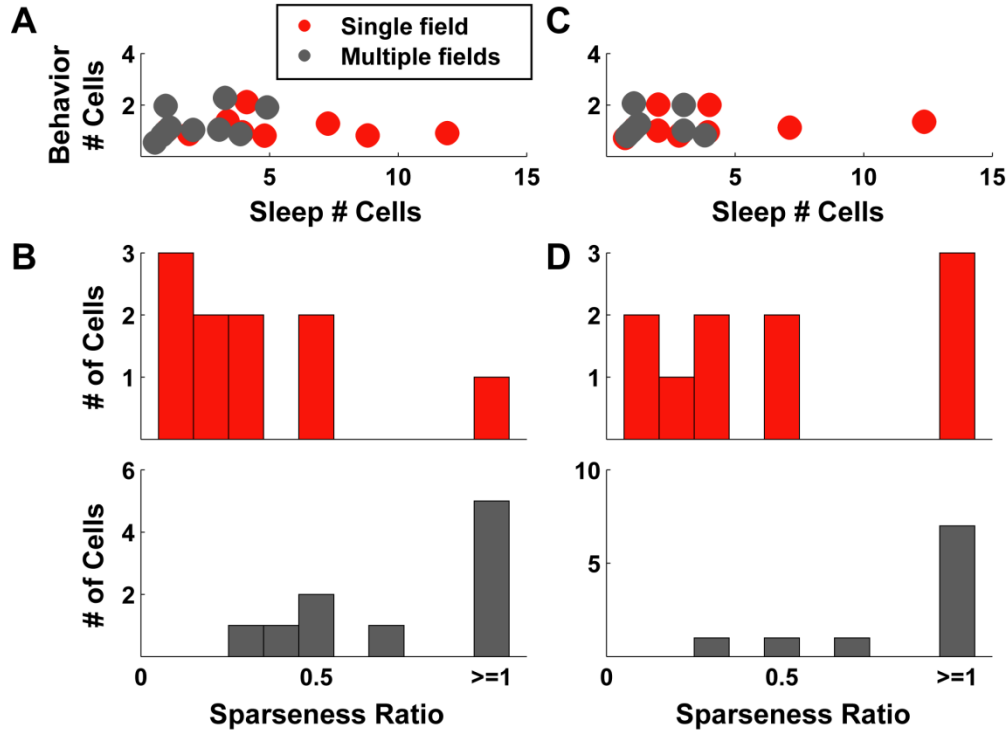


**Figure 2.13. Analyses with Velocity Filtered Data.** Rate maps were speed filtered to exclude firing that occurred when rats were stationary (speed < 2 cm/s). (A,C) Scatter plots showing the number of active cells during behavior vs. the number of cells detected during the sleep session with the most clusters for each tetrode (A) or the first day that an active cell during behavior was detected on a tetrode (C). Each point represents data from one tetrode (tetrodes recording cells with only single fields are red and tetrodes recording a cell with multiple fields are gray). For both conditions, tetrodes recording cells with only single fields had significantly more sleep clusters than tetrodes recording at least one cell with multiple fields (Mann-Whitney  $U$ -test,  $p < 0.05$ ). To aid in visualization of overlapping points, jitter was added to the points. (B,D) Histograms show sparseness ratios (number of active cells during behavior / number of sleep clusters) for tetrodes recording cells with only single fields (top panel; red bars) and tetrodes recording at least one cell with multiple fields (bottom panel; gray bars) for the sleep session with the most clusters (B) or the first day that an active cell during behavior was detected (D). For both conditions, tetrodes recording cells with only single fields had significantly lower sparseness ratios than tetrodes recording at least one cell with multiple fields (B: Mann-Whitney  $U$ -test,  $p < 0.01$ ; D: Mann-Whitney  $U$ -test,  $p < 0.05$ ).

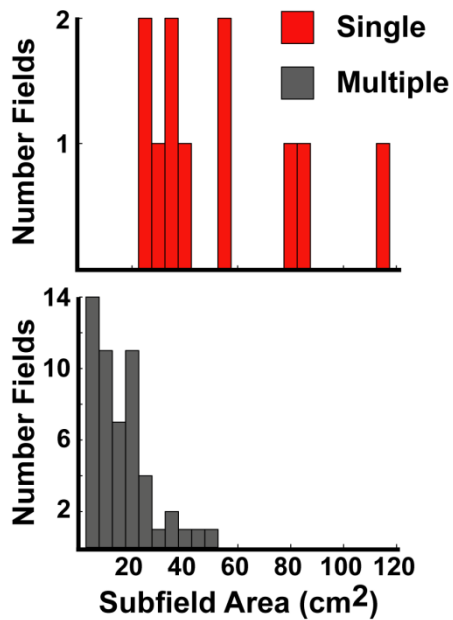


**Figure 2.14. Subfield Size for DG Cells.** Histograms show the area of each individual field of cells with only single fields recorded on a tetrode (top panel; red bars) and cells from tetrodes that recorded at least one unit with multiple fields (bottom panel; gray bars).

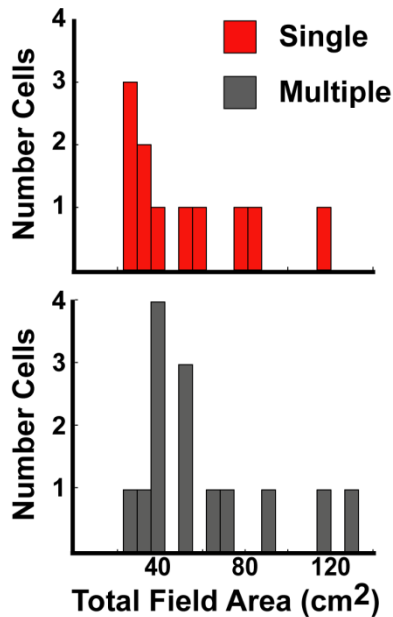


**Figure 2.15. Combined Field Size for DG Cells.** Histograms show total area (area of all fields summed) for each cell in the two groups. Top panel (red bars) show cells with single fields and bottom panel (gray bars) show cells multiple fields.

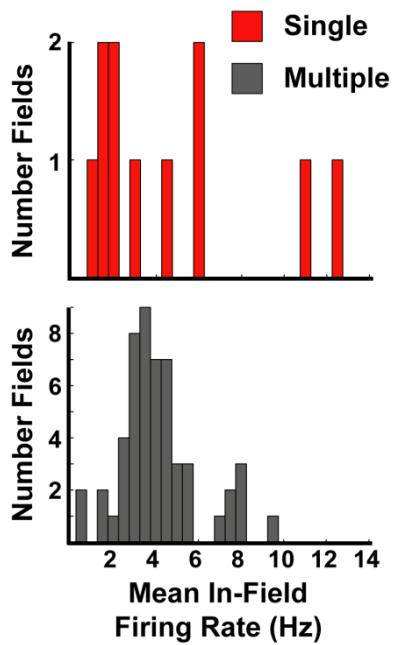


**Figure 2.16. In-Field Firing Rates for DG Cells.** Histograms show mean in-field firing rates for the two groups. Top panel (red bars) show cells with single fields and bottom panel (grey bars) show cells multiple fields.

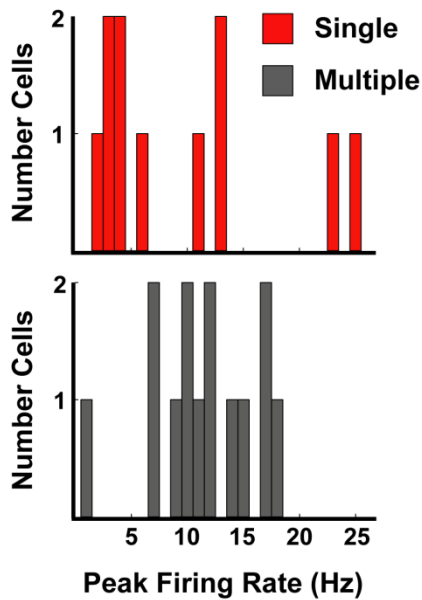


**Figure 2.17. Peak Firing Rate for DG Cells.** Histograms show the peak firing rate for each cell in the two groups. Top panel (red bars) show cells with single fields and bottom panel (grey bars) show cells multiple fields.

0.3). The spatial information scores of cells recorded on single field tetrodes was higher than those of cells recorded on tetrodes detecting units with multiple fields (single median 1.50 bits/spike,  $IQR_{25to75}$  0.95-1.93; multiple median 1.12 bits/spike,  $IQR_{25to75}$  0.74-1.40; Mann-Whitney  $U$ -test;  $p = 0.05$ ); however, this was only a trend (Figure 2.18). No differences were obtained when we analyzed data from only the first day that active cells were recorded on a tetrode (see Table 2.1).

Shown in slice work, Scharfman (1992) reported that mossy cells fire in bursts when injecting a pulse of depolarizing current, whereas granule cells do not show this physiological profile. Therefore, we decided to examine the “burstiness” of active cells on tetrodes recording units with single fields or multiple fields based on the criterion used in Harris et al. (2001). The burst index was defined as the number of times two consecutive spikes occurred within 6 ms during a cell’s spike train divided by the total number of inter spike intervals. Figure 2.19 shows that cells on tetrodes recording at least one unit with multiple fields were significantly more bursty than cells on tetrodes recording units with only single fields (single median 0.12,  $IQR_{25to75}$  0.05-0.13; multiple median 0.15,  $IQR_{25to75}$  0.12-0.16; Mann-Whitney  $U$ -test;  $p < 0.05$ ). Harris et al. (Harris et al., 2001) extended the duration of the inter spike intervals up 15 ms; therefore, we looked at an extended range of times (i.e., 9, 12, and 15 ms) and only detected trends for 9 and 12 ms and no difference for 15 ms time span, which was possibly do to the small sample size (see Table 2.1). No difference was detected when we used the data from only the first day that active cells were recorded to exclude repeated samples compared to the day with the most sleep clusters.

Additional differences were observed between cells recorded on tetrodes with units that had single fields and multiple fields, when looking at the firing properties of cells recorded during sleep. The burst index was calculated for all cells recorded on both groups of tetrodes (Figure 2.20). The 6 ms burst index for cells on tetrodes with single fields was substantially lower than cells on tetrodes

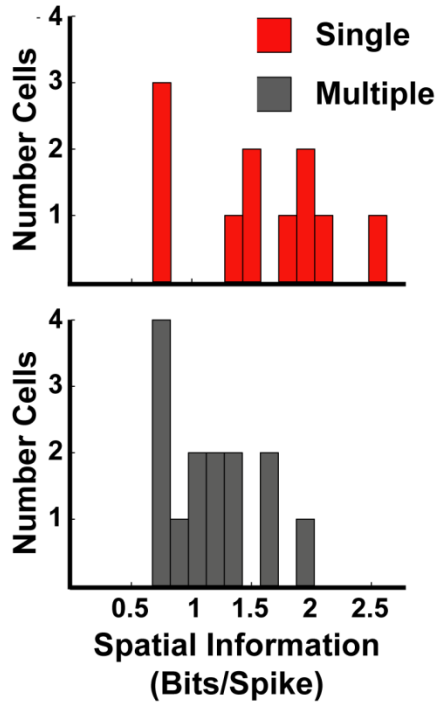


**Figure 2.18. Spatial Information for DG Cells.** Histograms show spatial information scores for each cell in the two groups. Top panel (red bars) show cells with single fields and bottom panel (grey bars) show cells with multiple fields.

Table 2.1

## Statistics for additional analyses with data not shown.

### HIGH - day with most recorded cells

#### Behavior

Comparison	P Value	Single Median	Single IQR 25	Single IQR 75	Multiple Median	Multiple IQR 25	Multiple IQR 75
Burst 9 Cell	0.052	0.17	0.10	0.21	0.23	0.20	0.24
Burst 12 Cell	0.067	0.22	0.14	0.28	0.28	0.24	0.31
Burst 15 Cell	0.13	0.25	0.18	0.33	0.33	0.28	0.36

#### Sleep

Comparison	P Value	Single Median	Single IQR 25	Single IQR 75	Multiple Median	Multiple IQR 25	Multiple IQR 75
Burst 9 ms	$8.8 \times 10^{-4}$	0.11	0.06	0.15	0.20	0.17	0.27
Burst 12 ms	$1.7 \times 10^{-3}$	0.13	0.07	0.22	0.24	0.20	0.32
Burst 15 ms	$1.6 \times 10^{-3}$	0.14	0.09	0.25	0.26	0.23	0.36
Channel Slope	0.021	0.20	0.17	0.23	0.17	0.13	0.20

### Day1 - first day that cell was recorded

#### Behavior

Comparison	P Value	Single Median	Single IQR 25	Single IQR 75	Multiple Median	Multiple IQR 25	Multiple IQR 75
Area of Each Field	$2.4 \times 10^{-5}$	42.07	31.11	66.57	15.11	8.00	22.00
Mean Infield Firing Rate	0.91	3.62	1.79	6.06	3.74	3.00	4.58
Peak Infield Firing Rate	0.67	7.90	3.40	12.99	6.17	4.37	9.01
Burst 6 Cell	0.12	0.10	0.05	0.13	0.15	0.12	0.17
Burst 9 Cell	0.075	0.15	0.10	0.20	0.23	0.18	0.26
Burst 12 Cell	0.075	0.21	0.14	0.27	0.28	0.23	0.31
Burst 15 Cell	0.095	0.25	0.18	0.33	0.33	0.27	0.36
Info Cell	0.13	1.50	0.93	1.88	1.13	0.74	1.60
Peak Cell	0.46	7.90	3.40	12.99	11.22	6.67	14.37
Area Cell	0.22	42.07	31.11	66.57	53.78	37.33	74.67
Sparseness Ratio	0.012	0.33	0.22	0.63	1.00	0.75	1.00

#### Sleep

Comparison	P Value	Single Median	Single IQR 25	Single IQR 75	Multiple Median	Multiple IQR 25	Multiple IQR 75
Duration(msec)	0.046	0.22	0.22	0.28	0.28	0.25	0.31
MFR (Hz)	$7.3 \times 10^{-4}$	0.07	0.02	0.21	0.43	0.17	0.73
Voltage	0.48	0.35	0.24	0.44	0.29	0.22	0.37
Burst 6 ms	$1.1 \times 10^{-6}$	0.04	0.02	0.09	0.16	0.13	0.21
Burst 9 ms	$3.5 \times 10^{-7}$	0.08	0.05	0.14	0.22	0.19	0.28
Burst 12 ms	$2.6 \times 10^{-7}$	0.11	0.07	0.18	0.26	0.23	0.32
Burst 15 ms	$2.3 \times 10^{-7}$	0.13	0.09	0.21	0.31	0.26	0.37
Normalized Amp Dif	$1.7 \times 10^{-3}$	0.48	0.35	0.60	0.32	0.22	0.37
Channel Slope	$9.4 \times 10^{-4}$	0.21	0.18	0.24	0.17	0.11	0.18



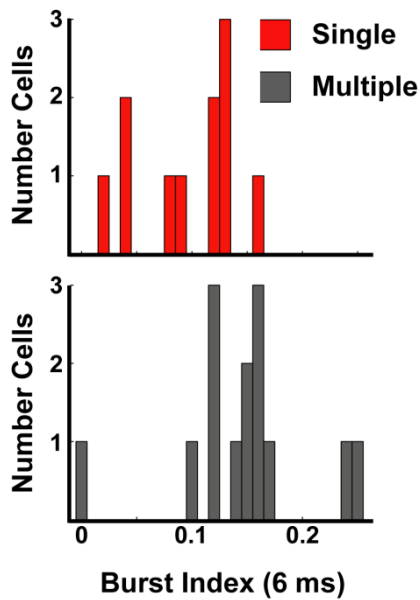


**Figure 2.19. Burst Index for DG Cells Recorded During Behavior.**

Histograms show the burst index for each cell in the two groups. The burst index indicates the percentage of spikes in a cell's spike train that occurred within 6 ms of each other. Top panel (red bars) show cells with single fields and bottom panel (grey bars) show cells multiple fields.

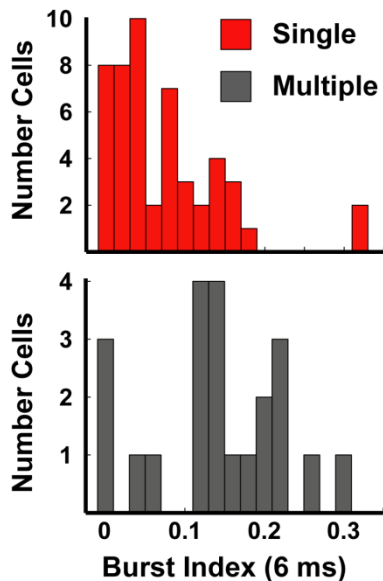


**Figure 2.20. Burst Index of DG Cells Recorded During Sleep.** Histograms show the burst index for each cell in the two groups. Red (top) and grey (bottom) plots represent data from tetrodes detecting cells with single or multiple fields, respectively.

with multiple fields (single median 0.04,  $IQR_{25to75}$  0.02-0.11; multiple median 0.14,  $IQR_{25to75}$  0.11-0.20; Mann-Whitney  $U$ -test;  $p < 0.001$ ). There were also significant differences between the two groups using durations of 9, 12, and 15 ms (see Table 2.1). The median firing rate during sleep for the cells on tetrodes recording units with single fields was 0.05 Hz with an  $IQR_{25to75}$  of 0.02-0.19, in contrast to 0.36 Hz with an  $IQR_{25to75}$  of 0.08-0.61 for cells detected on tetrodes with units that had multiple fields (Figure 2.21; Mann-Whitney  $U$ -test;  $p < 0.01$ ). This suggests that cells recorded on single field tetrodes fire more sparsely than cells recorded on multiple field tetrodes.

Two anatomical differences between mossy and granule cells are size of the cell bodies and the spacing between cells. Mossy cells have large somas that are not densely packed with other cells of the polymorphic cell layer. In contrast, granule cells have smaller cell bodies that are densely packed with other granule cells. In addition to detecting more granule cells, the densely packed granule cells might be closer to the tetrode causing a difference in the amplitudes that the spikes are simultaneously recorded on the four channels of the tetrode compared to the less densely packed cells of the hilus. Therefore, we compared the difference between channels on the tetrode with the largest and smallest amplitudes of the two groups. The normalized difference in amplitude index was calculated by taking the difference between the channels with the largest and smallest amplitudes and then dividing by the sum. Values closer to zero represent similarly sized amplitudes, whereas values closer to one represent larger differences. There was a considerable difference between the largest and smallest amplitudes on the cells recorded on tetrodes classified as single fields and multiple fields (Figure 2.22; single median 0.45,  $IQR_{25to75}$  0.31-0.58; multiple median 0.34,  $IQR_{25to75}$  0.24-0.41; Mann-Whitney  $U$ -test;  $p < 0.05$ ). When sorting all normalized channels of the tetrode (dividing each by the amplitude of the largest channel) in ascending order and comparing the slopes, there was also a significant difference (data not shown). The cells recorded on tetrodes classified as single fields had a larger slope than cells recorded on tetrodes with multiple fields (single median 0.20,  $IQR_{25to75}$  0.17-0.23; multiple

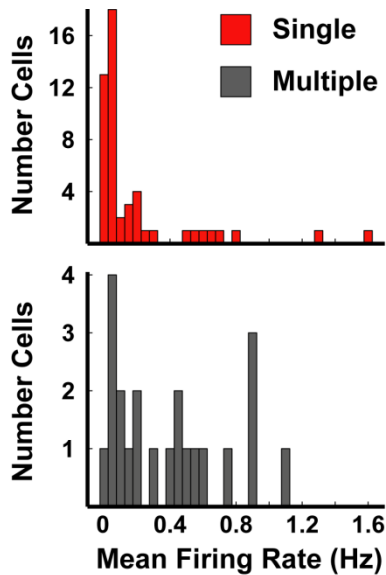


**Figure 2.21. Mean Firing Rates for DG Cells Recorded During Sleep.** Histograms show the mean firing rate for each cell in the two groups. Red (top) and grey (bottom) plots represent data from tetrodes detecting cells with single or multiple fields, respectively.

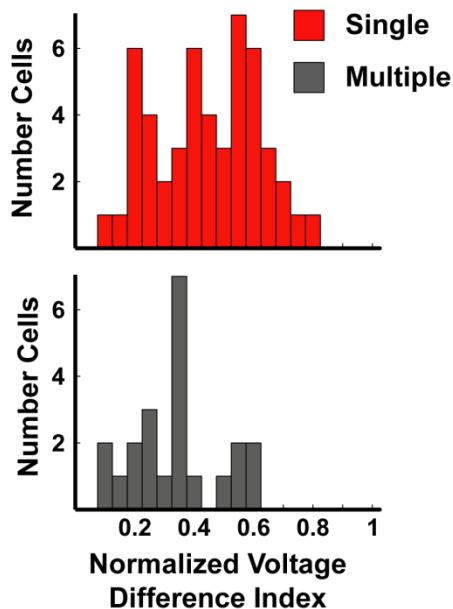


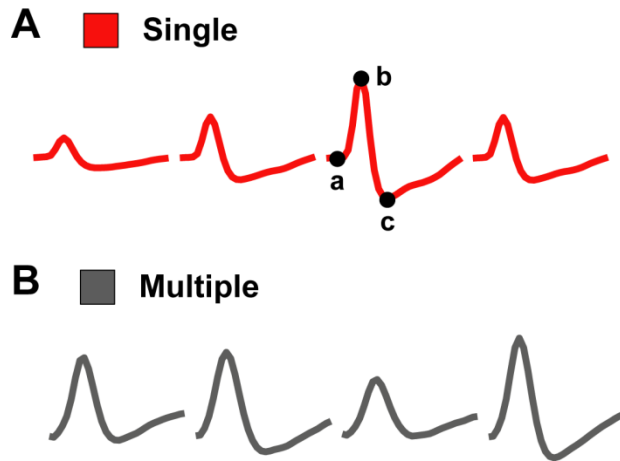
**Figure 2.22. Normalized Voltage Index for DG Cells Recorded During Sleep.** Histograms show normalized voltage difference between the channels with the largest and smallest amplitudes on the tetrode for each cell in the two groups. The index was calculated by determining the difference between the amplitudes of the two channels and dividing by the sum of the two amplitudes. Red (top) and grey (bottom) plots represent data from tetrodes detecting cells with single or multiple fields, respectively.

median 0.17,  $IQR_{25to75}$  0.13-0.20; Mann-Whitney  $U$ -test;  $p < 0.05$ ), which corroborated the difference seen with the normalized difference in amplitude index. This emphasizes another distinction between the two groups of recorded cells.

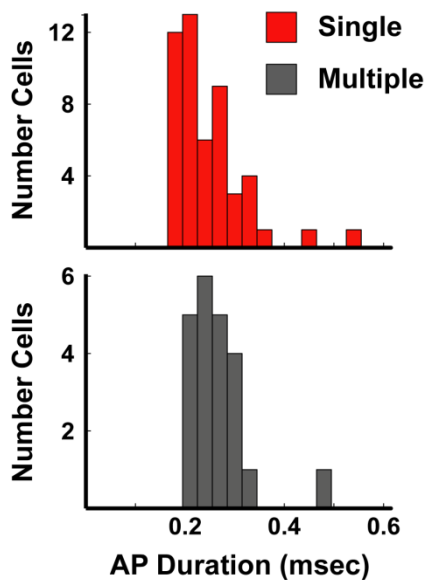
In brain slices, Scharfman (1992) reported that the duration of the action potential was longer in mossy cells than granule cells, while Henze and Buzsaki (2007) also reported that the action potential duration for mossy cells was long and broad in anesthetized rats. Therefore, we examined the features of the extracellular waveform recorded during sleep for both groups (Figure 2.23) in an attempt to further dissociate the cells recorded on a tetrode classified as either single or multiple fields. The time between the peak of the action potential and trough of the after hyperpolarization was measured on the mean waveform with the largest amplitude for each cell (see points B and C on the red waveform in Figure 2.20 for an example). Figure 2.24 only shows a trend for cells on tetrodes classified as single fields to have action potential durations that are shorter than seen for cells in the second group (single median 0.23  $\mu$ sec,  $IQR_{25to75}$  0.22-0.28; multiple median 0.27  $\mu$ sec,  $IQR_{25to75}$  0.25-0.31; Mann-Whitney  $U$ -test;  $p = 0.07$ ). In addition, we also compared the maximum voltage (see points A and B on the red waveform in Figure 2.20 for an example) of the mean waveform between the two groups. There was a trend for the voltages of cells recorded on tetrodes detecting cells with single fields to be larger than the second group of cells (Figure 2.25; single median 0.38 mV,  $IQR_{25to75}$  0.29-0.48; multiple median 0.28 mV,  $IQR_{25to75}$  0.22-0.41; Mann-Whitney  $U$ -test;  $p = 0.07$ ).

### **2.3 Conclusion**

Previous reports describing the spatial firing pattern of excitatory cells in the dentate gyrus are rare, which is in part due to the challenges of recording a sparse firing population of cells located in granule cell layer. To further complicate the situation, clearly interpreting the results is hindered because the



**Figure 2.23. Example Waveforms Recorded During Sleep.** Examples of the mean waveforms recorded during sleep on four channels of a tetrode. Red and grey waveforms were recorded on tetrodes detecting cells with single (A) or multiple (B) fields, respectively. The points labeled a, b, and c on the waveform on the third channel in (A) represent the locations used to determine voltage (height of a to b) and duration (time between b and c) of the action potential.



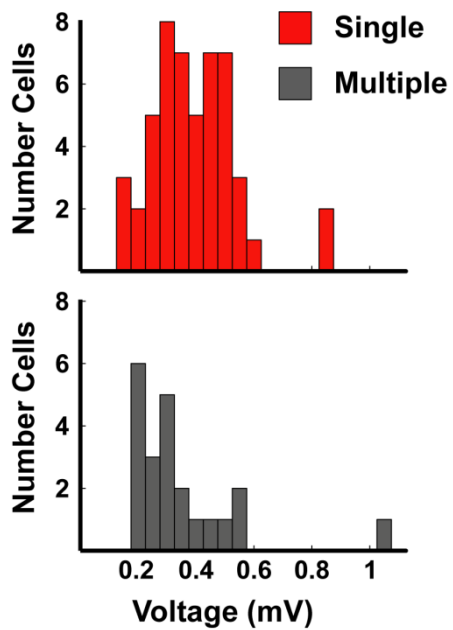


**Figure 2.25. Voltage of Action Potentials for DG Cells Recorded During Sleep.** Histograms show the maximum voltage for each cell in the two groups. Red (top) and grey (bottom) plots represent data from tetrodes detecting cells with single or multiple fields, respectively.

dentate gyrus is the only region of the hippocampal formation (i.e., CA1, CA2, CA3, and dentate) that has multiple types of excitatory cells (granule and mossy cells). The few studies reporting the spatial firing pattern of dentate gyrus cells have shown that putative granule cells fire in multiple locations, which are distributed irregularly throughout the environment, but occasionally cells recorded in the dentate fire in a single location (Jung and McNaughton, 1993; Gothard et al., 2001; Leutgeb et al., 2007), but no data has been reported describing the spatial firing properties of hilar cells. In the present study, we provided the first evidence demonstrating that cells localized to the polymorphic cell layer of the dentate gyrus fire in multiple location that are distributed irregularly throughout an enclosure, which was strikingly similar to the previously reported granule cell spatial firing patterns. Therefore, the active cells with spatial firing were partitioned into two groups: (1) cells recorded on tetrodes detecting units with only single fields and (2) cells recorded on tetrodes detecting a least one unit with multiple fields. These results provide strong evidence revealing two distinct populations of cells in the dentate gyrus that both convey spatial information. The first group is typically recorded on tetrodes detecting many additional cells during sleep that are silent during behavior (except for a small minority with single fields); thus, they fire more sparsely than the second group of cells recorded on tetrodes detecting fewer clusters with the majority firing in both sleep and multiple locations in the environment. Another set of parameters have further differentiated the two groups. Group one had a lower mean firing rate during sleep and appreciably less pronounced bursting during both behavior and sleep. Consequently, we believe that examining these properties has allowed the first reported characterization of two different cell types in the dentate gyrus (i.e. granule and hilar cells) in freely moving animals. Furthermore, the electrophysiological differences between the two groups resemble the differences reported between granule and mossy cells in both slice and anesthetized animals leading us to speculate that these are granule and mossy cells. However, we cannot exclude the possibility that cells firing in multiple

locations throughout an enclosure are one of the many types of inhibitory cells, as opposed to mossy cells. For a detailed discussion see Chapter 4.

## **2.4 Experimental Procedure**

### **2.4a Subjects and Surgery**

Seven male, Long-Evans rats, between 5 and 6 months old, were purchased from Charles River Laboratories and individually housed on a 12-hour light/dark cycle with *ad libitum* access to water. Under aseptic conditions, rats were implanted with a custom designed recording drive containing 20 independently movable tetrodes. All surgeries and animal procedures complied with National Institutes of Health guidelines and were approved by the Institutional Animal Care and Use Committees at John Hopkins University and the University of Texas Health Science Center at Houston. In all animals, 5 tetrodes targeted the CA3 region and 13 tetrodes targeted the DG. To optimize the proportion of tetrodes entering the DG and CA3, recordings were performed during surgery to identify the location of the lateral edge of CA3, which served as a landmark for the medial/lateral placement of the drives (range 3.2 to 4.9 mm lateral to bregma). For the anterior/posterior placement of the drive, the most lateral tetrode was placed 3.2 to 4.4 mm posterior to bregma.

### **2.4b Training and Recording**

Initially, chocolate sprinkles were dispersed throughout a cardboard box (63.5 L x 66 W x 59.7 H cm) and rats gradually learned to forage for the reward. The reward was eventually reduced to a few pieces of chocolate periodically tossed into the chamber. After the rats acclimated several days to foraging and the environment, the surroundings were switched to a larger box (135 L x 135 W x 30 H cm) with white wooden walls located in a second room that also housed the recording equipment. Training continued in this environment until units were detected and experiments were initiated. Briefly, a series of experiments were



conducted over 9 to 14 days which involved rats foraging in an open environment or circumnavigating a track. Prior to and following the experiment, extensive periods of sleep were recorded (30 min-1hr). Results from the sleep data and any session that rats actively foraged in an open environment were examined and shown in this report, whereas the behavior recorded as rats ran on a circular track was excluded.

#### **2.4c Electrophysiological Recordings**

A Cheetah Data Acquisition System (Neuralynx, Tucson, AZ) was used to obtain electrophysiological recordings. This system simultaneously acquired up to 72 channels (18 tetrodes) of single-unit data and continuously recorded local EEG activity from 21 channels. Neural signals were recorded with fine microwire electrodes (nichrome or platinum-iridium) and preamplified. The signals, which were conducted through fine-wire recording cables and a motorized 80-channel commutator, were amplified (1 – 5 k) and filtered between 600 Hz and 6 KHz to optimize recording neural spikes or 1 Hz and 300 Hz for recording local field potential. Units and local field potential were sampled at 32 kHz and 1 kHz, respectively. The headstage contained a circular array of red (front of head) and blue (back of head) LEDs and a linear, caudally-projecting 13 cm extension that contained green LEDs. These were recorded at 30 Hz with an overhead camera to track the rat's momentary position. Neural and positional data were synchronized in time and stored on Dell computers for later offline analyses.

Tetrode advancement occurred over approximately three weeks, in which each tetrode was independently lowered in small increments on a daily basis until the tetrode tip was assumed to be located in proper hippocampal subregion. The advancement of tetrodes was assessed by examining the changing patterns in EEG activity in conjunction with units appearing and disappearing. After entering the CA1 layer, denoted by EEG ripples and a second series of detectable cells that were located approximately 400  $\mu$ m deeper than cortical units (separated by the corpus callosum and alveus), tetrodes were advanced at a similar rate for an additional 300  $\mu$ m until gamma activity and dentate spikes in

the EEG were detected (Bragin et al., 1995b; Bragin et al., 1995a). This denoted that tetrodes were approaching the dentate granule layer and the tetrodes were lowered approximately 20  $\mu\text{m}$  per day until units were observed. Once the tetrodes were putatively located in the proper positions, the advancement of most tetrodes was permanently stopped. However, if all units were lost on a tetrode, it was slightly adjusted and allowed to stabilize for 12 hrs before the start of the next experiment.

#### **2.4d Unit Isolation**

Single-units were isolated offline, using an in-house written program compatible for PCs, based on multiple waveform characteristics (i.e., relative amplitude, area under the waveform, and valley depth) detected concurrently on four slightly different locations. Data recorded during active behavior were isolated from tetrodes with an *a priori* knowledge of recording location; however, sleep data were isolated using a blind method, but some features in the data made a few of the sleep recordings recognizable. The isolation quality of each cell was rated 1 (very good) to 5 (poor) depending on the cluster's separation from background noise and other clusters. All cells rated as poor or marginal isolation were excluded from all analyses. Additionally, cells that fired less than 75 spikes and had a statistically insignificant ( $p > 0.01$ ; Monte-Carlo statistics) spatial information score that was less than  $< 0.5$  bits/spike were considered inactive. The spatial information score was calculated using the same algorithm used in Skaggs et al., (Skaggs et al., 1996).

#### **2.5e Data Analysis**

The number of times a cell fired and the total time the rat spent in each pixel of a 64 x 48 grid was calculated and stored in two separate matrices. The firing matrix was divided by the time matrix to create a ratemap for the cell then smoothed using an adaptive binning algorithm as described in Skaggs et al., 1996. Ratemaps were used to calculate the number of fields for each cell. All pixels in the ratemap with a mean firing rate that exceeded 20% of the cell's peak

firing rate and contiguous with the edges of a minimum of 10 pixels were considered fields. The area of each field was estimated by converting the number pixels to centimeters using a conversion ratio established by the distance between the video camera and floor of the environment. The mean infield firing rate was ascertained by averaging the mean firing rate of each pixel in the field.

For sleep, the mean firing rate was determined from the number of spikes that each cell fired for the duration of sleep. The voltage and duration for every action potential was based on the average waveform found on the channel of the tetrode with the largest amplitude. The amplitude was measured from the peak of the waveform to the lowest point prior to the peak. To establish the duration of the spike, the width from the peak of the waveform to the lowest point in the valley was measured and then divided by the sampling rate of the video (32 Hz).

Four data points were recorded during four consecutive days from one tetrode that was localized to the dentate molecular layer. The waveforms of these data points had a thin spike on only one of the tetrode channels and the two dimensional spatial autocorrelograms resembled autocorrelograms of “grid” cells. Furthermore, these data points resembled the data recorded from the perforant path fibers reported in Leutgeb et al., (Leutgeb et al., 2007); consequently, these data were excluded from all analyses related to active behavior reported in this study. Two rats refused to forage for food reward and the majority of the environment was under sampled; therefore, data from these rats were also excluded from analyses.

To exclude repeated samples, we looked at recordings from a tetrode with active cells on the day that the most sleep clusters were detected and the first day that an active cell was detected. Analyses reported in the results are based on recordings from the day with the most sleep clusters; however, results based on the first day that an active cell was detected were reported in the supplementary material chart 1 and show similar trends.

## **2.5f Histological Procedures**

After completing the last experiment, lesions were made on a subset of tetrodes to aid in track identification. Rats were euthanized the following day by perfusing with formalin through the heart. Coronal slices (40  $\mu\text{m}$ ) were cut from the brain on a freezing microtome, mounted, and stained with Cresyl Violet. Sections were photographed under a Motic SMZ-168 stereo scope (Motic Instruments Inc., Richmond, BC, Canada), captured with a moticam 2000 camera (Motic Instruments Inc., Richmond, BC, Canada) or IC Capture DFK 41BU02 camera (The Imaging Source, Charlotte, NC, USA), and stored as JPEG files on a Dell computer. High magnification images were taken under a Zeiss Axioplan (Carl Zeiss Optical, Inc., Chester, VA, USA). Electrode tracks and the tetrode that generated them were identified and assigned to an anatomical layer depending on the region where the track stopped.

## CHAPTER 3 QUANTITATIVE EVIDENCE FOR PATTERN COMPLETION AND PATTERN SEPARATION PROCESSES IN CA3 AND DG

### 3.1 Introduction

The hippocampal formation is implicated in many mnemonic processes. One salient feature of hippocampal output is the location-specific firing of pyramidal cells, which are implicated in spatial and context-dependent memories (O'Keefe and Nadel, 1978; Wood et al., 2000). The recollection of these memories theoretically utilizes an autoassociative attractor network that functions by implementing two competitive, yet complementary processes (Hopfield, 1982; Marr, 1971; Tsodyks, 1999). *Pattern completion* can reproduce a previously stored output pattern from a partial or degraded input pattern (Marr, 1971; Guzowski et al., 2004; McNaughton and Morris, 1987), and many models suggest that the CA3 region of the hippocampus is responsible for this phenomenon via its recurrent collaterals (Marr, 1971; McNaughton and Morris, 1987; Rolls and Treves, 1998) and the propensity for the recurrently connected cells to undergo long-term potentiation (Harris and Cotman, 1986; Zalutsky and Nicoll, 1990). The process of pattern completion, modeled with a sigmoidal curve, reflects a pattern of activity in CA3 neurons that remains similar despite a partial or degraded pattern of activity in the input structures (McClelland and Goddard, 1996). In contrast, *pattern separation* decreases redundancy among incoming information and then outputs patterns that overlap less than the inputs (Rolls and Kesner, 2006; McNaughton and Nadel, 1990; Guzowski et al., 2004). In theory, the dentate gyrus could perform pattern separation and prevent spurious recall by producing sparse representations from entorhinal cortex input (McNaughton and Nadel, 1990; McNaughton and Morris, 1987).

Strong evidence supporting the hypothesis that CA3 is necessary for pattern completion came from Nakazawa and colleagues (2002), who found that removing most extramaze cues during a spatial memory task altered both the behavior and CA1 place fields of a CA3 NMDA-receptor knockout mouse more than a wild-type mouse. Simultaneous recordings from CA3 and CA1 showed that the population of CA3 cells represented the change between a familiar and cue-altered environment more coherently than CA1 (Lee et al., 2004b), suggesting that CA3 was pattern completing or generalizing compared to CA1. Regarding the process of storing new memories, Gilbert et al. (2001) used a delayed-match-to-sample for spatial location task to assess pattern separation and found that rats with ablated granule cells performed worse when spatial similarity was increased compared to vehicle injected controls. Furthermore, data from Leutgeb et al. (2007) showed that DG neurons fired in multiple locations in the environment and that each of the cells individual firing fields independently change their firing rates when the shape of the environment was altered. The variation in firing rates for the different environments was suggested as a mechanism to express pattern separation (Leutgeb et al., 2007).

Previous studies specifically focused on the function of each hippocampal subregion and made implicit assumptions about how environmental manipulations changed the hippocampal input representations; however, the cell populations that provided these inputs were rarely examined. To directly compare the input and output representations and quantitatively determine whether the CA3 and DG networks actively perform pattern completion and pattern separation, CA3 and its primary afferents (i.e., DG, LEC, and MEC) were recorded in freely moving rats during the same experimental conditions. We show that the primary input structures (LEC, MEC, and DG) change their representations between a familiar and cue-altered environment more than the downstream CA3 subfield. In contrast, we found that the dentate gyrus representation changes more than its input representations (i.e. LEC and MEC). Furthermore, even though individual LEC cells showed poor spatial tuning, a weak local-cue-related signal was observed at the population level that

contrasted with the global-cue-related signal represented by the MEC. These findings are consistent with longstanding computational models proposing that (1) CA3 is an associative memory system performing pattern completion in order to recall previous memories from partial inputs and (2) the DG performs pattern separation to help store different memories in ways that reduce interference when the memories are subsequently recalled.

### **3.2 Results**

Multiple recording probes were implanted on fourteen rats targeting the CA3 and dentate gyrus subfields of the hippocampal formation (Figure 3.1 A,B) and its primary input structures (Figure 3.1 C,D). Seven rats had tetrodes simultaneously targeting subfields CA3 and DG, three rats had tetrodes targeting LEC, and four rats had tetrodes targeting MEC. As tetrodes were individually lowered to the targeted regions (see experimental procedures 3.4 for details), rats were trained in a stable, controlled environment to circumnavigate clockwise (CW) around a track with prominent local cues, which was located in the center of a black curtained environment containing six distinct global cues (standard session; STD in Figure 3.2). During daily recordings, three standard sessions were interleaved with two mismatch sessions, consisting of a set of global cues being rotated CW and a set of local cues on the track being rotated in the opposite direction (counterclockwise; CCW) by the same amount (Figure 3.2). Mismatch angles were equivalent to the sum of absolute value of both rotations and covered a range of angles (i.e. mismatches of 45°, 90°, 135°, and 180°). Rats with recording probes targeting the hippocampal formation were exposed to two sets of each mismatch angle over 4 days, whereas rats with tetrodes targeting LEC and MEC were exposed to a range of sets (1-9) for 2 to 18 days. For the LEC experiments, the rat with 9 sets had an additional 6 mismatch sessions that were not part of a complete set. There was an additional 4 days of experiments with three 90° mismatch sessions, two 135° mismatch sessions, and one 45° mismatch session.

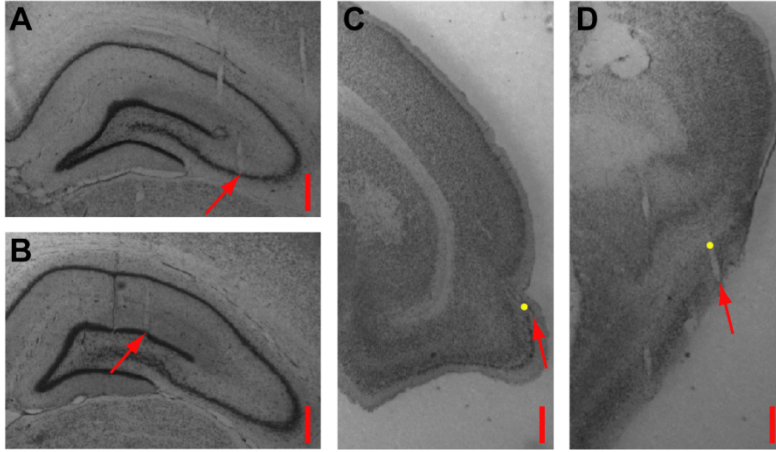


**Figure 3.1. Histology Localizing Tetrodes to CA3, DG, LEC, and MEC.** Histology examples showing locations of tetrodes targeting (A) CA3, (B) DG, (C) LEC, and (D) MEC. Scale bar equals 500  $\mu\text{m}$ . Arrows indicate tips of tetrode tracks. Yellow dots represent recording location for two example cells recorded from MEC and LEC.

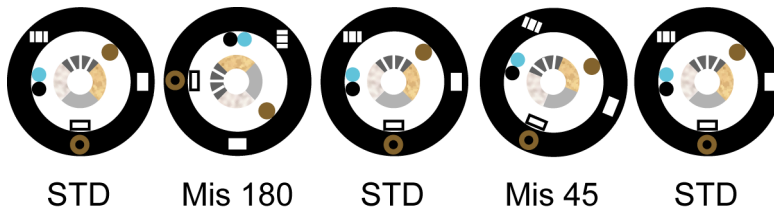


**Figure 3.2. Schematic Illustrating One Day of Recording.** Circular track with prominent local cues positioned in the center of a black curtain enclosure containing distinctive global cues. One day of the experimental protocol consisted of three standard sessions interleaved with two mismatch sessions consisting of the local and distal cues being rotated in the same amount but either clockwise or counterclockwise, respectively. The mismatch angles illustrated were 180° and 45°.



Cells were partitioned into putative excitatory (mean firing rate  $<10$  Hz) or inhibitory cells (mean firing rate  $\geq 10$  Hz), and only the excitatory cells that fired 20 or more spikes were considered active and included in the following analyses (Figure 3.3). Of the putative principal cells, approximately 37% of CA3 ( $n = 146/399$ ), 28% of DG ( $n = 96/341$ ), 77% of LEC ( $n = 44/57$ ), and 80% of MEC ( $n = 77/96$ ) were considered active during the first daily standard session. As previously reported, the spatial information for LEC cells was lower than CA3, DG, and MEC (Figure 3.4). Single units in CA3, DG, LEC, and MEC showed a variety of responses to the cue manipulations. The responses of individual cells were separated into five types and examples are shown in figure 3.5. Cells with firing patterns that rotated with the global cues were classified as CW, whereas cells with firing patterns that followed the local cues were categorized as CCW. Some cells fired during the preceding standard session, but stopped firing during the mismatch session. Other cells only fired during the mismatch session. Cells that started or stopped firing during the mismatch sessions were classified as 'Appear' or 'Disappear', respectively. The final category was 'Ambiguous' and these were cells with responses that could not be grouped with certainty into the previously mentioned classes (i.e., a cell with two fields rotating in different directions during the mismatch).

To compare the response of the CA3 population with its primary inputs, a spatial population correlation analysis was performed. The normalized mean firing rate of every cell was calculated for 360 positions on the circular track (binned every  $1^\circ$ ). All cells were stacked and population firing rate vectors were constructed at each location on the track. The firing rate vectors for each bin of the standard session prior to the mismatch session were correlated with the firing rate vectors from either the mismatch session or the next subsequent standard session to create spatial population correlation matrices (Fig 3.6). The results for

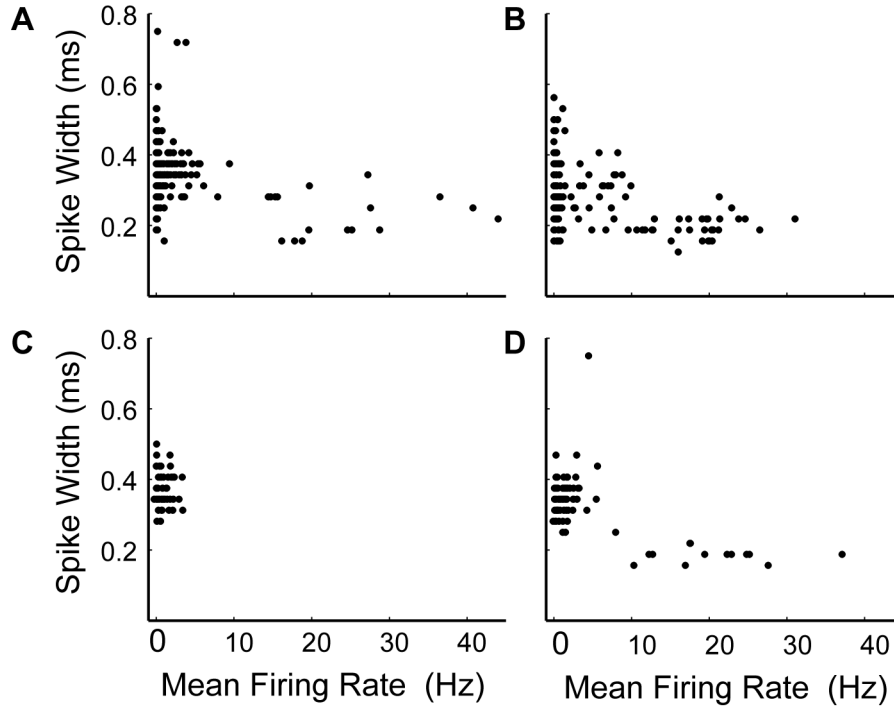


**Figure 3.3. Categorization of Putative Excitatory and Inhibitory Neurons.**

Scatter plots of mean firing rate (Hz) on the abscissa and spike width (ms) on the ordinate for all well isolated CA3 (A), DG (B), LEC (C), and MEC (D) cells. For the MEC and CA3 cells, two distinct groups were observed (putative principal cells with a mean firing rate  $< 10$  Hz and putative interneurons with a mean firing rate  $\geq 10$  Hz). A less obvious distinction was seen for DG cells, but to remain uniform across regions the criterion used to identify putative principal cells in CA3 and MEC was applied. No LEC cells had a firing rate that exceeded 5 Hz.

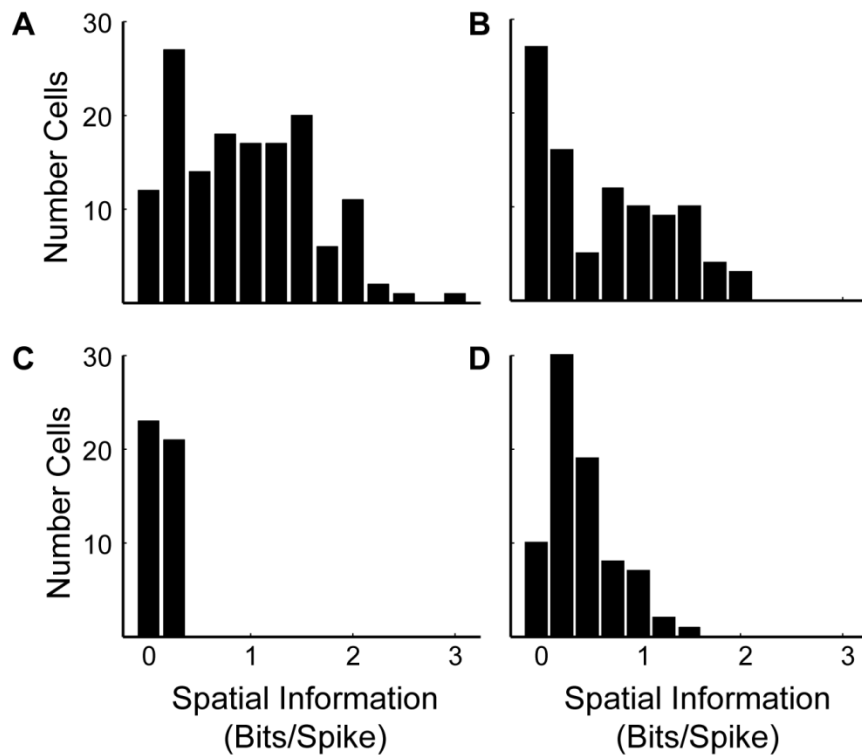


**Figure 3.4. Distribution of Spatial Information Scores on Circular Track.** Histograms show the spatial information scores based on two dimensional rate maps for CA3 (A), DG (B), LEC (C), and MEC (D) cells. The information scores for MEC and LEC have been reported previously (Yoganarasimha, 2010).

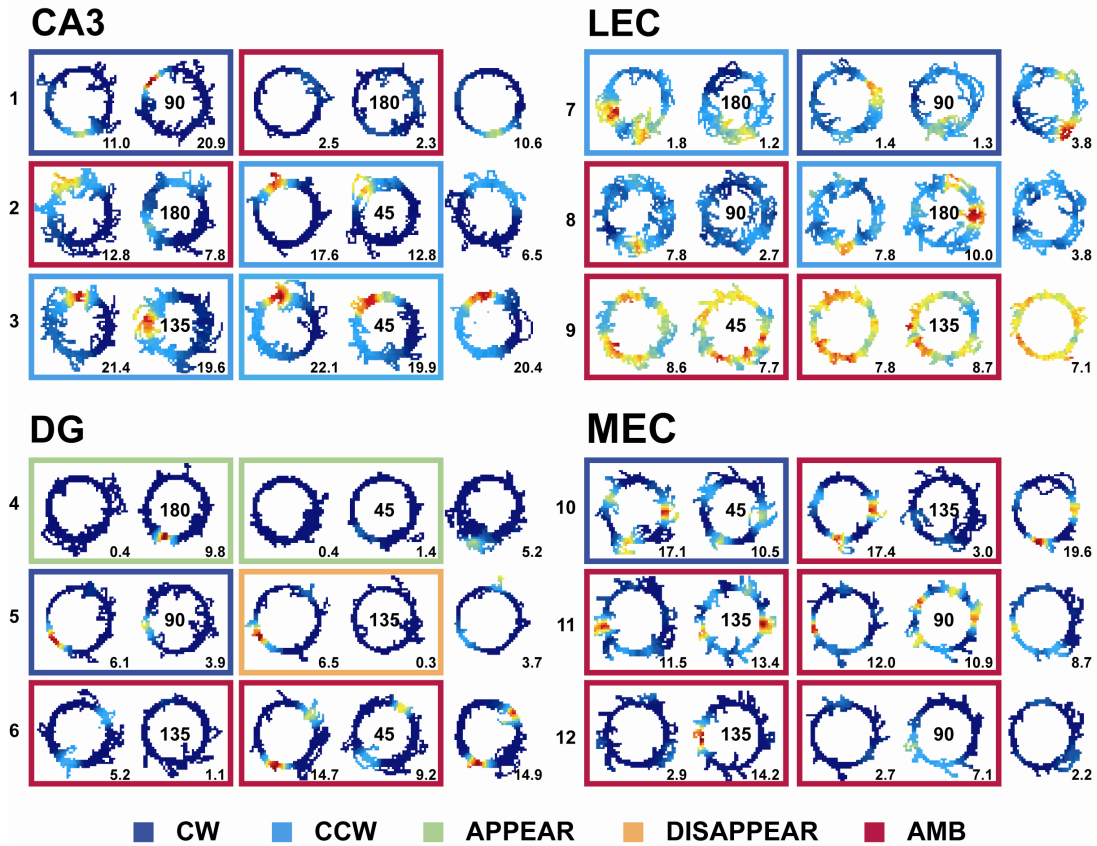


**Figure 3.5. Example Rate Maps for Four Recorded Regions Showing Variety of Cellular Responses After Rotating the Local and Global Cues.** Rate maps showing representative cells from DG, CA3, LEC, and MEC that changed their firing patterns between the standard and mismatch sessions. Series of rate maps represent five consecutive sessions for one day. Blue shows areas with no firing and red shows peak rates, which are labeled on the lower right corner of each map. Colored boxes around ratemaps indicate response type (CW-dark blue; CCW-light blue; Appear-green; Disappear-orange; Ambiguous (AMB)-maroon). Angles in the center of all mismatch session ratemaps for each group (columns 2 and 4) indicate the total mismatch angle.

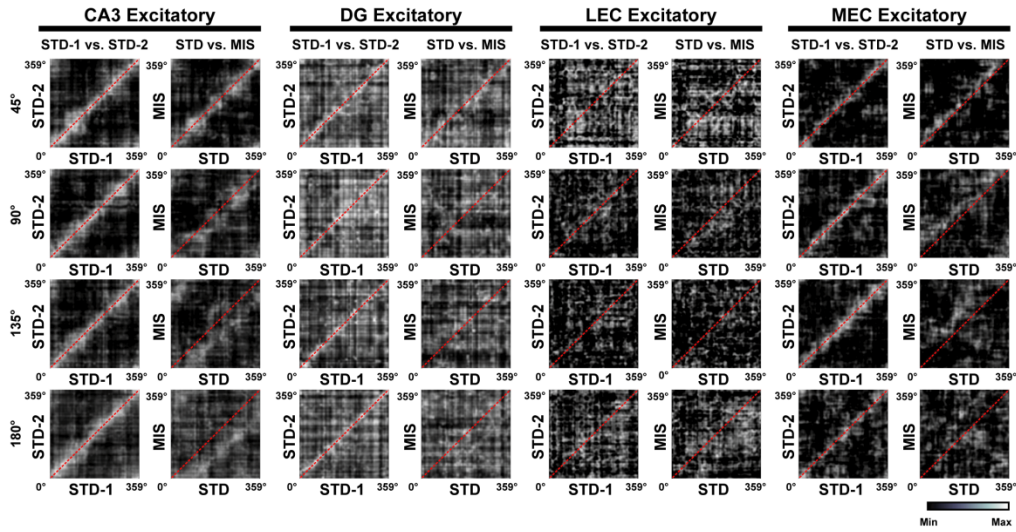


**Figure 3.6. Correlation Matrices Between Vectors of Positional Firing Rates for Population of Recorded Cells.** Correlation matrices between normalized firing rate vectors from CA3, DG, LEC, and MEC. For each cell, the firing rate for every bin was normalized to its peak firing rate. The matrix was created by correlating firing rate vectors for a standard session with those of the subsequent mismatch or standard session. Positions ( $^{\circ}$ ) on the linearized track in the standard and/or mismatch sessions are shown on the ordinate and abscissa. MEC, LEC, and DG representations became increasingly decorrelated between STD and MIS sessions with increasing mismatch angles, as the correlation matrices lost most of their structure. In contrast, the CA3 representations maintained a stronger band of correlation, even in the  $180^{\circ}$  mismatch; however, the band of correlation did progressively become more decorrelated as the mismatch angle increased.

CA3 replicated the findings from Lee et al. (2004b). Briefly, the correlation matrices for CA3 comparing the standard sessions preceding and following all mismatch angles, produced a high correlation on the diagonal, showing that a significant number of CA3 cells fired at a similar location in both standard sessions. Like the population correlation matrices between the standard sessions, in every mismatch rotation CA3 sustained a band of highly correlated activity, albeit the band shifted downward indicating that the CA3 cells were controlled by the local cues.

When analyzing the response of the DG cells during the 45° mismatch, there was a weak band of correlated activity near the diagonal. For all mismatch angles greater than 45°, the DG spatial population correlation matrices appeared decorrelated and lacked the coherence observed in the population of CA3 cells. Even the standard sessions for DG appeared less structured, which suggests that the DG representation might continually change from one session to the next. Every LEC correlation matrix appeared decorrelated due to the lack of structure suggesting that the LEC representation, unlike the CA3 representation, might change from one session to the next. The MEC representation was highly correlated along the diagonal for all the correlation matrices between the standard sessions. Furthermore, the correlation matrices indicated that the MEC representation maintained a structured band of correlation for all mismatch types, but the band significantly degraded during the session with the largest mismatch angle. In contrast to CA3, the band of correlation shifted upward indicating that the MEC cells were controlled by the global cues.

For each region, the sample sizes in the correlation matrix were different (CA3, 45°  $n = 72$ , 90°  $n = 83$ , 135°  $n = 85$ , and 180°  $n = 89$ ; DG, 45°  $n = 43$ , 90°  $n = 46$ , 135°  $n = 44$ , and 180°  $n = 53$ ; LEC, 45°  $n = 14$ , 90°  $n = 30$ , 135°  $n = 22$ , and 180°  $n = 21$ ; MEC, 45°  $n = 34$ , 90°  $n = 39$ , 135°  $n = 42$ , and 180°  $n = 33$ ). Since the sample size could affect the correlations in the matrices, the CA3 data

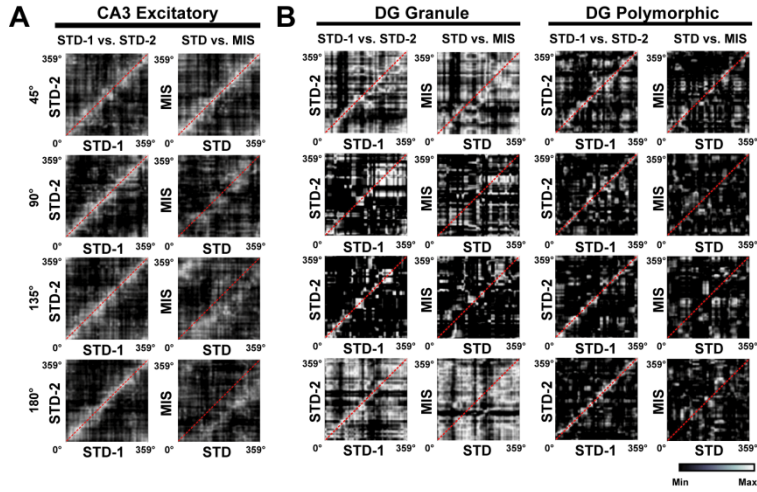


**Figure 3.7. Controls for Hippocampal Formation Spatial Population Correlation Matrices.** (A) Correlation matrices controlling for difference sample sizes in CA3 and DG. (B) Correlation matrices between normalized firing rate vectors from DG granule and polymorphic cell layers. Insufficient cell numbers from each layer prevents statistical quantification.

were randomly subsampled to match the sample sizes of the DG correlation matrices. Figure 3.7A shows that the structured band of high correlation seen in the CA3 population remained after controlling for the difference in sample sizes. Despite the smaller sample sizes in MEC, the MEC showed better correlation than DG; therefore, we believe that the difference in cell number is not an important factor. Unfortunately, the sample size of LEC was not large enough to run the control analysis.

The DG is the only region in the hippocampus proper with two excitatory cell types (i.e., granule and mossy cells) and both types of cells may perform different computations. Consequently, we attempted analyzing the DG data based on putative recordings from granule and hilar cells. No differences were observed between the different layers in DG (Figure 3.7B; presumed polymorphic and granule); however, a statistical comparison could not be made because of insufficient sample sizes for each layer. Since the subfields of the hippocampus receive input from different layers of the entorhinal cortex (i.e. CA1 receives input from layer 3 and both CA3 and DG receive input from layer 2), we also attempted to partition the MEC and LEC recording into different layers. No conclusions could be reached about the different entorhinal layers because of insufficient sample sizes for each layer (Figure 3.8).

The magnitude that the population shifted in response to all of the mismatch rotations was quantified by reducing each of the two dimensional correlation matrices into a one dimensional structure (Figure 3.9). The mean correlation at each of the 360 diagonals in the correlation matrices was calculated and plotted for each region at every mismatch angle (Figure 3.10). The maximum mean correlation for all CA3 STD versus STD correlation matrices (gray lines) occurred at the zero diagonal indicating that the representations were similar from one familiar environment to the next. For the probe sessions, the amount that the peak of the mean correlation shifted increased as the size of



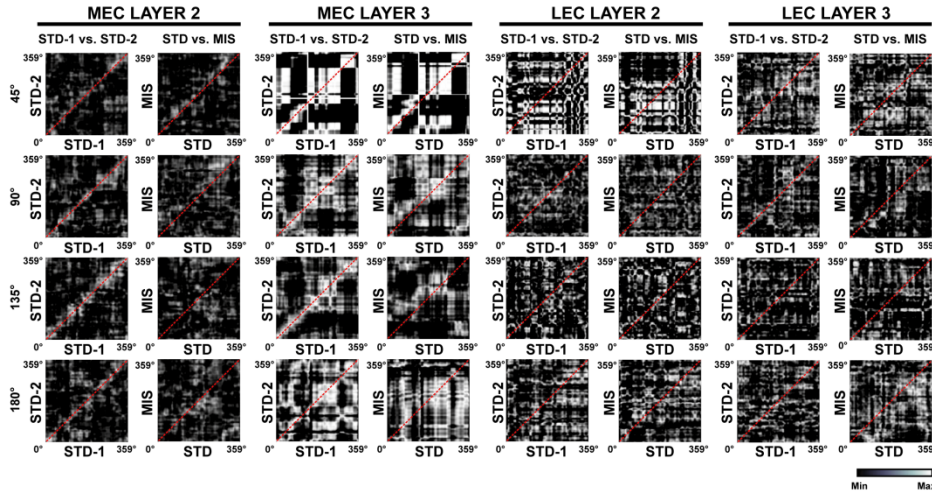


**Figure 3.8. Spatial Population Correlation Matrices for Superficial Layers of the Entorhinal Cortex.** Correlation matrices between normalized firing rate vectors from layers II and III of the MEC and LEC. Insufficient cell numbers from each layer prevent statistical quantification.

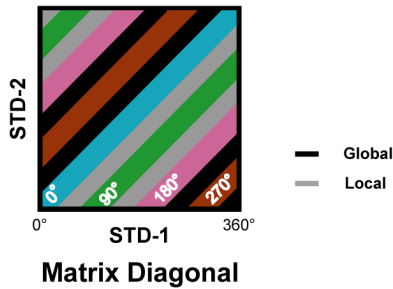


**Figure 3.9. Schematic of Method for Calculating Mean Correlations for Diagonals of Correlation Matrix.** Illustration showing regions of the population correlation matrices used to calculate the mean correlations for the 360 diagonals. The cyan, green, violet, and brown lines show the regions of the matrix used to determine the mean correlations for diagonals 0, 90, 180, and 270, respectively. The shaded gray area in the correlation matrix (diagonals 1-179) represents a local cue response, whereas the black region (diagonals 181-359) indicates a global cue response.

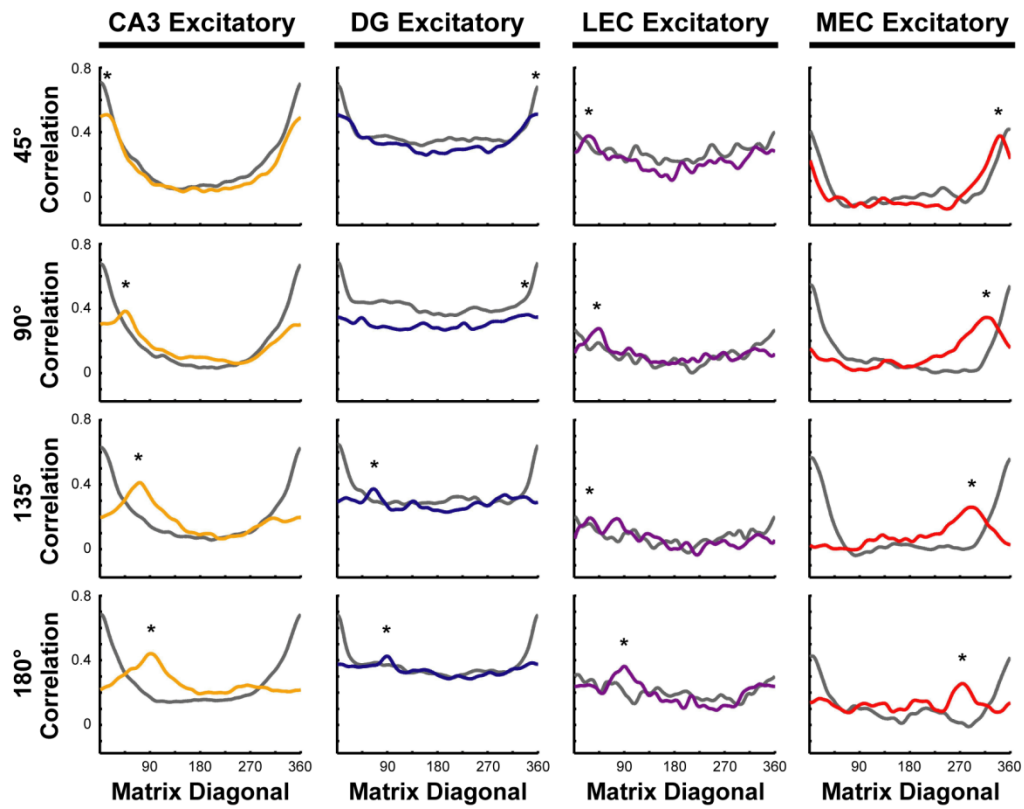


**Figure 3.10. Mean Correlations for Diagonals of Correlation Matrices.** Plots show the mean correlations of CA3, DG, LEC, and MEC population correlation matrices. Gray and colored lines show the mean correlations from the STD-1 vs. STD-2 and STD vs. MIS matrices, respectively. Local and global cue control correspond to diagonals 1-179 and 181-359, respectively.

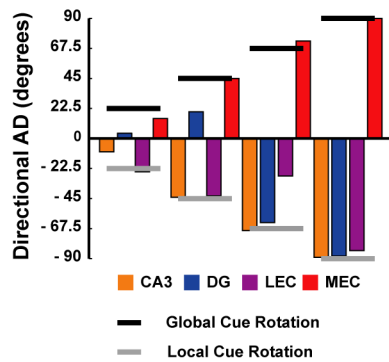


**Figure 3.11. Cue Control Over Population.** Bar plots showing the directional response of the population from all regions. Black and gray horizontal bars indicate the amount that global and local cues were rotated, respectively. The peaks from MEC representation always follow the global cues, whereas the peaks from the LEC and CA3 representations follow the local cues. DG does not consistently follow a cue set.

mismatch angle increased. When the mismatch angles were greater than 45°, the location of the CA3 mismatch peak directly corresponded to the amount of the local cue rotation (Figure 3.10; Figure 3.11; Monte Carlo;  $p < 0.001$ ). For the 45° rotation, the peak of the mean correlation slightly under-rotated and occurred at bin 12 instead of 22; however, the shift in the population was still in the direction of the local cue rotation. Furthermore, when examining the amplitude at the peak of the mean correlation, there was a decrease in the mean correlations as the mismatch angles increased.

The population responses of the regions sending afferents to the CA3 subfield were strikingly different than observed in CA3. For the MEC input, the representation was strongly influenced by the global cues (Figure 3.10; Figure 3.11; Monte Carlo;  $p < 0.003$ ), thus shifting in the opposite direction from CA3. The amount that the MEC representations rotated for all mismatch angles was within 5 degrees of the rotation angles for the global cue set. As expected, there was an inverse relationship between the amplitude of the peak (i.e., the mean correlation) and the size of the mismatch angle such that increasing the mismatch angle caused the amplitude to decrease. The MEC representation appeared fairly stable across standard sessions. For LEC, even though individual cells showed poor spatial tuning, a weak local-cue-related signal was observed at the population level. For every mismatch angle except for 135°, the amount that the peak shifted was within 3 degrees of the local cue rotation (Figure 3.10; Figure 3.11; Monte Carlo;  $p < 0.002$ ). The 1-D LEC 135 correlation matrix showed two adjacent peaks; the peak with the largest amplitude (mean  $R = 0.1947$ ) occurred at 29 degrees, whereas the second largest peak (mean  $R = 0.1894$ ) shifted an amount that was 77 degrees. Unlike CA3, the amplitude of the peaks for every STD versus STD and STD versus MIS were relatively small for LEC. The highest mean correlations for the population of DG neurons, similar to the pyramidal cells of CA3, occurred between the standard sessions at diagonal 0. For mismatch angles of 135° and 180°, there was a small peak

corresponding to the amount the local cues were rotated (Figure 3.10; Figure 3.11; Monte Carlo;  $p < 0.002$ ). In contrast, the largest correlations for the smaller rotation angles (i.e.  $45^\circ$  and  $90^\circ$ ) under-rotated, but were closer to the amount that the global cues were rotated (Figure 3.10; Figure 3.11; Monte Carlo;  $p < 0.03$ ). For the DG population, the amplitude of the peaks for all mismatch angles were greatly diminished compared to the standard sessions.

To examine the influence of the global and local cue sets, a subset of cells that fired in consecutive sessions (i.e., standard and following mismatch) from all four regions was examined and the responses to the rotations were quantified using circular statistics. The angle of rotation for each cell was assigned based on the amount that the cell's linearized rate map in the mismatch session needed to be shifted ( $0 - 355^\circ$ ;  $5^\circ$  bins) to produce the highest correlation between the rate maps of the standard and mismatch sessions. For each mismatch amount, the degree that the location of each cell's firing rotated between the standard and mismatch session, as well as the mean vector, is plotted in figure 3.12. The angle of the mean vector (magnified in insets) shows the average rotation of cells, whereas the magnitude of the mean vector is proportional to the variability of the distribution around the angle (i.e., the longer the vector the less dispersed the distribution). For all mismatch angles, the magnitude of the CA3 vector was significant and pointed in the direction that the local cues were rotated (Figure 3.12; Rayleigh test;  $p < 0.0006$ ) suggesting that the response of individual cells was similar and that it was controlled by the local cues.

In contrast to CA3, the magnitudes of the mean vectors for the upstream structures projecting into CA3 were variable. For the largest mismatch angles ( $135^\circ$  and  $180^\circ$ ), individual cells recorded from DG were heavily dispersed and none of the mean vectors were significant (Figure 3.12; Rayleigh test;  $p > 0.15$ ). However, the smallest mismatch angles were significantly clustered (Figure 3.12; Rayleigh test;  $p < 0.04$ ). The mean rotation angle for all mismatch rotations, except for  $90^\circ$ , appeared to be influenced by the local cues, whereas the  $90^\circ$  mismatch showed a weak bias towards the distal cues. For LEC, the mean rotation for every mismatch angle was in the direction of the local cues; however,

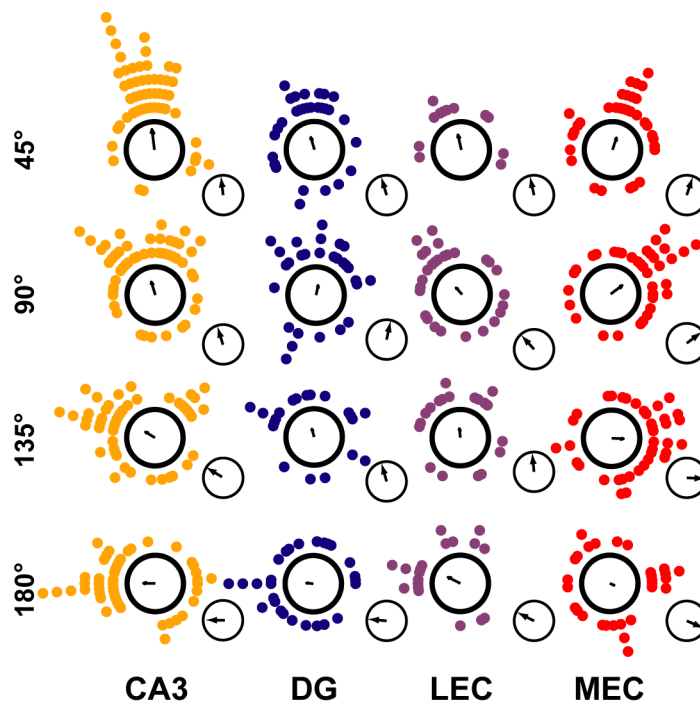


**Figure 3.12. Rotation Analysis Showing Responses of Individual Cells to Manipulations.** Each dot illustrates the amount of rotation (angle in polar plot) for the spatial firing of a cell between the STD and MIS sessions. The mean vectors of the distributions are shown in the center of the polar plots and the mean angles are shown as insets. Rows show results from the four mismatch sessions (45°, 90°, 135°, and 180°) for the region indicated below each column. MEC (red) representations were controlled primarily by the global cues, whereas the very weak spatial representations of the LEC (purple) were controlled primarily by the local cues. DG (blue) representations showed a mixed effect, whereas CA3 (orange) representations were strongly controlled by the local cues.

the significance of the mean vectors was variable (Figure 3.12; 45° and 180°, Rayleigh test,  $p < 0.03$ ; 90°, Rayleigh test,  $p = 0.06$ ; 135°, Rayleigh test,  $p > 0.14$ ). For every mismatch rotation, the mean rotation angle for MEC neurons was controlled by the global cues. Moreover, the mean vectors were significant for mismatch angles of 45, 90, and 135 degrees (Figure 3.12; Rayleigh test;  $p < 0.002$ ). In contrast, MEC neurons were not clustered during the 180° mismatch (Figure 3.12; Rayleigh test;  $p > 0.4$ ). All rats with recordings from the same region showed similar patterns (Figure 3.13). Recordings from CA3 and DG occurred during the first four days that the animals were exposed to the manipulations, whereas most LEC recordings occurred after the fourth day that the rats had experienced the mismatch. As LEC tetrodes were advanced, units detected in the deep LEC layers (i.e. layers 5 and 6) were encountered prior to the superficial LEC layers (i.e. layers 2 and 3); therefore, more cells from deep LEC were recorded during the first four days of the experiment. Since the deep layers of LEC do not project to the hippocampus, the data was not included in this study. The length of time that the LEC rats were exposed to the manipulation might have caused the weak local response; however, this is unlikely because Lee et al. (Lee et al., 2004b) recorded CA3 for eight days and saw similar responses across rats. For MEC, similar responses were seen before the first 4 mismatch sessions and subsequent probe trials (Figure 3.14).

The comparisons between the different regions at both the population and individual cellular levels pooled data that was recorded across many sessions and rats. A distinct possibility exists that concurrently recorded cells from each region might show a similar response to the mismatch manipulations, but which set of cues control the response could vary from session to session. This situation would cause the combined response to appear disjointed, even though each ensemble was coherent. To control for this effect, we examined from each region data sets with at least 2 simultaneously recorded cells that fired in both the standard and the mismatch session. Examples of different ensembles

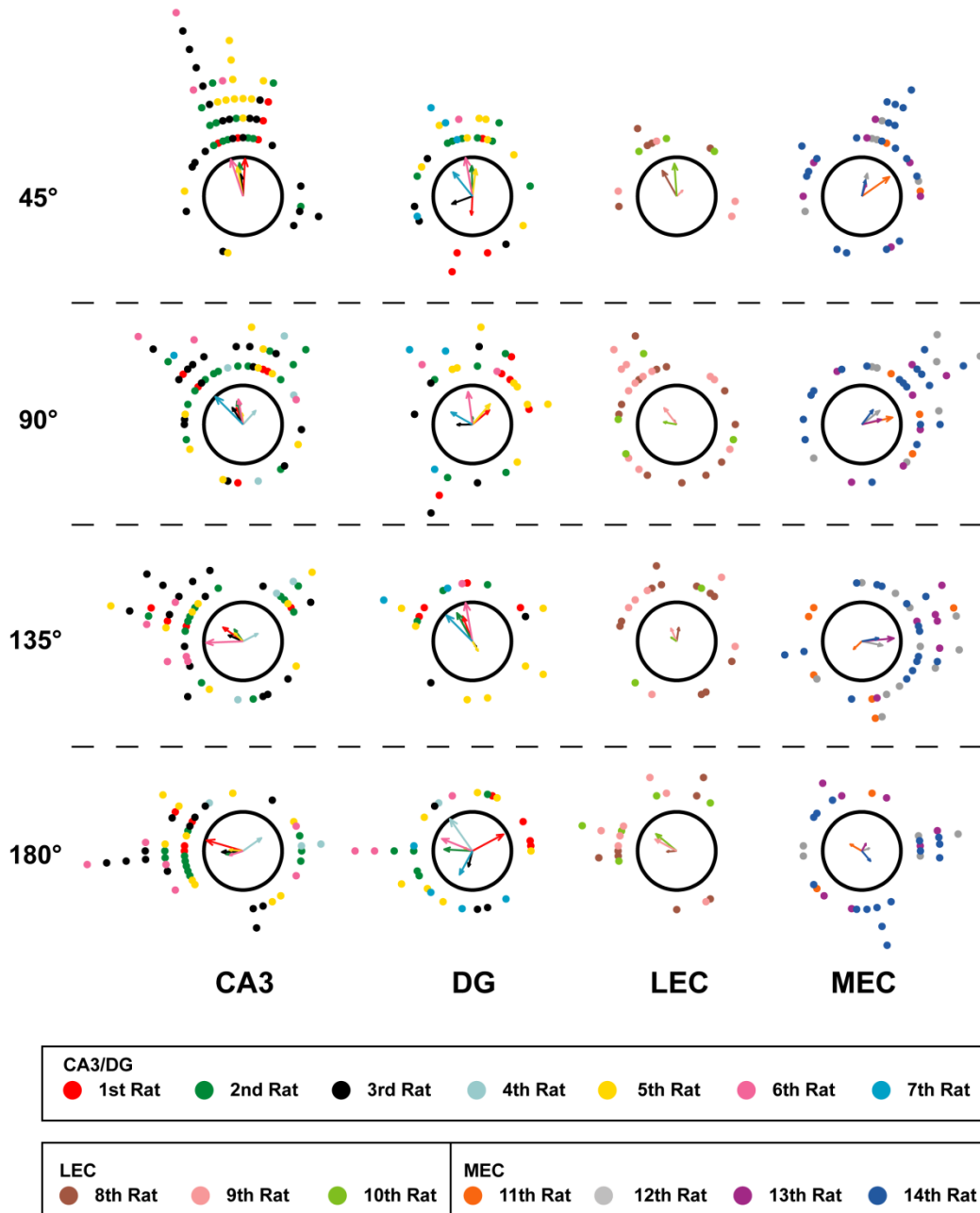


**Figure 3.13. Comparison between individual subjects.** Each colored point shows the amount of rotation (angle in polar plot) for the spatial firing of a cell between the STD and MIS sessions for one rat (n = 14). Simultaneous DG and CA3 recordings were from seven rats, whereas LEC and MEC recordings were from three and four different rats, respectively. Colored arrows represent the mean vectors for each rat. Rows represent data from the four mismatch sessions and columns show the four regions. The distribution of spatial firing responses does not appear to be an artifact caused by one individual rat.



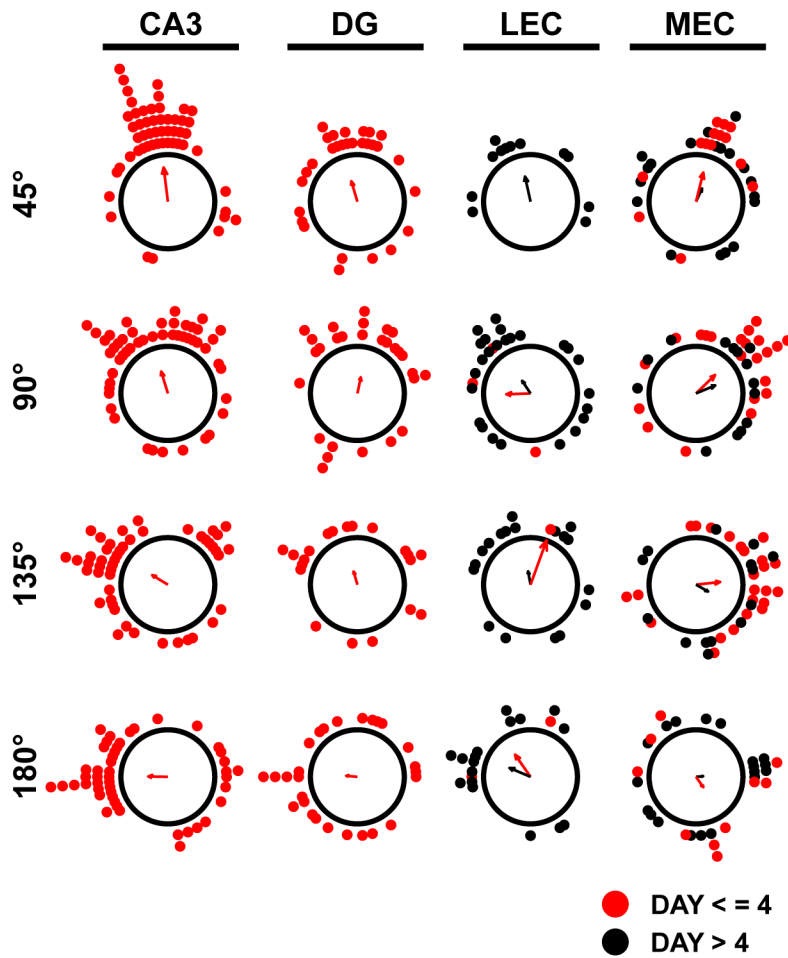


**Figure 3.14. Comparison between the first four days and subsequent days of recording.** Red represents data recorded before the fifth day and black shows recordings following the fourth day. All recordings from CA3 and DG rats occurred during the first four days. MEC recordings transpired throughout the series of experiments, whereas the majority of LEC recordings took place after the fourth day. There was considerable overlap between the amount of rotation (angular coordinate) for the spatial firing for MEC cells between the STD and MIS sessions across all days of recording.

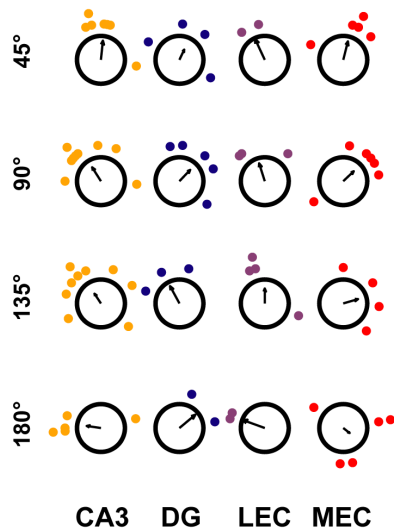


**Figure 3.15. Examples of Simultaneously Recorded Cells in Each Region.** Each point represents the amount of rotation (angle in polar plot) for the spatial firing of a cell between the STD and MIS sessions. Ensembles were defined as a minimum of two cells that reach criterion (mean firing rate < 10 Hz and the number of spikes  $\geq 20$ ) in both the standard and mismatch sessions. The mean vector of each ensemble is shown in the center of the polar plots and the direction of the arrow indicates the mean angle that each ensemble rotated. Rows show the mismatch session and columns indicated the regions (CA3-orange; DG-blue; LEC-purple; MEC-red).

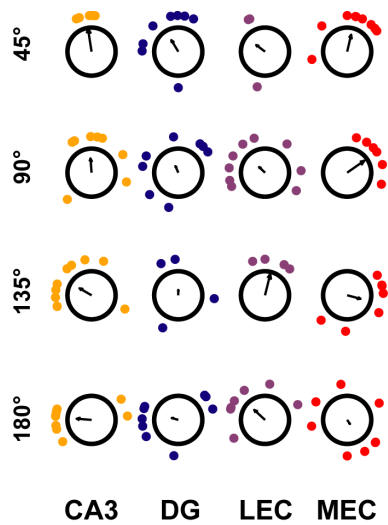


**Figure 3.16. Secondary Statistics on Responses of Ensembles in Each Region.** Each dot represents the mean rotation (angular coordinate) of one set of simultaneously recorded cells (i.e., ensemble) from CA3, DG, LEC, or MEC. The mean vector of all the ensembles is shown in the center of the polar plots and the direction of the arrow indicates the mean angle of rotation for all of the ensembles. Rows show the mismatch session and columns indicated the regions (CA3-orange; DG-blue; LEC-purple; MEC-red). All ensembles were significantly clustered for CA3 (Rayleigh test;  $p < 0.04$ ), whereas the DG ensembles were never significantly clustered (Figure 3.16; Rayleigh test;  $p > 0.07$ ). For MEC, ensembles were significantly clustered near the amount that the global cues were rotated during the mismatch angles of 45° and 90° (Figure 3.16; Rayleigh test;  $p < 0.007$ ). For LEC, ensembles were significantly clustered near the amount that the local cues were rotated during the mismatch angles of 135° and 180° (Figure 3.16; Rayleigh test;  $p < 0.007$ ).

recorded from the four regions for every mismatch rotation are shown in Figure 3.15. The angle of rotation for each cell that was part of an ensemble was used to calculate the average rotation and mean vector for every ensemble. For every mismatch angle, circular statistics, which were secondary statistics, were calculated on the ensembles from each region (Figure 3.16). During each probe session, all ensembles were significantly clustered for CA3 (Figure 3.16; Rayleigh test;  $p < 0.04$ ), whereas none of the DG ensembles were significantly clustered (Figure 3.16; Rayleigh test;  $p > 0.07$ ). For MEC, ensembles were significantly clustered near the amount that the global cues were rotated during the smallest mismatch angles (Figure 3.16; Rayleigh test;  $p < 0.007$ ), whereas the ensembles were fairly distributed during largest mismatch angles (Figure 3.16; Rayleigh test;  $p > 0.09$ ). Despite diffuse distributions seen with the larger mismatch angles, the average rotation of all the ensembles was in the direction that the global cues were rotated. Ensemble clustering in LEC was opposite to the pattern seen in MEC (Figure 3.16; mismatch angle  $< 90^\circ$ ; Rayleigh test;  $p > 0.3$ ; mismatch  $135^\circ$ ; Rayleigh test;  $p < 0.03$ ; mismatch  $180^\circ$ ; Rayleigh test;  $p < 0.07$ ). It is a distinct possibility that different sets of cues could control the response of cells of one rat from session to session; therefore, an additional control was run to check the coherence of simultaneously recorded DG and CA3 cells. Similar to the results that were observed in either the DG or CA3 regions, the CA3 ensembles were significantly clustered except for  $135^\circ$  mismatch, whereas DG ensembles were not significantly clustered (Figure 3.17; Rayleigh test; DG all mismatch angles,  $p > 0.15$ ; CA3 mismatch angles  $45^\circ$ ,  $90^\circ$ , and  $180^\circ$ ,  $p < 0.04$ ; CA3 mismatch  $135^\circ$ ,  $p > 0.2$ ).

Figure 3.18 (A&B) shows that the number of cells in each ensemble ranged from 2-11 (CA3), 2-4 (DG), 2-4 (LEC), and 2-10 (MEC). To test whether the size of the ensemble would affect the average length of the mean vector, simulations were run to calculate the average mean vector length for ensembles with 2-11 cells, assuming that the underlying population of rotation angles was

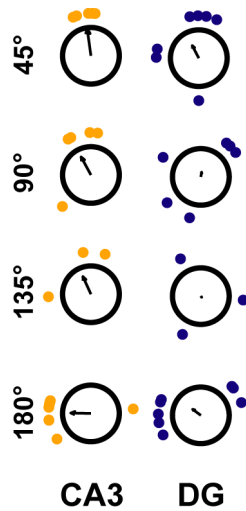


**Figure 3.17. Secondary Statistics on Responses of Ensembles Concurrently Recorded from DG and CA3.** Each dot represents the mean rotation (angular coordinate) of one set of simultaneously recorded cells (i.e. ensemble) from CA3 and DG. The mean vector of all the ensembles is shown in the center of the polar plots and the direction of the arrow indicates the mean angle of rotation for all of the ensembles. Rows show the mismatch session and columns indicate the regions (CA3-orange; DG-blue).

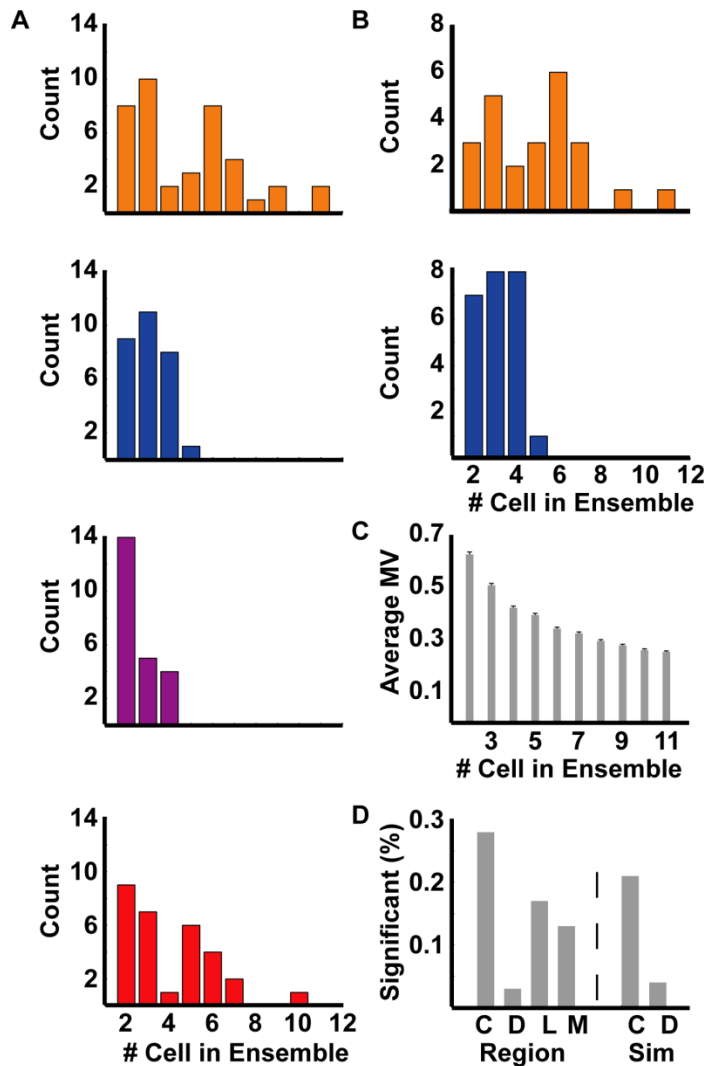


**Figure 3.18. Ensemble Coherence.** Histograms of the number of cells in each ensemble for the four regions (A) and DG and CA3 recorded simultaneously (B). Orange, blue, purple, and red bars represent data from CA3, DG, LEC, and MEC, respectively. Distributions show that CA3 and MEC have more cells in an ensemble than DG and LEC. (C) To show that small sample sizes can artificially increase the size of the average mean vector, the average mean vector length was calculated for ensembles with 2-11 cells from an underlying distribution of random orientations. Simulations were run 1000 times for each ensemble cell size (2-11) such that a data point (angle of rotation for each cell in the ensemble) was randomly sampled from a uniform distribution with replacement. The mean vector length was largest for ensembles with two cells and exponentially decreased as the number of cell in an ensemble increased. (D) Percentage of significant mean vector lengths for each region (left of dash) and simultaneously recorded CA3 and DG (right of dash).

randomly distributed. Each simulation was run 1000 times for ensembles with cell sizes ranging from 2-11 such that a data point (angle of rotation for each cell in the ensemble) was randomly sampled from a uniform distribution with replacement. Mean vectors were computed for each simulation and the average mean vector length for the 1000 ensembles was determined (Figure 3.18 C). As expected, the average mean vector was largest for ensembles with two cells and decreased exponentially as the number of cell in an ensemble increased. We then determined whether the length of the mean vector from an ensemble was significant based on the number of cells in each ensemble and the simulated results. The mean vector length was considered significant at the  $p < 0.05$  level if it was greater than 950 of the 1000 mean vector lengths from the simulated data with the same number of cells in the ensemble. For ensembles from each region (Figure 3.18 D; left of dash), there were more significant mean vectors for CA3 (28%;  $n = 11/40$ ) than in DG (3%;  $n = 1/29$ ), LEC (17%;  $n = 4/23$ ), and MEC (13%;  $n = 4/30$ ); however, the larger number of significant vectors in CA3 was only a trend ( $p < 0.1$ ). Similar results were seen for simultaneously recorded DG and CA3 ensembles (Figure 3.18 D, right of dash; CA3, 21%,  $n = 5/24$ ; DG, 4%,  $n = 1/24$ ; chi-square;  $p > 0.1$ ).

Single units in CA3, DG, LEC, and MEC showed a variety of responses to the cue manipulations. To quantify the responses of individual cells included in the population analyses, the response of each cell to the manipulation was categorized. The responses of individual cells were separated into five types (see Figure 3.5 for representative examples). Cells were categorized as CW, CCW, and AMB based on the correlation value used to determine the rotation angle. If the maximum correlation between the standard and mismatch session was below 0.6, cells were considered ambiguous. Cells with high maximum correlations ( $R \geq 0.6$ ) at locations corresponding to a clockwise or counterclockwise rotation were classified as CW or CCW, respectively. The categories appear and disappear were based on the number of spikes a cell fired (active considered  $\geq 20$  spikes) in the standard and mismatch sessions. Figure

3.19 shows the percentage of cells classified as clockwise, counterclockwise, appear, disappear, or ambiguous for each region. The distributions of cell responses were significantly different for the four regions (Figure 3.19; chi-square;  $p < 0.001$ ).

### **3.3 Conclusions**

The present study examined the flow of information through the hippocampal formation by comparing how the input representations (DG, LEC, and MEC) and output representations (CA3) changed between a familiar and cue-altered environment. Three striking findings were reported. First, there was a dissociation between the information the hippocampal formation received from the MEC and LEC. The MEC representation was controlled by global cues, whereas the LEC representation was influenced by the local cues despite individual LEC cells conveying a weak spatial signal (Yoganarasimha et al., 2010; Hargreaves et al., 2005) (Figure 3.4). Second, the DG population response appeared to change more than the MEC and LEC input representations, suggesting that DG performs pattern separation on its inputs to decrease the redundancy amongst incoming information and then outputs patterns that overlap less than the inputs. However, when looking at individually recorded ensembles, there were no considerable differences detected in the number of significant mean vectors between the four regions. This cast doubt on the theory that DG is performing pattern separation. Finally, the CA3 representation remains more constant between familiar and cue-altered environments than the representations of its primary input structures. This finding is consistent with longstanding computational models proposing that CA3 is an associative memory system performing pattern completion in order to recall previous memories from partial inputs. For a detailed discussion see Chapter 4.



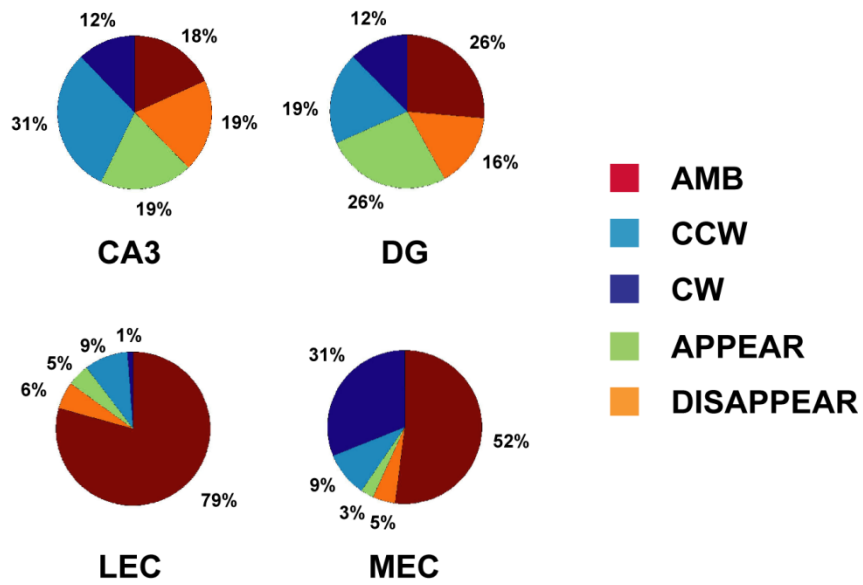


**Figure 3.19. Categorical Response of Individual Cells to Mismatch Session.** Pie charts showing the percentage of CA3, DG, LEC, and MEC cells that were classified as clockwise, counterclockwise, appear, disappear, or ambiguous.

### **3.4 Experimental Procedure**

#### **3.4a Subjects and Surgery**

Fourteen male, Long-Evans rats, which were approximately 5-6 months old and weighted 489-760 grams, were purchased from Charles River Laboratories. Each rat was housed in a single cage and exposed to a 12-hour light/dark circadian cycle, while having *ad libitum* access to water and food.

After approximately fourteen days of habituation, surgeries were performed on the rats to implant a custom-built, recording drive that contained 20 independently moveable tetrodes (2 of which were references). All tetrodes targeted structures on the right cerebral hemisphere. The drives with tetrodes targeting MEC and LEC (rats 151, 156, 159, 165, 174, 184, and 191) were fabricated as a single bundle with a diameter of 2.3 mm. The first two drives simultaneously targeting CA3 and DG (rat 153 and rat 173) were made as a single bundle. Five of the most anterior and lateral positioned tetrodes targeted CA3, whereas the most posterior and medial 13 tetrodes targeted DG. For the last 5 rats (189, 195, 197, 227, and 232), drives were constructed with two groups of tetrodes (5 targeting CA3 and 13 targeting DG) that were displaced by ~415  $\mu\text{m}$  (medial-lateral) and the most anterior tetrodes of each group separated on average by ~400  $\mu\text{m}$ . This configuration was optimally designed for the most lateral tetrodes in each group to reach the lateral edge of the DG granule cell layer and CA3a layers, which are separated by ~1 mm.

All surgeries occurred under aseptic conditions, which complied with National Institutes of Health guidelines and were approved by the Institutional Animal Care and Use Committees at John Hopkins University and the University of Texas Health Science Center at Houston. To optimally increase the proportion of tetrodes entering the DG, recordings were performed during surgery to identify the location of the lateral edge of CA3, which served as a landmark for the

medial/ lateral placement the drives. For the anterior/posterior placement of the drive, the most lateral tetrode was placed 3.2 to 4.4 mm posterior to bregma. For the drives with tetrodes targeting the MEC, the most lateral tetrode was placed 9.8 to 10.9 mm posterior to bregma and 4.8 to 5 mm lateral to the midline. For the drives with tetrodes targeting the LEC, the most lateral tetrode was placed 7.2 to 7.7 mm posterior to bregma and 3.2 to 4.6 mm lateral to the midline.

### **3.4b Training and Recording**

Seven days after habituating to their new environments, rats were familiarized to human contact (30 minutes/day) and trained to sleep in a small dish (~ 25.4 cm) located on a pedestal (30 minutes to an hour/day). Once the rats recovered from the surgical procedure (5-7 days), their body weight was reduced to 80-90% of the free-feeding weight by rationing the food. After a daily session of advancing tetrodes, rats were trained in a controlled and stable environment (Figure 3.20) to run laps around a circular track (239 cm and 20.3 cm outer circumference and width, respectively). The track, which was centered in a black-curtained enclosure with six salient cues located on the periphery, was divided into four arcs of equal length, but the surface of each arc was textured with different material. During initial training sessions, chocolate sprinkles were dispersed around the track and rats gradually learned to continuously navigate clockwise for the reward. To prevent the rats from moving counterclockwise, a cardboard panel was placed in front of the rat until it reversed directions and continued circumnavigating clockwise. As behavior progressively improved, the reward was eventually reduced to one to two random locations on the track. Training continued in this environment until units were detected and experiments were initiated. For the DG and CA3 rats, training lasted on average ~16 days. For MEC and LEC rats, training lasted on average ~12 and ~11 days, respectively. All MEC and LEC experiments were conducted by Dr. Doreswamy Yoganarasimha and Geeta Rao; however, I performed all analyses presented in this dissertation.



**Figure 3.20. Stable, controlled environment for the double rotation experiment.** Picture shows the standard configuration of local and global cues in the double rotation experiment.

The double rotation experiments were conducted for 4 days on rats with DG and CA3 recordings, 10-22 days on rats with LEC recordings, and 2-10 days on rats with MEC recordings. For experiments with simultaneous recordings from DG and CA3, two sleep sessions (sleep 1 lasting 1 hr and sleep 2 lasting 30 minutes), separated by two hours when the rat was returned to its home cage, were recorded prior to the start of the experiment. During behavior, rats ran five track sessions and a final session of foraging in an open box. Track sessions consisted of three standard sessions (STD; local and global cue relationship remained constant) interleaved with two mismatch sessions (MIS; local and global cues were rotated by equal increments, but in opposite directions, producing mismatch angles of 45°, 90°, 135°, or 180°). For example, a 180° mismatch represents a 90° local cue rotation plus a 90° distal cue rotation. Mismatch angles were chosen in pseudorandom order. Results from the data recorded as rats ran on a circular track are presented in this chapter and the data from the sleep and open-field foraging sessions are presented in chapter 2. Experiments with tetrodes targeting the entorhinal cortex were identical to the DG/CA3 experiments except that only one 30 minute sleep session was recorded prior to the start of the behavior and two open field foraging sessions were recorded after the track sessions (see (Savelli et al., 2008). All experiments concluded with a 30 minute sleep session.

### **3.4c Electrophysiological Recordings**

A Cheetah Data Acquisition System (Neuralynx, Tucson, AZ) concurrently obtained up to 72 channels (18 tetrodes) of single-unit data and local EEG activity from 21 channels. Neural signals were detected simultaneously on four fine microwire electrodes (nichrome or platinum-iridium) that were wound together to form a tetrode. The signals, which were preamplified in the headstage to conduct the signal through fine-wire recording cables and a motorized 80-channel commutator, were amplified for a second time (1,000 - 5,000 gain) and optimized for recording neural spikes or local field potentials (LFPs) by filtering between 0.6 and 6 KHz or 1 Hz and 300 Hz, respectively. The

spike waveforms of units above a threshold of 30-70  $\mu\text{V}$  were sampled for 1 ms at 32 kHz, whereas LFPs were continuously sampled at 1 kHz. The rat's momentary position was tracked with an overhead camera recording a circular array of light emitting diodes (red and blue) positioned over the head of the rat and a 13 cm extension behind the head with additional diodes (green) at 30 Hz.

The tetrodes targeting DG and CA3 were independently advanced by small increments everyday for approximately three weeks. Units appearing and disappearing in conjunction with the changing patterns in LFP activity were used to assess the movement of tetrodes. After entering the CA1 layer, positioned approximately 400  $\mu\text{m}$  deeper than the cortical layer 6, tetrodes were advanced at ~40-148  $\mu\text{m}$  (the larger movements occurred after leaving CA1) each day for an additional 300  $\mu\text{m}$ . For tetrodes targeting DG, advancement was significantly reduced to 10-20  $\mu\text{m}$  per day once gamma activity and dentate spikes in the LFP were detected (Bragin et al., 1995b; Bragin et al., 1995a). These signals suggested that tetrodes were encroaching upon the granule layer of the dentate gyrus. Once units were detected during sleep, recordings were performed as the animal circumnavigated a track and foraged in an open field. A tetrode was no longer advanced after it detected units that fired on the track or open-field (see below). Any tetrode only detecting cells that were considered inactive during behavior were advanced by 10  $\mu\text{m}$ . This continued until at least five putative DG cells were simultaneously detected that fired during behavior and then tetrodes were no longer moved while the double rotation experiments were conducted. For rats 227 and 232, DG tetrodes that did not detect cells during the experiment were advanced by 10  $\mu\text{m}$  each day. For tetrodes targeting CA3, tetrodes were daily advanced by ~50  $\mu\text{m}$  in an attempt to enter the CA3 layer at the same time as DG units were detecting cells. For the entorhinal cortex, each tetrode position was estimated from the total distance it was advanced after entering the brain. The number of times each tetrode passed through a region with multiple units and a region that was relatively quiet as well as the changing patterns in LFP activity provided additional insight. The presence of theta rhythm in the LFP and units with grid cell activity indicated that tetrodes were in the MEC area. After

each day of recording, tetrodes were advanced  $\sim 150\ \mu\text{m}$  to sample different cells across the multiple days of recording. Experiments concluded, after all tetrodes stopped detecting cells, which indicated that tetrodes were in Layer I. For MEC, theta phase reversal also suggested when tetrodes were in Layer I (Alonso and Garcia-Austt, 1987b; Alonso and Garcia-Austt, 1987a). Final recording site localization was determined using histological analysis (see below).

### **3.4d Unit Isolation**

Multiple waveform characteristics (i.e., spike amplitude peak, area under the waveform, and valley depth) recorded simultaneously on the four wires, located in slightly different positions, were used to isolate single-units offline with an interactive software program that was designed in-house. A cell's isolation quality was rated 1 (very good) to 5 (poor) depending on the distance each cluster was separated from other clusters and from background noise. Cluster isolation was judged prior to examining any of the behavioral firing correlates of the cells. All cells rated as fair or better (categories 1, 2, and 3) were potentially included in all analyses (see Data Analysis for specific inclusion criteria). Cells that fired 20 spikes or more in one track session and had a mean firing rate  $< 10$  Hz were considered active excitatory cells.

### **3.4e Data Analysis**

To create ratemaps, a ratio of the number of times a cell fired and the total time the rat spent in each pixel ( $\sim 2.29\ \text{cm}^2$ ) of a  $64 \times 48$  grid was calculated. For rats 227 and 232, each square pixel was  $\sim 2.61\ \text{cm}^2$  because the distance between the camera and track was  $\sim 46\ \text{cm}$  shorter than for every other rat. Each bin of the two-dimensional ratemap was smoothed using an adaptive binning algorithm and the cell's spatial information score was computed (see (Skaggs et al., 1996)). All analyses were performed on data that excluded off track firing by filtering the data to include only spikes occurring within the outside ( $\sim 76\ \text{cm}$ ) and inside ( $\sim 56\ \text{cm}$ ) diameters of the track. Circular, two-dimensional data were linearized and every cell's mean firing rate was calculated for every one degree

of the track. The linearized firing rate maps were smoothed using a Gaussian smoothing algorithm.

Spatial population correlation matrices were created by constructing population firing rate vectors at each of the 360 locations on the track for any cell that fired more than 20 spikes in either of the two sessions being correlated and that had a mean firing rate less than 10 Hz. The firing rate vectors for each bin of the standard session were correlated to the firing rate vectors for each bin of either the mismatch session or the next subsequent standard session using a Pearson product-moment correlation. This produced a 360 x 360 correlation coefficient matrix that was partitioned into regions associated with clockwise or counterclockwise rotations. A band of high correlation located in either region shows that the population of cells rotated their firing location coherently in the corresponding direction. To quantify the location of each band, the average of the correlations was calculated for each diagonal of the correlation matrix. Briefly, the correlations along the central diagonal of the correlation matrix were averaged and then the correlation matrix was circularly shifted by one degree to the left. Determining the mean correlation along the diagonal and circularly shifting the correlation matrix continued until the correlation matrix was shifted 360 degrees and returned to the original position. For every region and mismatch angle, the greatest mean correlation and the corresponding angle were determined for all STD versus STD and STD versus MIS matrices. To show that the location of the peak correlations did not occur by chance at either the amount that the local or global cues were rotated, the linearized mismatch session ratemaps were randomly shifted by a minimum of 5 degrees for every cell. Population firing rate vectors were created from the randomized data and correlated to the population firing rate vectors from the preceding standard session. The mean correlations surrounding the amount of each rotated cue set ( $\pm 10$  bins) was calculated for correlation matrix created from the shuffled data. This procedure was repeated 1000 times and the location of the peak of the actual data was considered significant at the  $p < .01$  level if less than 10 of the



mean correlations from the shuffled data were greater than the score from the unshuffled data.

For every cell that fired more than 20 spikes in both the standard and mismatch sessions and had a mean firing rate lower than 10 Hz, the amount that each cell's firing location shifted was calculated. The linearized ratemap in the standard session (STD) was compared to the linearized ratemap for the mismatch session and quantified via a Pearson product-moment correlation. After shifting the mismatch session ratemap by 5°, it was again compared to the standard session ratemap by calculating the similarity between the two ratemaps. These comparisons continued until the mismatch ratemap was shifted back to the original position. The amount of the shift producing the highest Pearson product-moment correlation indicated the degree that the firing location was rotated. When the correlations were the highest for the bins between 5 and 175 degrees or 185 to 355 degrees, it suggested that the place fields followed the distal or local cues, respectively. For each separate region, 2 or more simultaneously recorded cells, active in both the standard and mismatch sessions, were considered part of an ensemble. For the concurrently recorded DG and CA3 ensembles, at least 2 cells from both regions (minimum of 4 cells) needed to be active in both the standard and mismatch sessions for inclusion in the analysis.

### **3.4f Histological Procedures**

After an additional nine to fourteen experiments in the DG/CA3 recorded rats or the last double rotation experiment in entorhinal cortex recorded rats, marker lesions were performed on a subset of tetrodes (10  $\mu$ A of positive current for 10 seconds). Lesions were used to help identify tracks during histological reconstruction. The following day, rats were euthanized with formalin perfused through the heart. This procedure was slightly altered for rats 227 and 232, since they were euthanized immediately after the last double rotation experiment without hippocampal lesions. Brains were coronally sliced (40  $\mu$ m) with a

freezing microtome, placed on glass microscope slides, and stained with Cresyl Violet. Images of sections were captured with a moticam 2000 camera (Motic Instruments Inc., Richmond, BC, Canada) or IC Capture DFK 41BU02 camera (The Imaging Source, Charlotte, NC, USA) that was attached to a Motic SMZ-168 stereo scope and saved as high resolution JPEG files on a Dell computer. Electrode tracks and the tetrode that generated them were identified and assigned to an anatomical layer depending on the region where the track stopped. For entorhinal cortex, the tetrode location during each experimental session was assigned to a specific layer based on reconstructing the depth of the tetrode track and assuming that the histological processing caused the neural tissue to shrink by a factor of 15%.

## **CHAPTER 4 GENERAL DISCUSSION**

### **4.1 Recap of Findings**

The current investigations have addressed the flow of information through the hippocampal formation and provided evidence for the theoretical concepts of pattern separation and pattern completion as mechanisms for storing and recalling memories. The initial study characterized the *in vivo* spatial firing properties for cells in the dentate gyrus (chapter 2) and the second study focused on the possible computations that neurons in the DG and CA3 subfields performed to encode and recall memories (chapter 3). Furthermore, a dissociation between two primary cortical inputs to the hippocampal formation was made in the third chapter, which showed that the MEC carried information about the global cue rotation, and the LEC carried information pertaining to the local cue rotation.

### **4.2 Hippocampal Circuitry**

The neural architecture of the hippocampal formation is well suited for information storage and recall. The DG and CA3 subfields receive direct input via the perforant pathway (Witter, 1993;Witter and Amaral, 2004) from layer II of the entorhinal cortex (MEC and LEC). Cells in the entorhinal cortex (~300,000) make contact with an expanded number of granule cells (~1,000,000) in the dentate (Amaral et al., 1990;Henze et al., 2000), which might permit neuronal activity patterns to be differentiated by redistributing overlapping neural activity from a smaller cell population in the entorhinal cortex into nonoverlapping activity in a much larger granule cell population (Marr, 1971;McNaughton and Morris, 1987;Rolls and Treves, 1998). After transforming perforant path input, the dentate mossy fiber projections are in a position to influence the activity of both CA3 pyramidal cells (~300,000) and mossy cells (~30,000) in the dentate polymorphic cell layer (Witter and Amaral, 2004;Morgan et al., 2007). It is

estimated that a granule cell can influence 14-28 pyramidal cells, yet each pyramidal cell receives contact from 50 granule cells (Witter and Amaral, 2004). Both the perforant path and mossy fibers innervate CA3, but the largest number of synapses results from recurrent collaterals of pyramidal cells themselves (Ishizuka et al., 1990; Li et al., 1994). Due to the Hebbian plasticity that couples coactive elements of a neuronal population, this circuitry theoretically permits the completion of the whole representation when a few neurons of the original set are activated (McNaughton and Morris, 1987). The primary efferents from CA3 (the Schaffer collaterals) project to CA1, but an additional feedback projection from CA3 pyramidal cells to hilar mossy cells exists, although it is less studied than the feedforward projection (Scharfman, 1994). In theory, the location of the mossy cells in the hippocampal circuitry is ideally suited to regulate the flow of information through the circuit because mossy cells are believed to disynaptically inhibit the output of nearby granule cells (Scharfman et al., 1990). However, direct evidence of mossy cells inhibiting nearby granule cells is lacking. The feedback projection and recurrent circuitry in the dentate complicates the simplistic trisynaptic loop model.

#### **4.3 Theories of Hippocampal Function**

The anatomical connections of the hippocampus as well as the convergence and divergence ratio of different cell types have lead to many theoretical models proposing that memory storage depends on an autoassociative attractor network and suggested that each hippocampal subfield has a different function. In theory, the hippocampus stores and recalls memories by implementing two competitive, yet complementary processes (Hopfield, 1982; Marr, 1971; Tsodyks, 1999). Pattern completion can reproduce a previously stored output pattern from a partial or degraded input pattern (Marr, 1971; Guzowski et al., 2004; McNaughton and Morris, 1987), and many models suggest that the CA3 region of the hippocampus is responsible for this phenomenon via its recurrent collaterals (Marr, 1971; McNaughton and Morris, 1987; Treves and Rolls, 1994). In contrast, pattern separation decreases

redundancy among incoming information and then outputs patterns that overlap less than the inputs, which in theory could be performed in the dentate gyrus (McNaughton and Nadel, 1990;McNaughton and Morris, 1987;Treves and Rolls, 1992;Rolls and Treves, 1994;Guzowski et al., 2004;Rolls and Kesner, 2006). In many models that implement pattern separation, expansion recoding plays a central role in permitting neuronal activity patterns to be differentiated by redistributing overlapping neural activity from a smaller population of cells into nonoverlapping activity in a much larger granule cell population (Marr, 1971;McNaughton and Morris, 1987;Rolls and Treves, 1998).

#### **4.4 Potential Mechanism for Memory Recall in CA3**

Behavioral evidence supporting the hypothesis that CA3 is necessary for pattern completion came from Gold and Kesner (2005) in a study that showed that chemically ablating CA3 decreased the ability of rats to find a reward location after reducing the number of available cues. Complementing the behavioral evidence, Nakazawa and colleagues (2002) found that mice lacking NMDA-receptors in CA3 showed behavioral deficits in a Morris water maze and that CA1 place cells showed a reduction in firing rate and place field size compared to wild-type mice when  $\frac{3}{4}$  of the extramaze cues were removed. Another experiment performed by Lee et al. (2004b) involved rotating distal and local cues in opposite directions, which created a mismatch at each point on a track between the sensory input provided from the distal and proximal cues, and found that location-specific firing of CA3 cells maintained similar patterns of activity in both conditions (i.e., CA3 performed pattern completion compared to CA1). These experimental results lend credibility to the theory that CA3 performs pattern completion, but lack the crucial test directly showing that the output of CA3 changes less than the primary inputs. To date, few studies have directly compared the output representation of CA3 with the input representations from DG, LEC, and MEC, but instead all previous studies have made assumptions as to how the manipulations may have effected each input representation.

When simultaneously recording DG and CA3, we were able to replicate the previous findings observed in Lee et al. (2004a) showing that the CA3 representation remained cohesive between a previously learned, stable environment and a cue-altered environment (chapter 3). The results were similar, even using a different set of rats and experimenters, but the task remained constant. Representations from the different subfields were compared between standard sessions (rats ran counterclockwise around the circular track for 15 laps in a familiar environment) and mismatch sessions (where the local and global cues were rotated in opposite direction by equal amounts). A significant difference between the two reports involved the comparison between hippocampal subfields. In the current study, we directly compared the CA3 representation (output) with the DG, LEC, and MEC representations (input), whereas Lee et al (2004a) compared CA1 (output) to CA3 (input). The CA3 representation showed a strong bias to cohesively follow the local cues both at the population level and with individually recorded cells (chapter 3) despite the DG input dramatically changing between the familiar and altered environments. The DG to CA3 mossy fiber projections have been proposed to be a detonator synapse that acts as a teaching signal to help CA3 encode new representations; however, under these conditions the CA3 representation remains more cohesive than DG. This suggests that CA3 may remain in the same attractor state despite a preprocessing stage where DG attempts to disambiguate the representations between the familiar and altered environments. Under the same experimental conditions, the MEC representation appeared to be coherent between the standard and mismatch sessions; however, at the larger mismatch angle (180 degrees), the representation appeared to degrade. Furthermore, the representation appeared to follow the global cues, which contrasted with the CA3 representation. For the LEC, the weak spatial signal appeared to be controlled by local cues, but the representations between the standard and mismatch sessions were not strongly correlated.

These results provide strong support for CA3 performing pattern completion. We believe that once the CA3 network learns the association

between the local and global cues, a stable attractor is established that represents the learned configurations (see standard vs. standard correlation matrices). During the probe session, one cortical input (LEC) conveys the local signal and the second cortical input (MEC) carries the information about the global cue rotation in the opposite direction. Instead of following the more coherent MEC signal, some of the CA3 neurons that were active in the attractor network are reactivated by the weak or partial LEC signal. The recurrently connected cells that underwent Hebbian plasticity during the initial learning may cause the neuronal population that encoded the familiar environment to fire. Thus, the network falls into a stable state despite receiving the conflicting MEC and DG signals.

An unresolved question is why CA3 follows the local cue rotation and the weak LEC signal instead of the global cue rotation and the more cohesive MEC signal. One possible explanation is based on the sequence of events at the start of the mismatch session. Between recordings sessions, rats sat on a pedestal in a room adjacent to the recording environment as the experimenters rearranged the sets of cues. The rats were then disoriented, to disrupt the rat's internal sense of direction (Knierim et al., 1995; Jeffery and O'Keefe, 1999), and brought into the cue-altered environment in an opaque box. In theory, the first moment that the rat could detect the dissociation between the alignment of the local and global cues occurred when it was placed onto the track to begin the session. When the rat was placed onto the track, presumably it paid attention to the local cues at the onset of the experiment. The LEC, which has been suggested to be gated by attention (Burwell, 2000), would then signal the local cue rotation to CA3. This partial signal from LEC may be sufficient to activate enough of the original population of CA3 cells that were active during the familiar, standard environment to then pattern complete the whole representation with a counterclockwise bias. A combination of computational and experimental work would be needed to test this prediction. The critical test would require controlling which input (local or global) CA3 initially received and then determining whether CA3 followed the corresponding cues. This is rather trivial in a simulation;

however, experimentally it is more challenging since it involves forcing a rat to pay attention to either the local or global cues at the onset of the experiment and showing that the animal performed the appropriate behavior.

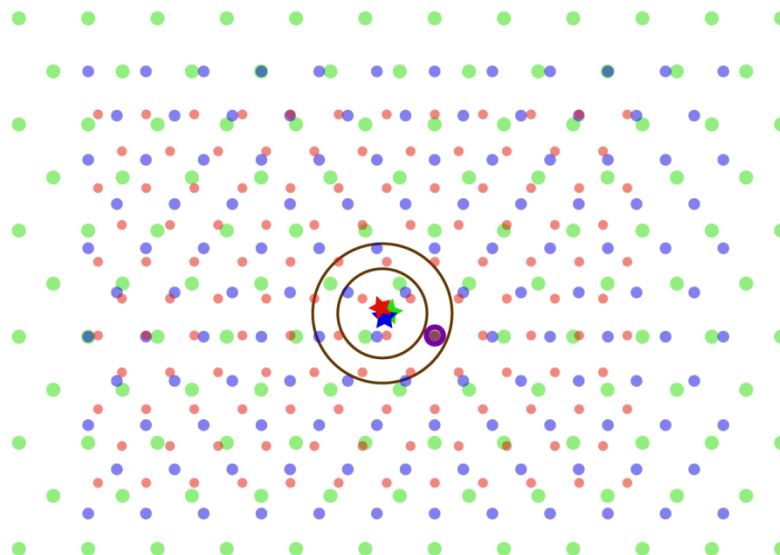
An alternative explanation for the CA3 representation being controlled by the local cues may result from the properties of individual CA3 cells during a rat's stereotyped behavior on the circular track. Lee et al. (2004b) showed that the center of CA3 place fields shifted backwards between the first and last lap (lap number 15) during the initial experience in the cue-altered environment. This backward shift in conjunction with the weak local cue signal, conveyed from the LEC, may cause the originally active CA3 population encoding the learned environment might be reactivated and follow the local cues. This idea can be addressed with two experiments. First, the rat's stereotyped trajectory should be altered such that it runs counterclockwise on the circular track. In this condition, the center of the CA3 place fields may shift backwards in a counterclockwise direction and cause the CA3 fields to follow the global cues. To complement this experiment, one should change the direction of the cue rotations (i.e., global and local cues are rotated counterclockwise and clockwise, respectively) while rats ran clockwise around the track. Under this condition, the center of the CA3 place fields would likely shift backwards in a clockwise direction similar to Lee et al. (2004b) and follow the global cues instead of the local.

In chapter three, the argument was made that CA3 performs pattern completion because its representation is more cohesive than the DG and LEC representations. While the MEC representation is fairly cohesive, the MEC population tends to follow the global cues, which contrasts with the CA3 cells following the local cues. Therefore, CA3 is unlikely to passively relay the results of information processing from the MEC. However, there is a possibility that the counterclockwise response of a CA3 cells can arise from combining the weak local signal from LEC and the global signal from the MEC. Fyhn et al. (Fyhn et al., 2007) reported that hippocampal place cells remap when the alignment of grid cells has shifted, whereas the location, but not firing rate, remained constant



when the underlying grid cell activity was stable. McNaughton (2006), O'Keefe and Burgess (2005), and Solstad (2006) have modeled the transformation from grid cells to place cells using a simple summation rule such that a hippocampal place cell fires only when the overlapping vertices of multiple grid cells are aligned in a single location. For grid cells in the MEC, the size and distance between each vertex of the grid increases along the dorsal-ventral axis (Hafting et al., 2005). Figure 4.1 illustrates this feature by showing three grid cells (cell 1 is red and the most dorsal of the three; cell 2 is blue and intermediate between cell 1 and 3; cell 3 is green and the most ventral of the three). All three cells fire in a repeating grid-like pattern, which covers the entire environment, and each point of the grid representing a vertex of an equilateral triangle. A circular track is located in the center of the environment and only one region on this confined space has three overlapping fields. In this simplified schematic, the three overlapping vertices would generate a place field (purple circle) in one of the CA3 cells during a standard session. Figure 4.1b represents the underlying grid firing pattern during a 90° mismatch session. All three grid cells were controlled by the global cues and rotated clockwise by 45 degrees; however, the pivot point for rotation differed slightly for all three cells. By allowing the grids to rotate around independent points, three vertices from the original three cells again overlap corresponding to a location that rotated 45° counterclockwise. This is one method to produce a counterclockwise rotation in a CA3 cell from a clockwise rotation in a small set ( $n=3$ ) of MEC cells. The likelihood that enough of the underlying MEC distribution is rotating at different pivot points to cause the plurality of CA3 cells to respond with a counterclockwise bias is highly unlikely. Running simulations to determine how often this occurs would be informative and address the question of whether is possible explanation or an alias of sampling. If the simulations show that the clockwise rotation of MEC cells frequently produces a counterclockwise bias in the population of CA3 cells, then coupling the local signal from the LEC with the MEC representation that followed the global cues might be enough to active the same set of CA3 place

A



B

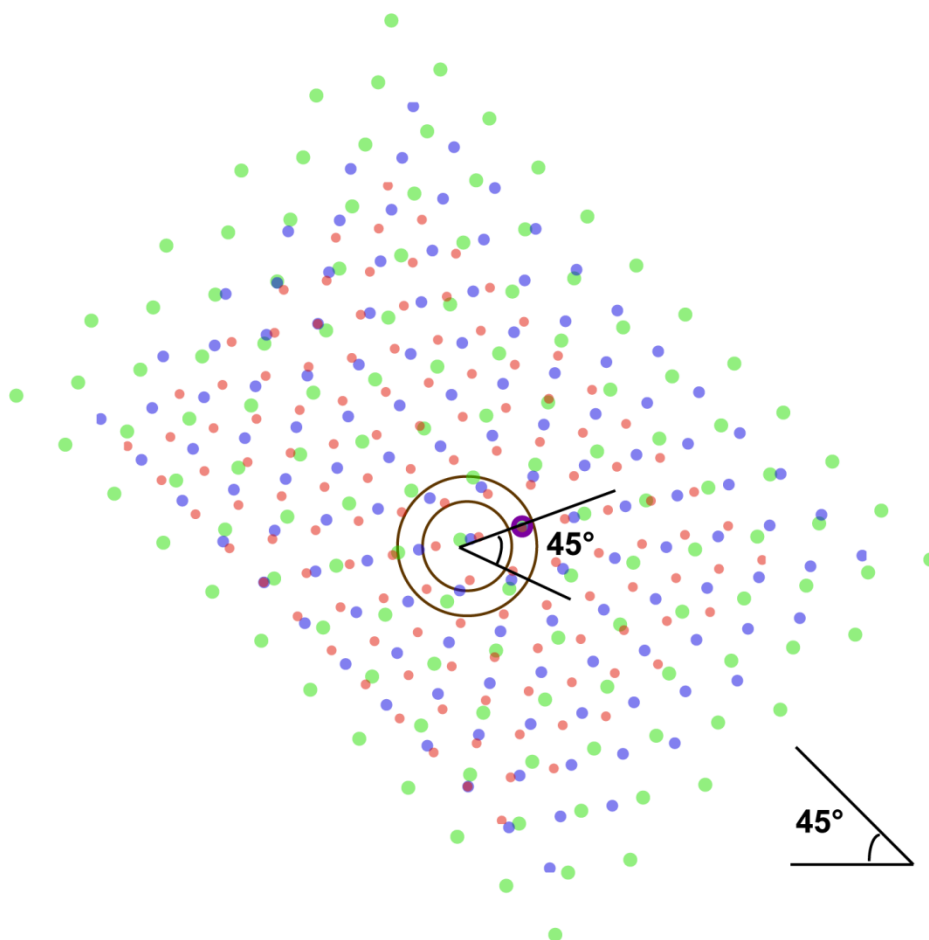


**Figure 4.1. Potential Method for a Counterclockwise Rotation in a CA3 Cell.**

(A) Schematic showing transformation from grid cell input to place cell output in the standard environment. Three grid cells have firing patterns, with vertices of different spacing and size (green, blue, and red), covering a large spatial area. When the vertices from the three grid cells align on the track (brown rings), a place field for one cell, indicated by a purple circle, is generated. Colored stars represent pivot points for underlying grids. (B) During a  $90^\circ$  mismatch session, the underlying grid cells rotate their firing pattern by  $45^\circ$  to follow the global cues; however, the point of rotation of all three grid cells is slightly offset. Some of the MEC cells may appear to rotate coherently, while other MEC neurons may appear to rotate and shift their fields. Despite each grid cell having a different point of rotation, three vertices still align at a point that has appeared to rotate  $45^\circ$  in the opposite direction. Coupling the input from the three grid cells with a weak counterclockwise signal from the LEC may be sufficient to drive the place cell that was originally active in the standard environment.

cells that were originally active in the standard session, but cause the CA3 cells to rotate their firing locations in a counterclockwise direction. This potential mechanism would not address the question of CA3 performing pattern completion.

#### **4.5 Characterizing the Spatial Firing of Cells from the Dentate Gyrus**

Before diving into a discussion about the functional role that the dentate gyrus plays in memory, a brief discussion regarding the classification of spatial firing for the different cell types in this under-characterized hippocampal subfield is warranted. An extensive body of literature examining the *in vitro* electrophysiological properties of different cell types of the dentate gyrus exists compared to *in vivo* studies from freely moving animals. The resting membrane potential of granule cells has been reported as extremely hyperpolarized (Lambert and Jones, 1990; Spruston and Johnston, 1992; Staley et al., 1992; Soltesz and Mody, 1994; Ylinen et al., 1995; Penttonen et al., 1997) compared to mossy cells (Scharfman and Schwartzkroin, 1988; Scharfman, 1992; Scharfman, 1994; Lubke et al., 1998; Henze and Buzsaki, 2007). This difference in resting membrane potential could contribute to differences observed in the sparseness, as reflected in the firing rates and ratio of active cells to sleep clusters, between cells recorded on tetrodes detecting units with only single fields and those detecting cells with multiple fields. Our results indicated that cells recorded on tetrodes with active cells firing in single locations do indeed have a lower mean firing rate during sleep and a lower percentage of active cells than cells recorded on tetrodes detecting active cells with multiple fields. The extremely hyperpolarized resting membrane potential of granule cells would cause granule cells to be more difficult to excite than mossy cells and fire at a lower rate. The extremely hyperpolarized resting membrane potential might further explain why the group of cells with a lower percentage of active cells fire in a single location. In contrast, exceeding the threshold for triggering a spike in cells with a higher resting membrane potential would likely occur more often in

multiple locations in the environment, thus it may account for the spatial firing observed in numerous places. It is possible that the functional properties reported for cells recorded on tetrodes detecting units with multiple fields might describe new born granule cells, as suggested by Alme et al. (2010). Nothing in this report disputes this theory.

One of the most salient distinctions between granule cells and mossy cells recorded in slice is the capacity to fire in burst. Granule cells recorded in slice do not fire trains of spikes either in response to a pulse of current or spontaneously, whereas in mossy cells bursting is prevalent (Scharfman, 1992). After injecting a depolarizing current step, granule cells show spike frequency adaptation in which the cell initially spikes but does not continue for the duration of the pulse. In contrast, mossy cells (both in slice and anesthetized animals) continue spiking through the duration of the pulse. Our results show that cells recorded on tetrodes detecting a cell with a single field are less prone to burst during sleep and behavior than cells recorded on tetrodes detecting a cell with multiple fields. These results resemble those reported in slice; therefore, we believe granule cells tend to fire in single locations and mossy cells tend to fire in multiple locations.

Previous studies describing the spatial firing pattern in the dentate gyrus have reported that putative granule cells fire in multiple locations that are distributed irregularly across the environment (Jung and McNaughton, 1993; Skaggs et al., 1996; Gothard et al., 2001; Leutgeb et al., 2007). In contrast, the present study reports that putative excitatory cells in the polymorphic cell layer fire in multiple places, dispersed irregularly throughout the environment, whereas the spatial firing of putative granule cells is confined to a single region. These conclusions are in part based on separating the data into two groups depending on the number of fields and then comparing the quantity of active cells to sleep clusters. In all subfields of the hippocampus, the majority of units are silent during behavior and these cells are only detected during sleep or under anesthesia (Ranck, Jr., 1973; Thompson and Best, 1989; Wilson and McNaughton, 1993; Skaggs et al., 1996). Similarly, the vast majority of granule

cells did not express the immediate-early gene *Arc* after behavioral exploration, which suggests that these cells were silent during behavior (Chawla et al., 2005). In this study, extended periods of deep sleep, unlike CA1 where quiet wakefulness and ripples are sufficient to detect sleep clusters, were recorded under the assumption that it would facilitate the detection of the extremely sparse firing population of granule cells. The pioneering study from Leutgeb et al. (2007) do not specifically describe the spatial firing properties of cells that were recorded on tetrodes with more than six sleep clusters. One possibility is that Leutgeb et al. (2007) did not record enough deep sleep to detect the extremely sparse firing granule cells and instead recorded the more active cells in the hilus. Another pioneering study, Jung and McNaughton (1993) stimulated the perforant path (primary input to the molecular layer of the dentate gyrus) to aid in the identification of putative granule cells and observed cells with both single and multiple fields. However, this technique does not exclude the possibility that cells from the polymorphic cell layer were recorded in this study, since Scharfman (1991) reported some hilar cells have dendrites in the molecular layer that can be excited by perforant path stimulation at a lower threshold for synaptic activation than granule cells.

In the current report, we showed that approximately 22% of putative granule cells were active while the animal foraged in a large environment. This percentage is considerably larger than previously reported (Barnes, 1990;Chawla et al., 2005). One potential explanation may be that many of the cells were silent during sleep despite recording for prolonged periods of time. To observe a percentage as low as 2%, one would need to record one active cell out of every 50 detected during sleep. It was observed that some tetrodes had numerous clusters during sleep, but no behaviorally active cells. These sleep clusters were not included in the ratio of active to sleep cells, since the spatial firing pattern of active cells was used to separate the two groups of cells. Including these cells in the sparseness index might have increased the similarity to the proportions that were previously reported. Another possibility contributing to the higher percentage of active cells may have been the method used to classify cells as

single or multiple fields. Using the current method based on peak rate and contiguous pixels, two fields in close proximity but with inflections would be counted as a single field. This misclassification would increase the percentage of active cells. To avoid miscategorizing cell types into an arbitrary taxonomy of single or multiple fields, one would need to unequivocally identify the cells being recorded. This is further complicated, not only because there are multiple excitatory cells in the dentate gyrus, but this region undergoes lifelong neurogenesis in which new cells are incorporated into the existing hippocampal circuitry (Zhao and Overstreet-Wadiche, 2008) that might have different spatial firing properties than the mature granule cells and mossy cells. Alme et al., (2010) report that a small excitable population of granule cells might correspond to the most recently generated cells, which is a distinct possibility. Nothing reported in the current study disputes this claim; however, we have strong evidence that the majority of cells recorded deep in the polymorphic layer show spatial firing in multiple locations throughout an enclosure. To unambiguously determine the properties of the complicated local circuitry in the dentate gyrus, it will likely require using molecular tools to specifically target the three types of excitatory cells in the dentate gyrus in combination with *in vivo* electrophysiological records from freely moving animals.

The anatomy of the hippocampus suggests that mossy cells play a central role in the recurrent circuitry within the dentate gyrus as well as in the only excitatory feedback pathway in the classic “trisynaptic loop” (Witter and Amaral, 2004;Scharfman, 1994;Buckmaster and Schwartzkroin, 1994;Jackson and Scharfman, 1996;Buckmaster et al., 1996;Wenzel et al., 1997). Given estimates of 1,000,000 granule cells and 30,000 mossy cells (Morgan et al., 2007), one can estimate that each mossy cell receives powerful, converging feed-forward excitation from as many as 400 granule cells. Early in the 1990’s Ishizuka et al. (1990) and Li et al. (1994) showed that the axon collaterals of dye injected CA3c pyramidal cells were present in the dentate gyrus polymorphic layer, which was later shown to be a monosynaptic connection capable of producing small depolarizations in mossy cells (Scharfman, 1994). The mossy cells are a node

for the convergence of excitatory inputs; however, these cells are also heavily innervated by perisomatic inhibition (Acsady et al., 2000; Murakawa and Kosaka, 2001) that would prevent mossy cells from spiking in response to every excitatory input. In the behaving animal, the input from CA3 typically represents a single location in the environment. Similarly, the results in the present study suggest that the firing pattern of putative granule cells represent single locations, whereas putative excitatory cells in the polymorphic layer tend to fire in multiple locations. This pattern of multi-punctate fields might be explained from the convergence of input representing single locations in the environment (Figure 4.2). In our proposed model, a subset of active granule cells would fire in a single location in the environment, which would drive the downstream mossy cell to fire in multiple locations that corresponded to the location of the active granule cells. Since a mossy cell may be functionally connected to 200-400 granule cells, 2% of which have been reported to be active in a given context (Chawla et al., 2005), it can be estimated that in any environment a mossy cell will receive powerful input from 2-8 active granule cells, thereby causing the mossy cell to fire in 2-8 locations and multiple contexts. These numbers would likely increase when considering the impact of the excitatory feedback from CA3c cells.

#### **4.6 Mechanism for Memory Storage in the Dentate Gyrus**

Many models that concentrate on the mnemonic function of memory storage suggest that the dentate gyrus creates a sparse representation from a distributed neural code in the cortex. This process of expansion recoding permits neuronal activity patterns to be differentiated by redistributing overlapping neural activity from a smaller population of cells into nonoverlapping activity in a much larger granule cell population (Marr, 1971; McNaughton and Morris, 1987; Rolls and Treves, 1998). Although we cannot address directly the notion that the DG performs pattern separation in chapter 2, it is noteworthy that one population of cells show sparse encoding, which is an integral part of the longstanding notion of DG as a pattern separator. For chapter 3, the analyses were restricted to neurons in each region that were active in a least one session.



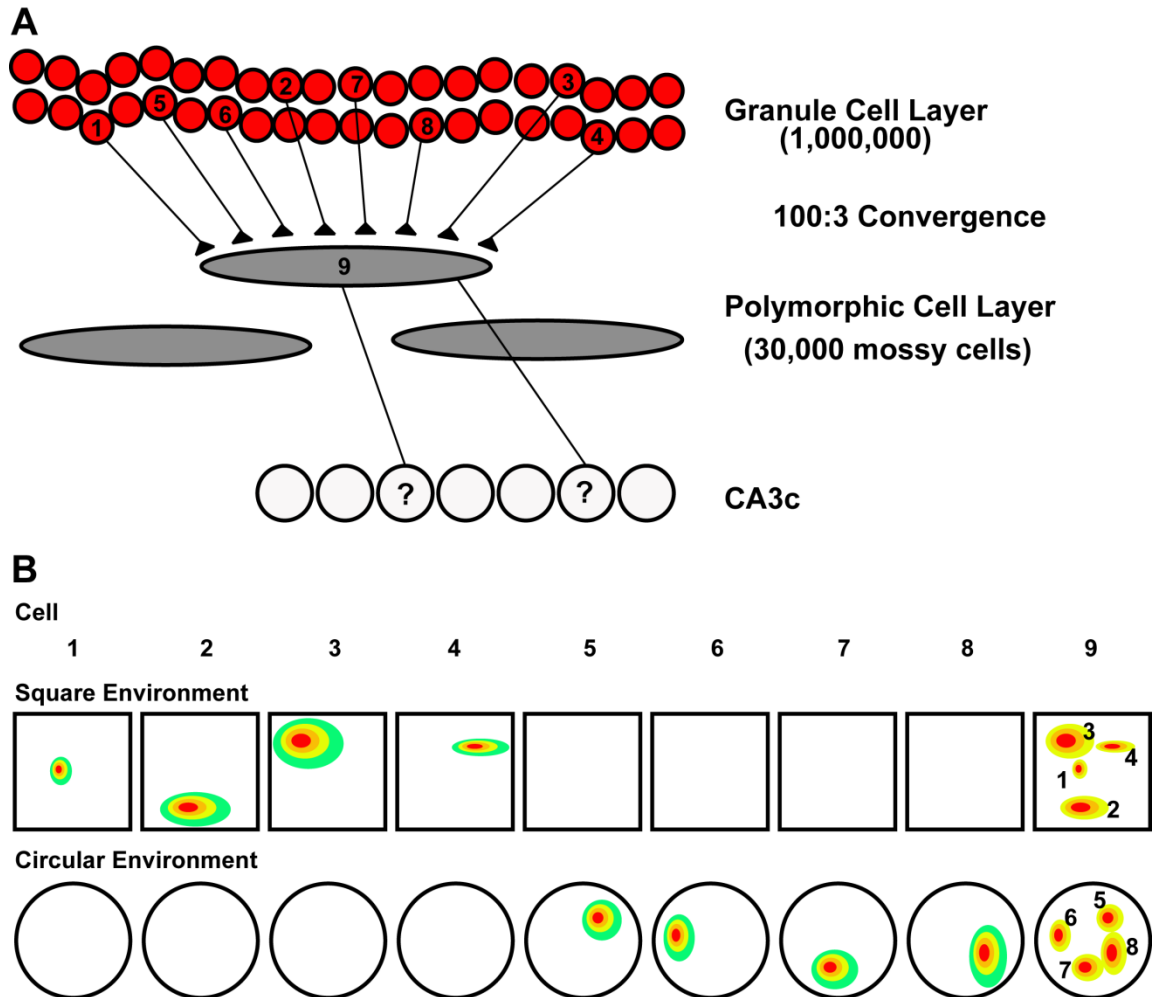


**Figure 4.2. Model of Hippocampal Local Circuitry.** (A) Illustration of dentate gyrus and CA3c neural network. The mossy cells (gray; ~30,000 cells) receive a powerful feedforward input from the granule cells (red; ~1,000,000) and a feedback input from the CA3c pyramidal cells (white). The feedforward and feedback signals converge onto a less densely packed region (convergence ratios of 100:3 from granule cells to mossy cells and unknown for CA3c pyramidal cells to mossy cells). For simplicity, one mossy cell (9) is innervated by a small subset of granule (1-8) and pyramidal cells. (B) Hypothetical examples of spatial firing for granule and mossy cells in a square and circular environment. The multi-punctate spatial firing pattern of the mossy cell (9) could depend on which set of inputs are active in the environment (either granule cells 1-4 with single fields in the square environment or granule cells 5-8 with single fields in the circular environments). In theory, each mossy cell would fire in multiple different contexts, since these cells receive powerful input from an estimated 200-400 granule cells.

These analyses ignore the number of cells that were silent while the animals circumnavigated the track, which decreases the sparseness. Nonetheless, we still show in Chapter 3 that the DG representations of two similar environments are less correlated than the cortical input representations. An attempt was made to partition the DG into individual components (i.e. granule cells and hilar cells), but the number of cells in each group was too small to make any statistical conclusions. However, the spatial population correlation matrices for both groups appeared decorrelated; therefore, we combined all recordings from the DG into one region. Further support for combining all cell types from the dentate was provided from behavioral and computational studies. Hunsaker and colleagues (2008) showed that lesions to both the dentate and to a lesser extent CA3c impaired an animal's ability to detect subtle changes in the distance between two objects in an environment and concluded that granule, hilar, and CA3c cells acted as a functional unit to perform pattern separation. This theory has been further extended in computational work from Myers and Scharfman (2009), who created a model of dentate gyrus function in which mossy cell activity directly affected the efficacy of pattern separation (i.e., increasing or decreasing the firing rate of mossy cells could increase or decrease pattern separation). Pattern separation would be significantly facilitated by having mossy cells fire in multiple locations in an environment. Since mossy cells feedback to basket cells that silence the original granule cell input, the repetitive mossy cell activity distributed across the environment might enhance the globally distributed inhibition of basket cells onto granule cells (Struble et al., 1978; Sik et al., 1997; Andersen et al., 2006), thus decreasing the percentage of overlapping activity in the granule cell population and amplifying pattern separation.

The dentate gyrus, in theory, could use multiple mechanisms to change its representation from one condition to the next. One mechanism that the dentate gyrus may use to perform pattern separation is the classic theory of expansion recoding. Originally proposed by Marr (1969) to explain how to decrease the overlap between a similar set of input patterns in a small population of cells that

project to a larger population of cells in the cerebellum, this theory was later expanded to the dentate gyrus of the hippocampus (McNaughton and Morris, 1987;McNaughton and Nadel, 1990). The dentate gyrus could perform pattern separation and prevent spurious recall by producing nonoverlapping, sparse representations from entorhinal cortex input (McNaughton and Morris, 1987;McNaughton and Nadel, 1990). This would be expressed as remapping (i.e. cells that start or stop firing between the standard and mismatch sessions). Indeed, the majority of cells in the dentate remapped (i.e. started or stopped firing during the mismatch session), which was a larger proportion than either the MEC or LEC. Another method for enhancing pattern separation is to increase the variability in the responses of individual cells to the cue manipulations. Individual cells that fired in sequential standard and mismatch sessions were not controlled by a specific cue set and were never significantly clustered. Even simultaneously recorded DG cells showed a variety of responses to the cue rotations and rarely were the mean vectors significantly larger than chance. Both of these mechanisms are likely being used by the dentate to disambiguate similar inputs and create different representations.

Leutgeb et al. (2007) found that DG cells with multiple fields could independently change the firing rates of each field as the shape of the environment was altered. The authors argued the changing patterns in firing rate could enhance the decorrelated state of the ensembles and differentiate each environment. This additional mechanism to express pattern separation cannot be excluded by the current study for the DG cells with multiple fields. It is a distinct possibility that for cells with multiple fields, each subfield may be independently controlled by either the global or local cues and, during the mismatch session, might rotate in either direction. This would alter the representation between the standard and mismatch sessions. Unfortunately, this could not be tested due to the difficulties of unambiguously tracking the fields during the mismatch sessions.

#### **4.7 Dissociation of Input Streams**

Hargreaves et al. (2005) reported that in an open-field environment MEC neurons convey significantly more spatial information than LEC neurons. Complementing this study, Yoganarasimha et al. (2010) showed that the disparity between hippocampal input regions remained even when the simple environment was switched to a cue-rich environment. Furthermore, the local field potentials in the MEC show a stronger theta oscillation than the local field potentials in the LEC (Deshmukh et al., 2010). The present report further dissociates the two primary inputs to the hippocampus by showing a weak local-cue-related signal in the LEC population, despite individual LEC cells showing poor spatial tuning, that contrasted with the global-cue-related signal in the MEC population. This study provides one of the first reported functional correlates for LEC neurons in freely moving animals. To my knowledge, only one other report has provided a functional role for the LEC neurons in foraging rats; Deshmukh and Knierim (in preparation) showed that the spatial information score of LEC neurons is higher in the presence of objects than without objects. Some LEC cells fired near the objects and other neurons developed place fields without an obvious relationship to any of the objects. These findings support the notion that two streams of information are transmitted to the hippocampus; a spatial “where” signal conveyed by the MEC and a nonspatial “what” signal conveyed by the LEC.

A longstanding view proposes that the spatial metric in the hippocampus results from a path integration mechanism (McNaughton et al., 1996). Originally, McNaughton (1996a;1996a;1996) and Whishaw (1999;1996;1997;1998;1998) believed that path integration was occurring in the hippocampus proper; however, after the landmark discovery of grid cells in the MEC it is now believed that this process occurs one synapse upstream of the hippocampus (O'Keefe and Burgess, 2005;McNaughton et al., 2006;Fuhs and Touretzky, 2006). The generation of the internal representation of space is thought to be derived from self-motion and directional heading without the use of external cues (i.e., distant

landmarks); however, these cues are theoretically used to orient the spatial representation. In the current study, evidence shows that the MEC population follows the global cue rotation. This, however, was expected because of the underlying neural circuitry that conveys a head direction signal (anterior dorsal thalamic nucleus → postsubiculum → MEC) and evidence showing that the preferred firing direction of head direction cells in the anterior dorsal thalamic nucleus was tightly coupled to the global cue rotation when rotating the local and global cues in equal, but opposite directions (Yoganarasimha et al., 2006). Furthermore, numerous reports indicate that rotating external cues in isolation controls the preferred firing direction of head direction cells in both the anterior dorsal thalamic nucleus and postsubiculum (Taube et al., 1990b; Taube and Burton, 1995; Taube, 1995).

#### **4.8 Overview Summary**

This dissertation examines the flow of information through the hippocampal formation and suggests potential mechanisms that each subfield may use to encode and recall memories. Many studies have ascribed functions to the different hippocampal subfields based on assumed properties of the upstream structure and rarely make direct comparisons between the input and output representations. The initial results from my dissertation describe the previously under-characterized spatial firing properties of neurons in the DG, which is one of the primary inputs into CA3. Strong evidence is provided that shows two populations of cells in the DG convey spatial information. One group has lower mean rates in sleep and behavior, a lower propensity to burst, more simultaneously recorded cells, and fires in a single location in an environment. The second group has higher firing rates in sleep and behavior, a higher propensity to burst, less simultaneously recorded cells, and fires in multiple locations in an environment. Based on previously characterized firing properties of granule and hilar cells recorded in slice and anesthetized animals, we concluded that cells with single fields were likely granule cells and cells with multiple fields were likely hilar cells. Despite reporting two groups of cells with

different firing properties in the dentate, data were combined because each group appeared to change representations between a familiar environment and cue-altered environment. Furthermore, previous reports have suggested that the local circuitry of the dentate works as a functional unit to orthogonalize similar inputs. To address the computations performed in the DG and CA3 networks, the input and output representations were compared between a learned, familiar environment and a cue-altered environment (see Figure 4.3). Evidence was provided that showed the dentate gyrus decreased the overlap between similar measured inputs and the DG representation was less cohesive than the representations in the MEC and LEC. This was theoretically achieved through the implementation of multiple mechanisms, all of which facilitate pattern separation. First, the ratio of presumed active to silent granule cells is small, thus creating a sparse representation. Second, more cells remapped in the DG network than in the distributed cortical networks. Finally, ensembles of cells were less coherent and never controlled by one set of cues. In contrast to DG, the population of CA3 cells appeared more coherent than its primary inputs. Despite a fairly cohesive representation in the MEC conveying information about the global cue rotation, the CA3 network followed the partial, weak local signal in the LEC. These results provide a direct, quantitative comparison between hippocampal input and output representations and support the longstanding theoretical models that the dentate gyrus performs pattern separation and that CA3 performs pattern completion.

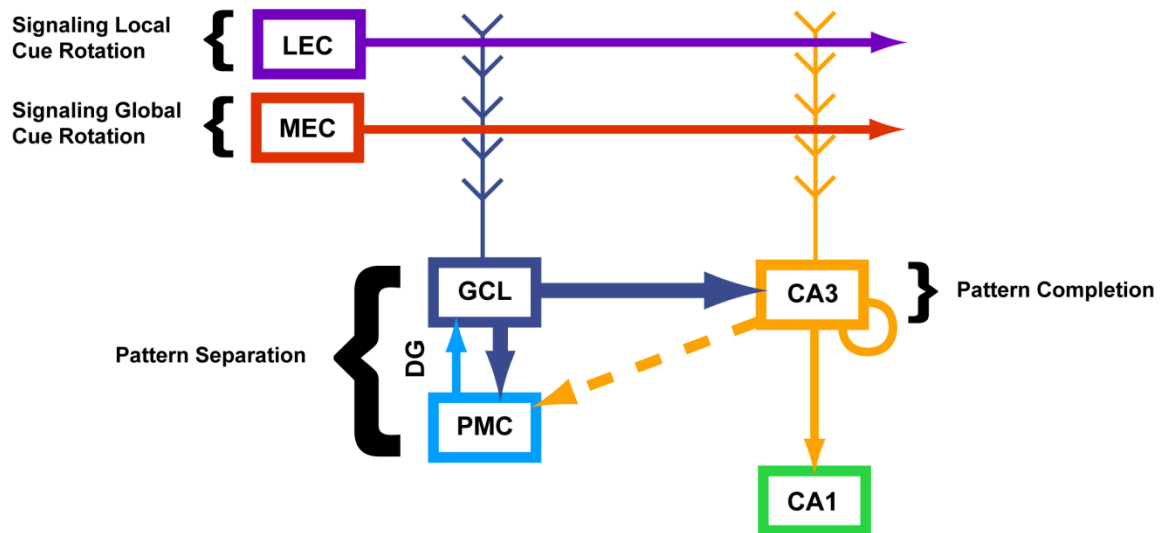


**Figure 4.3. Summary of Mechanisms for Storing and Recalling Memories.**

During the double rotation experiment, the CA3 representation remains more coherent than the combined input from MEC, LEC, and DG. The MEC and LEC signal a rotation in the global and local cues, respectively. Despite the conflicting signals, the weak LEC signal may be sufficient to activate a few CA3 neurons in the attractor network representing the learned environment. Because of the previous learning between recurrently connected CA3 cells, other previously coactive neurons may be reactivated and generate a more cohesive representation than seen in the input structures. Meanwhile, the DG network attempts to disambiguate the altered and learned environments by creating different representations. The DG may create a sparse code in the granule cell layer from a distributed code in the cortex, change the population of active cells (i.e., remap), independently alter the location/rate of each field for cells with multiple fields (suggested by Leutgeb et al. (2007), and respond to either the global or local cue sets in order to change the representations between environments.

## BIBLIOGRAPHY

1. Acsady, L., I. Katona, F. J. Martinez-Guijarro, G. Buzsaki, and T. F. Freund. 2000. Unusual target selectivity of perisomatic inhibitory cells in the hilar region of the rat hippocampus. *J. Neurosci.* 20:6907-6919.
2. Aggleton, J. P., P. R. Hunt, and J. N. Rawlins. 1986. The effects of hippocampal lesions upon spatial and non-spatial tests of working memory. *Behav. Brain Res.* 19:133-146.
3. Aigner, T. G., D. L. Walker, and M. Mishkin. 1991. Comparison of the effects of scopolamine administered before and after acquisition in a test of visual recognition memory in monkeys. *Behav. Neural Biol.* 55:61-67.
4. Aimone, J. B., W. Deng, and F. H. Gage. 2010. Adult neurogenesis: integrating theories and separating functions. *Trends Cogn Sci.* 14:325-337.
5. Aimone, J. B., J. Wiles, and F. H. Gage. 2006. Potential role for adult neurogenesis in the encoding of time in new memories. *Nat. Neurosci.* 9:723-727.
6. Alme, C. B., R. A. Buzzetti, D. F. Marrone, J. K. Leutgeb, M. K. Chawla, M. J. Schaner, J. D. Bohanick, T. Khoboko, S. Leutgeb, E. I. Moser, M. B. Moser, B. L. McNaughton, and C. A. Barnes. 2010. Hippocampal granule cells opt for early retirement. *Hippocampus* 20:1109-1123.



7. Alonso, A. and E. Garcia-Austt. 1987a. Neuronal sources of theta rhythm in the entorhinal cortex of the rat. I. Laminar distribution of theta field potentials. *Exp. Brain Res.* 67:493-501.
8. Alonso, A. and E. Garcia-Austt. 1987b. Neuronal sources of theta rhythm in the entorhinal cortex of the rat. II. Phase relations between unit discharges and theta field potentials. *Exp. Brain Res.* 67:502-509.
9. Alvarado, M. C. and J. W. Rudy. 1995a. A comparison of kainic acid plus colchicine and ibotenic acid-induced hippocampal formation damage on four configural tasks in rats. *Behav. Neurosci.* 109:1052-1062.
10. Alvarado, M. C. and J. W. Rudy. 1995b. Rats with damage to the hippocampal-formation are impaired on the transverse-patterning problem but not on elemental discriminations. *Behav. Neurosci.* 109:204-211.
11. Alvarez, P., S. Zola-Morgan, and L. R. Squire. 1995. Damage limited to the hippocampal region produces long-lasting memory impairment in monkeys. *J. Neurosci.* 15:3796-3807.
12. Amaral, D. G., N. Ishizuka, and B. Claiborne. 1990. Neurons, numbers and the hippocampal network. *Prog. Brain Res.* 83:1-11.
13. Amaral, D. G. and M. P. Witter. 1989. The three-dimensional organization of the hippocampal formation: a review of anatomical data. *Neuroscience* 31:571-591.

14. Anagnostaras, S. G., S. Maren, and M. S. Fanselow. 1999. Temporally graded retrograde amnesia of contextual fear after hippocampal damage in rats: within-subjects examination. *J. Neurosci.* 19:1106-1114.
15. Andersen, P., R. G. Morris, D. G. Amaral, T. Bliss, and J. O'Keefe. 2006. *The Hippocampus Book*. Oxford University Press.
16. Asanuma, H. and I. Rosen. 1972. Topographical organization of cortical efferent zones projecting to distal forelimb muscles in the monkey. *Exp. Brain Res.* 14:243-256.
17. Barefoot, H. C., C. J. Maclean, H. F. Baker, and R. M. Ridley. 2003. Unilateral hippocampal and inferotemporal cortex lesions in opposite hemispheres impair learning of single-pair visual discriminations as well as visuovisual conditional tasks in monkeys. *Behav. Brain Res.* 141:51-62.
18. Barnes, C. A. 1990. Effects of aging on the dynamics of information processing and synaptic weight changes in the mammalian hippocampus. *Prog. Brain Res.* 86:89-104.
19. Bartlett, F. C. 1932. *Remembering: A Study in Experimental and Social Psychology*. University Press, Cambridge.
20. Baxter, M. G. and A. A. Chiba. 1999. Cognitive functions of the basal forebrain. *Curr. Opin. Neurobiol.* 9:178-183.

21. Baxter, M. G. and E. A. Murray. 2001. Opposite relationship of hippocampal and rhinal cortex damage to delayed nonmatching-to-sample deficits in monkeys. *Hippocampus* 11:61-71.
22. Bayer, S. A. 1983. 3H-thymidine-radiographic studies of neurogenesis in the rat olfactory bulb. *Exp. Brain Res.* 50:329-340.
23. Bekhterev, V. 1900. Demonstration eines Gehirns mit Zerstörung der vorderen und inneren Theile der Hirnrinde beider Schläfenlappen. *Neurol Zentralbl* 19:990-991.
24. Binder, J. R., P. S. Bellgowan, T. A. Hammeke, E. T. Possing, and J. A. Frost. 2005. A comparison of two fMRI protocols for eliciting hippocampal activation. *Epilepsia* 46:1061-1070.
25. Blackstad, T. W. 1956. Commissural connections of the hippocampal region in the rat, with special reference to their mode of termination. *J. Comp Neurol.* 105:417-537.
26. Blackstad, T. W., K. Brink, J. Hem, and B. Jeune. 1970. Distribution of hippocampal mossy fibers in the rat. An experimental study with silver impregnation methods. *J. Comp Neurol.* 138:433-449.
27. Bontempi, B., C. Laurent-Demir, C. Destrade, and R. Jaffard. 1999. Time-dependent reorganization of brain circuitry underlying long-term memory storage. *Nature* 400:671-675.

28. Bower, M. R., D. R. Euston, and B. L. McNaughton. 2005. Sequential-context-dependent hippocampal activity is not necessary to learn sequences with repeated elements. *J. Neurosci.* 25:1313-1323.
29. Bragin, A., G. Jando, Z. Nadasdy, J. Hetke, K. Wise, and G. Buzsaki. 1995a. Gamma (40-100 Hz) oscillation in the hippocampus of the behaving rat. *J. Neurosci.* 15:47-60.
30. Bragin, A., G. Jando, Z. Nadasdy, L. M. van, and G. Buzsaki. 1995b. Dentate EEG spikes and associated interneuronal population bursts in the hippocampal hilar region of the rat. *J. Neurophysiol.* 73:1691-1705.
31. Bucci, D. J., R. G. Phillips, and R. D. Burwell. 2000. Contributions of postrhinal and perirhinal cortex to contextual information processing. *Behav. Neurosci.* 114:882-894.
32. Buckmaster, C. A., H. Eichenbaum, D. G. Amaral, W. A. Suzuki, and P. R. Rapp. 2004. Entorhinal cortex lesions disrupt the relational organization of memory in monkeys. *J. Neurosci.* 24:9811-9825.
33. Buckmaster, P. S. and A. L. Jongen-Relo. 1999. Highly specific neuron loss preserves lateral inhibitory circuits in the dentate gyrus of kainate-induced epileptic rats. *J. Neurosci.* 19:9519-9529.
34. Buckmaster, P. S. and P. A. Schwartzkroin. 1994. Hippocampal mossy cell function: a speculative view. *Hippocampus* 4:393-402.

35. Buckmaster, P. S., B. W. Strowbridge, and P. A. Schwartzkroin. 1993. A comparison of rat hippocampal mossy cells and CA3c pyramidal cells. *J. Neurophysiol.* 70:1281-1299.
36. Buckmaster, P. S., H. J. Wenzel, D. D. Kunkel, and P. A. Schwartzkroin. 1996. Axon arbors and synaptic connections of hippocampal mossy cells in the rat in vivo. *J. Comp Neurol.* 366:271-292.
37. Burwell, R. D. 2000. The parahippocampal region: corticocortical connectivity. *Ann. N. Y. Acad. Sci.* 911:25-42.
38. Cacucci, F., C. Lever, T. J. Wills, N. Burgess, and J. O'Keefe. 2004. Theta-modulated place-by-direction cells in the hippocampal formation in the rat. *J. Neurosci.* 24:8265-8277.
39. Cave, C. B. and L. R. Squire. 1992. Intact and long-lasting repetition priming in amnesia. *J. Exp. Psychol. Learn. Mem. Cogn* 18:509-520.
40. Chawla, M. K., J. F. Guzowski, V. Ramirez-Amaya, P. Lipa, K. L. Hoffman, L. K. Marriott, P. F. Worley, B. L. McNaughton, and C. A. Barnes. 2005. Sparse, environmentally selective expression of Arc RNA in the upper blade of the rodent fascia dentata by brief spatial experience. *Hippocampus* 15:579-586.
41. Chen, L. L., L. H. Lin, E. J. Green, C. A. Barnes, and B. L. McNaughton. 1994. Head-direction cells in the rat posterior cortex. I. Anatomical distribution and behavioral modulation. *Exp. Brain Res.* 101:8-23.

42. Chudasama, Y., J. W. Dalley, F. Nathwani, P. Bouger, and T. W. Robbins. 2004. Cholinergic modulation of visual attention and working memory: dissociable effects of basal forebrain 192-IgG-saporin lesions and intraprefrontal infusions of scopolamine. *Learn. Mem.* 11:78-86.
43. Clark, R. E., A. N. West, S. M. Zola, and L. R. Squire. 2001. Rats with lesions of the hippocampus are impaired on the delayed nonmatching-to-sample task. *Hippocampus*. 11:176-186.
44. Clayton, N. S., T. J. Bussey, and A. Dickinson. 2003. Can animals recall the past and plan for the future? *Nat. Rev. Neurosci.* 4:685-691.
45. Clayton, N. S. and A. Dickinson. 1998. Episodic-like memory during cache recovery by scrub jays. *Nature* 395:272-274.
46. Clayton, N. S., D. P. Griffiths, N. J. Emery, and A. Dickinson. 2001. Elements of episodic-like memory in animals. *Philos. Trans. R. Soc. Lond B Biol. Sci.* 356:1483-1491.
47. Cobb, S. R. and C. H. Davies. 2005. Cholinergic modulation of hippocampal cells and circuits. *J. Physiol* 562:81-88.
48. Cohen, N. J. and H. Eichenbaum. 1993. Memory, amnesia, and the hippocampal system. MIT Press, Cambridge, MA.

49. Cohen, N. J. and L. R. Squire. 1980. Preserved learning and retention of pattern-analyzing skill in amnesia: dissociation of knowing how and knowing that. *Science* 210:207-210.
50. Conroy, M. A., R. O. Hopkins, and L. R. Squire. 2005. On the contribution of perceptual fluency and priming to recognition memory. *Cogn Affect. Behav. Neurosci.* 5:14-20.
51. Daum, I., S. Channon, and A. G. Canavan. 1989. Classical conditioning in patients with severe memory problems. *J. Neurol. Neurosurg. Psychiatry* 52:47-51.
52. Davidson, T. L., M. G. McKernan, and L. E. Jarrard. 1993. Hippocampal lesions do not impair negative patterning: a challenge to configural association theory. *Behav. Neurosci.* 107:227-234.
53. Davis, C. D., F. L. Jones, and B. E. Derrick. 2004. Novel environments enhance the induction and maintenance of long-term potentiation in the dentate gyrus. *J. Neurosci.* 24:6497-6506.
54. Deshmukh, S. S., D. Yoganarasimha, H. Voicu, and J. J. Knierim. 2010. Theta modulation in the medial and the lateral entorhinal cortices. *J. Neurophysiol.* 104:994-1006.
55. Desmond, N. L., C. A. Scott, J. A. Jane, Jr., and W. B. Levy. 1994. Ultrastructural identification of entorhinal cortical synapses in CA1 stratum lacunosum-moleculare of the rat. *Hippocampus* 4:594-600.

56. Dickerson, B. C. and H. Eichenbaum. 2010. The episodic memory system: neurocircuitry and disorders. *Neuropsychopharmacology* 35:86-104.
57. Diekelmann, S. and J. Born. 2010. The memory function of sleep. *Nat. Rev Neurosci.* 11:114-126.
58. Disterhoft, J. F., D. A. Coulter, and D. L. Alkon. 1986. Conditioning-specific membrane changes of rabbit hippocampal neurons measured in vitro. *Proc. Natl. Acad. Sci. U. S. A* 83:2733-2737.
59. Dusek, J. A. and H. Eichenbaum. 1997. The hippocampus and memory for orderly stimulus relations. *Proc. Natl. Acad. Sci. U. S. A* 94:7109-7114.
60. Duva, C. A., S. B. Floresco, G. R. Wunderlich, T. L. Lao, J. P. Pinel, and A. G. Phillips. 1997. Disruption of spatial but not object-recognition memory by neurotoxic lesions of the dorsal hippocampus in rats. *Behav. Neurosci.* 111:1184-1196.
61. Ebbinghaus, H. 1885. Memory: A Contribution to Experimental Psychology. Dover, New York.
62. Eichenbaum, H. 2004. Hippocampus: cognitive processes and neural representations that underlie declarative memory. *Neuron* 44:109-120.
63. Eichenbaum, H., P. Dudchenko, E. Wood, M. Shapiro, and H. Tanila. 1999. The hippocampus, memory, and place cells: is it spatial memory or a memory space? *Neuron* 23:209-226.



64. Eichenbaum, H. C. N. J. 2001. From Conditioning to Conscious Recollection: Memory Systems of the Brain. Oxford University Press, New York.
65. Eifuku, S., H. Nishijo, T. Kita, and T. Ono. 1995. Neuronal activity in the primate hippocampal formation during a conditional association task based on the subject's location. *J. Neurosci.* 15:4952-4969.
66. Ekstrom, A. D., M. J. Kahana, J. B. Caplan, T. A. Fields, E. A. Isham, E. L. Newman, and I. Fried. 2003. Cellular networks underlying human spatial navigation. *Nature* 425:184-188.
67. Ergorul, C. and H. Eichenbaum. 2006. Essential role of the hippocampal formation in rapid learning of higher-order sequential associations. *J. Neurosci.* 26:4111-4117.
68. Everitt, B. J. and T. W. Robbins. 1997. Central cholinergic systems and cognition. *Annu. Rev. Psychol.* 48:649-684.
69. Fanselow, M. S. 1990. Factors governing one-trial contextual conditioning. *Animal Learning Behavior* 18:264-270.
70. Ferbinteanu, J. and M. L. Shapiro. 2003. Prospective and retrospective memory coding in the hippocampus. *Neuron* 40:1227-1239.
71. Ferrier, D. 1876. The functions of the brain. Elder Smith, London.

72. Finger, T. E. 1976. Gustatory pathways in the bullhead catfish. 1. Connections of the anterior ganglion. *J. Comp Neurol* 165:513-526.
73. Fortin, N. J., K. L. Agster, and H. B. Eichenbaum. 2002. Critical role of the hippocampus in memory for sequences of events. *Nat. Neurosci.* 5:458-462.
74. Frank, L. M., G. B. Stanley, and E. N. Brown. 2004. Hippocampal plasticity across multiple days of exposure to novel environments. *J. Neurosci.* 24:7681-7689.
75. Fricke, R. and W. M. Cowan. 1978. An autoradiographic study of the commissural and ipsilateral hippocampo-dentate projections in the adult rat. *J. Comp Neurol.* 181:253-269.
76. Fuhs, M. C. and D. S. Touretzky. 2006. A spin glass model of path integration in rat medial entorhinal cortex. *J. Neurosci.* 26:4266-4276.
77. Fyhn, M., T. Hafting, A. Treves, M. B. Moser, and E. I. Moser. 2007. Hippocampal remapping and grid realignment in entorhinal cortex. *Nature* 446:190-194.
78. Gaarskjaer, F. B. 1978a. Organization of the mossy fiber system of the rat studied in extended hippocampi. I. Terminal area related to number of granule and pyramidal cells. *J. Comp Neurol.* 178:49-72.

79. Gaarskjaer, F. B. 1978b. Organization of the mossy fiber system of the rat studied in extended hippocampi. II. Experimental analysis of fiber distribution with silver impregnation methods. *J. Comp Neurol.* 178:73-88.
80. Gaffan, D. 1994. Dissociated effects of perirhinal cortex ablation, fornix transection and amygdalectomy: evidence for multiple memory systems in the primate temporal lobe. *Exp. Brain Res.* 99:411-422.
81. Gallagher, M. and P. C. Holland. 1992. Preserved configural learning and spatial learning impairment in rats with hippocampal damage. *Hippocampus* 2:81-88.
82. Ge, S., E. L. Goh, K. A. Sailor, Y. Kitabatake, G. L. Ming, and H. Song. 2006. GABA regulates synaptic integration of newly generated neurons in the adult brain. *Nature* 439:589-593.
83. Geinisman, Y., R. W. Berry, J. F. Disterhoft, J. M. Power, and E. A. Van der Zee. 2001. Associative learning elicits the formation of multiple-synapse boutons. *J. Neurosci.* 21:5568-5573.
84. Georges-Francois, P., E. T. Rolls, and R. G. Robertson. 1999. Spatial view cells in the primate hippocampus: allocentric view not head direction or eye position or place. *Cereb. Cortex* 9:197-212.
85. Gilbert, P. E., R. P. Kesner, and I. Lee. 2001. Dissociating hippocampal subregions: double dissociation between dentate gyrus and CA1. *Hippocampus* 11:626-636.

86. Gilboa, A., G. Winocur, R. S. Rosenbaum, A. Poreh, F. Gao, S. E. Black, R. Westmacott, and M. Moscovitch. 2006. Hippocampal contributions to recollection in retrograde and anterograde amnesia. *Hippocampus* 16:966-980.
87. Giovanello, K. S., D. Schnyer, and M. Verfaellie. 2009. Distinct hippocampal regions make unique contributions to relational memory. *Hippocampus* 19:111-117.
88. Gold, A. E. and R. P. Kesner. 2005. The role of the CA3 subregion of the dorsal hippocampus in spatial pattern completion in the rat. *Hippocampus* 15:808-814.
89. Gold, J. J., R. O. Hopkins, and L. R. Squire. 2006. Single-item memory, associative memory, and the human hippocampus. *Learn. Mem.* 13:644-649.
90. Good, M. and R. C. Honey. 1991. Conditioning and contextual retrieval in hippocampal rats. *Behav. Neurosci.* 105:499-509.
91. Gothard, K. M., K. L. Hoffman, F. P. Battaglia, and B. L. McNaughton. 2001. Dentate gyrus and ca1 ensemble activity during spatial reference frame shifts in the presence and absence of visual input. *J. Neurosci.* 21:7284-7292.
92. Gothard, K. M., W. E. Skaggs, and B. L. McNaughton. 1996a. Dynamics of mismatch correction in the hippocampal ensemble code for space:

- interaction between path integration and environmental cues. *J. Neurosci.* 16:8027-8040.
93. Gothard, K. M., W. E. Skaggs, K. M. Moore, and B. L. McNaughton. 1996b. Binding of hippocampal CA1 neural activity to multiple reference frames in a landmark-based navigation task. *J. Neurosci.* 16:823-835.
94. Griffin, A. L., H. Eichenbaum, and M. E. Hasselmo. 2007. Spatial representations of hippocampal CA1 neurons are modulated by behavioral context in a hippocampus-dependent memory task. *J. Neurosci.* 27:2416-2423.
95. Guzowski, J. F., J. J. Knierim, and E. I. Moser. 2004. Ensemble dynamics of hippocampal regions CA3 and CA1. *Neuron* 44:581-584.
96. Hafting, T., M. Fyhn, S. Molden, M. B. Moser, and E. I. Moser. 2005. Microstructure of a spatial map in the entorhinal cortex. *Nature* 436:801-806.
97. Haist, F., A. P. Shimamura, and L. R. Squire. 1992. On the relationship between recall and recognition memory. *J. Exp. Psychol. Learn. Mem. Cogn* 18:691-702.
98. Hannula, D. E. and C. Ranganath. 2008. Medial temporal lobe activity predicts successful relational memory binding. *J. Neurosci.* 28:116-124.

99. Hargreaves, E. L., G. Rao, I. Lee, and J. J. Knierim. 2005. Major dissociation between medial and lateral entorhinal input to dorsal hippocampus. *Science* 308:1792-1794.
100. Harris, E. W. and C. W. Cotman. 1986. Long-term potentiation of guinea pig mossy fiber responses is not blocked by N-methyl D-aspartate antagonists. *Neurosci. Lett.* 70:132-137.
101. Harris, K. D., H. Hirase, X. Leinekugel, D. A. Henze, and G. Buzsaki. 2001. Temporal interaction between single spikes and complex spike bursts in hippocampal pyramidal cells. *Neuron* 32:141-149.
102. Henke, K., A. Buck, B. Weber, and H. G. Wieser. 1997. Human hippocampus establishes associations in memory. *Hippocampus* 7:249-256.
103. Henze, D. A. and G. Buzsaki. 2007. Hilar mossy cells: functional identification and activity in vivo. *Prog. Brain Res.* 163:199-216.
104. Henze, D. A., N. N. Urban, and G. Barrionuevo. 2000. The multifarious hippocampal mossy fiber pathway: a review. *Neuroscience* 98:407-427.
105. Herry, C., F. Ferraguti, N. Singewald, J. J. Letzkus, I. Ehrlich, and A. Luthi. 2010. Neuronal circuits of fear extinction. *Eur. J. Neurosci.* 31:599-612.

106. Hetherington, P. A. and M. L. Shapiro. 1997. Hippocampal place fields are altered by the removal of single visual cues in a distance-dependent manner. *Behav. Neurosci.* 111:20-34.
107. Hirsh, R. 1974. The hippocampus and contextual retrieval of information from memory: a theory. *Behav. Biol.* 12:421-444.
108. Hopfield, J. J. 1982. Neural networks and physical systems with emergent collective computational abilities. *Proc. Natl. Acad. Sci. U. S. A* 79:2554-2558.
109. Hopkins, R. O., C. E. Myers, D. Shohamy, S. Grossman, and M. Gluck. 2004. Impaired probabilistic category learning in hypoxic subjects with hippocampal damage. *Neuropsychologia* 42:524-535.
110. Hsu, D. 2007. The dentate gyrus as a filter or gate: a look back and a look ahead. *Prog. Brain Res.* 163:601-613.
111. Hughes, A. 1971. Topographical relationships between the anatomy and physiology of the rabbit visual system. *Doc. Ophthalmol.* 30:33-159.
112. Hull, C. L. 1934a. The concept of the habit-family hierarchy and maze learning: Part I. *Psychological Review* 41:34-54.
113. Hull, C. L. 1934b. The concept of the habit-family hierarchy and maze learning: Part II. *Psychological Review* 41:134-153.

114. Hunsaker, M. R., J. S. Rosenberg, and R. P. Kesner. 2008. The role of the dentate gyrus, CA3a,b, and CA3c for detecting spatial and environmental novelty. *Hippocampus* 18:1064-1073.
115. Ishizuka, N., J. Weber, and D. G. Amaral. 1990. Organization of intrahippocampal projections originating from CA3 pyramidal cells in the rat. *J. Comp Neurol.* 295:580-623.
116. Jackson, J. H. 1865. Selected Writings of John Hughlings Jackson. Hodder and Stoughton, London.
117. Jackson, M. B. and H. E. Scharfman. 1996. Positive feedback from hilar mossy cells to granule cells in the dentate gyrus revealed by voltage-sensitive dye and microelectrode recording. *J. Neurophysiol.* 76:601-616.
118. Jackson-Smith, P., R. P. Kesner, and A. A. Chiba. 1993. Continuous recognition of spatial and nonspatial stimuli in hippocampal-lesioned rats. *Behav. Neural Biol.* 59:107-119.
119. Jacobs, B. L., S. L. Foote, and F. E. Bloom. 1978. Differential projections of neurons within the dorsal raphe nucleus of the rat: a horseradish peroxidase (HRP) study. *Brain Res.* 147:149-153.
120. Jarrard, L. E. 1978. Selective hippocampal lesions: differential effects on performance by rats of a spatial task with preoperative versus postoperative training. *J. Comp Physiol Psychol.* 92:1119-1127.



121. Jeffery, K. J. and J. M. O'Keefe. 1999. Learned interaction of visual and idiothetic cues in the control of place field orientation. *Exp. Brain Res.* 127:151-161.
122. Johnson, A. and A. D. Redish. 2007. Neural ensembles in CA3 transiently encode paths forward of the animal at a decision point. *J. Neurosci.* 27:12176-12189.
123. Jones, M. W. and M. A. Wilson. 2005. Phase precession of medial prefrontal cortical activity relative to the hippocampal theta rhythm. *Hippocampus* 15:867-873.
124. Jung, M. W. and B. L. McNaughton. 1993. Spatial selectivity of unit activity in the hippocampal granular layer. *Hippocampus* 3:165-182.
125. Kaplan, M. S. and J. W. Hinds. 1977. Neurogenesis in the adult rat: electron microscopic analysis of light radioautographs. *Science* 197:1092-1094.
126. Kennedy, P. J. and M. L. Shapiro. 2004. Retrieving memories via internal context requires the hippocampus. *J. Neurosci.* 24:6979-6985.
127. Kim, J. J. and M. S. Fanselow. 1992. Modality-specific retrograde amnesia of fear. *Science* 256:675-677.

128. Kim, J. J., R. A. Rison, and M. S. Fanselow. 1993. Effects of amygdala, hippocampus, and periaqueductal gray lesions on short- and long-term contextual fear. *Behav. Neurosci.* 107:1093-1098.
129. Kiss, J., A. Csaki, H. Bokor, M. Shanabrough, and C. Leranth. 2000. The supramammillo-hippocampal and supramammillo-septal glutamatergic/aspartatergic projections in the rat: a combined [3H]D-aspartate autoradiographic and immunohistochemical study. *Neuroscience* 97:657-669.
130. Knierim, J. J. 2002. Dynamic interactions between local surface cues, distal landmarks, and intrinsic circuitry in hippocampal place cells. *J. Neurosci.* 22:6254-6264.
131. Knierim, J. J., H. S. Kudrimoti, and B. L. McNaughton. 1995. Place cells, head direction cells, and the learning of landmark stability. *J. Neurosci.* 15:1648-1659.
132. Knierim, J. J., H. S. Kudrimoti, and B. L. McNaughton. 1996a. Neuronal mechanisms underlying the interaction between visual landmarks and path integration in the rat. *Int. J. Neural Syst.* 7:213-218.
133. Knierim, J. J., H. S. Kudrimoti, and B. L. McNaughton. 1998. Interactions between idiothetic cues and external landmarks in the control of place cells and head direction cells. *J. Neurophysiol.* 80:425-446.

134. Knierim, J. J., I. Lee, and E. L. Hargreaves. 2006. Hippocampal place cells: parallel input streams, subregional processing, and implications for episodic memory. *Hippocampus* 16:755-764.
135. Knierim, J. J., W. E. Skaggs, H. S. Kudrimoti, and B. L. McNaughton. 1996b. Vestibular and visual cues in navigation: a tale of two cities. *Ann. N. Y. Acad. Sci.* 781:399-406.
136. Knierim, J. J. and E. Van. 1992. Visual cortex: cartography, connectivity, and concurrent processing. *Curr. Opin. Neurobiol.* 2:150-155.
137. Knowlton, B. J. and L. R. Squire. 1993. The learning of categories: parallel brain systems for item memory and category knowledge. *Science* 262:1747-1749.
138. Knowlton, B. J., L. R. Squire, and M. A. Gluck. 1994. Probabilistic classification learning in amnesia. *Learn. Mem.* 1:106-120.
139. Kumaran, D. and E. A. Maguire. 2005. The human hippocampus: cognitive maps or relational memory? *J. Neurosci.* 25:7254-7259.
140. Lambert, J. D. and R. S. Jones. 1990. A reevaluation of excitatory amino acid-mediated synaptic transmission in rat dentate gyrus. *J. Neurophysiol.* 64:119-132.

141. Lee, I., G. Rao, and J. J. Knierim. 2004a. A double dissociation between hippocampal subfields: differential time course of CA3 and CA1 place cells for processing changed environments. *Neuron* 42:803-815.
142. Lee, I., D. Yoganarasimha, G. Rao, and J. J. Knierim. 2004b. Comparison of population coherence of place cells in hippocampal subfields CA1 and CA3. *Nature* 430:456-459.
143. Lenck-Santini, P. P., E. Save, and B. Poucet. 2001. Place-cell firing does not depend on the direction of turn in a Y-maze alternation task. *Eur. J. Neurosci.* 13:1055-1058.
144. Leutgeb, J. K., S. Leutgeb, M. B. Moser, and E. I. Moser. 2007. Pattern separation in the dentate gyrus and CA3 of the hippocampus. *Science* 315:961-966.
145. Leutgeb, J. K., S. Leutgeb, A. Treves, R. Meyer, C. A. Barnes, B. L. McNaughton, M. B. Moser, and E. I. Moser. 2005a. Progressive transformation of hippocampal neuronal representations in "morphed" environments. *Neuron* 48:345-358.
146. Leutgeb, S., J. K. Leutgeb, C. A. Barnes, E. I. Moser, B. L. McNaughton, and M. B. Moser. 2005b. Independent codes for spatial and episodic memory in hippocampal neuronal ensembles. *Science* 309:619-623.

147. Leutgeb, S., J. K. Leutgeb, A. Treves, M. B. Moser, and E. I. Moser. 2004. Distinct ensemble codes in hippocampal areas CA3 and CA1. *Science* 305:1295-1298.
148. Li, X. G., P. Somogyi, A. Ylinen, and G. Buzsaki. 1994. The hippocampal CA3 network: an in vivo intracellular labeling study. *J. Comp Neurol.* 339:181-208.
149. Li, Y., Y. Mu, and F. H. Gage. 2009. Development of neural circuits in the adult hippocampus. *Curr. Top. Dev. Biol.* 87:149-174.
150. Loy, R., D. A. Koziell, J. D. Lindsey, and R. Y. Moore. 1980. Noradrenergic innervation of the adult rat hippocampal formation. *J. Comp Neurol.* 189:699-710.
151. Lubke, J., M. Frotscher, and N. Spruston. 1998. Specialized electrophysiological properties of anatomically identified neurons in the hilar region of the rat fascia dentata. *J. Neurophysiol.* 79:1518-1534.
152. Ludvig, N., H. M. Tang, B. C. Gohil, and J. M. Botero. 2004. Detecting location-specific neuronal firing rate increases in the hippocampus of freely-moving monkeys. *Brain Res.* 1014:97-109.
153. Maaswinkel, H., L. E. Jarrard, and I. Q. Whishaw. 1999. Hippocampectomized rats are impaired in homing by path integration. *Hippocampus* 9:553-561.

154. Maguire, E. A., N. Burgess, J. G. Donnett, R. S. Frackowiak, C. D. Frith, and J. O'Keefe. 1998. Knowing where and getting there: a human navigation network. *Science* 280:921-924.
155. Maguire, E. A., D. G. Gadian, I. S. Johnsrude, C. D. Good, J. Ashburner, R. S. Frackowiak, and C. D. Frith. 2000. Navigation-related structural change in the hippocampi of taxi drivers. *Proc. Natl. Acad. Sci. U. S. A.* 97:4398-4403.
156. Manns, J. R. and H. Eichenbaum. 2006. Evolution of declarative memory. *Hippocampus* 16:795-808.
157. Manns, J. R. and H. Eichenbaum. 2009. A cognitive map for object memory in the hippocampus. *Learn. Mem.* 16:616-624.
158. Manns, J. R., M. W. Howard, and H. Eichenbaum. 2007. Gradual changes in hippocampal activity support remembering the order of events. *Neuron* 56:530-540.
159. Maren, S., G. Aharonov, and M. S. Fanselow. 1997. Neurotoxic lesions of the dorsal hippocampus and Pavlovian fear conditioning in rats. *Behav. Brain Res.* 88:261-274.
160. Maren, S. and M. S. Fanselow. 1997. Electrolytic lesions of the fimbria/fornix, dorsal hippocampus, or entorhinal cortex produce anterograde deficits in contextual fear conditioning in rats. *Neurobiol. Learn. Mem.* 67:142-149.

161. Markus, E. J., Y. L. Qin, B. Leonard, W. E. Skaggs, B. L. McNaughton, and C. A. Barnes. 1995. Interactions between location and task affect the spatial and directional firing of hippocampal neurons. *J. Neurosci.* 15:7079-7094.
162. Marr, D. 1969. A theory of cerebellar cortex. *J. Physiol* 202:437-470.
163. Marr, D. 1971. Simple memory: a theory for archicortex. *Philos. Trans. R. Soc. Lond B Biol. Sci.* 262:23-81.
164. Matsumura, N., H. Nishijo, R. Tamura, S. Eifuku, S. Endo, and T. Ono. 1999. Spatial- and task-dependent neuronal responses during real and virtual translocation in the monkey hippocampal formation. *J. Neurosci.* 19:2381-2393.
165. McClelland, J. L. and N. H. Goddard. 1996. Considerations arising from a complementary learning systems perspective on hippocampus and neocortex. *Hippocampus* 6:654-665.
166. McClelland, J. L., B. L. McNaughton, and R. C. O'Reilly. 1995. Why there are complementary learning systems in the hippocampus and neocortex: insights from the successes and failures of connectionist models of learning and memory. *Psychol. Rev* 102:419-457.
167. McNaughton, B. L., C. A. Barnes, J. L. Gerrard, K. Gothard, M. W. Jung, J. J. Knierim, H. Kudrimoti, Y. Qin, W. E. Skaggs, M. Suster, and K. L.

- Weaver. 1996. Deciphering the hippocampal polyglot: the hippocampus as a path integration system. *J. Exp. Biol.* 199:173-185.
168. McNaughton, B. L., C. A. Barnes, J. Meltzer, and R. J. Sutherland. 1989. Hippocampal granule cells are necessary for normal spatial learning but not for spatially-selective pyramidal cell discharge. *Exp. Brain Res.* 76:485-496.
169. McNaughton, B. L., C. A. Barnes, and J. O'Keefe. 1983. The contributions of position, direction, and velocity to single unit activity in the hippocampus of freely-moving rats. *Exp. Brain Res.* 52:41-49.
170. McNaughton, B. L., F. P. Battaglia, O. Jensen, E. I. Moser, and M. B. Moser. 2006. Path integration and the neural basis of the 'cognitive map'. *Nat. Rev. Neurosci.* 7:663-678.
171. McNaughton, B. L. and R. G. Morris. 1987. Hippocampal synaptic enhancement and information storage within a distributed memory system. *TINS* 10:408-415.
172. McNaughton, B. L. and L. Nadel. 1990. Hebb-Marr networks and the neurobiological representation of action in space. *In* Neuroscience and connectionist theory. M. A. Gluck and D. E. Rumelhart, editors. Erlbaum, Hillsdale. 1-63.
173. Middlebrooks, J. C., R. W. Dykes, and M. M. Merzenich. 1980. Binaural response-specific bands in primary auditory cortex (AI) of the cat:



- topographical organization orthogonal to isofrequency contours. *Brain Res.* 181:31-48.
174. Milner, B. 1962. Les troubles de la memoire accompagnant des lesions hippocampiques bilaterales. Paris.
175. Moita, M. A., S. Rosis, Y. Zhou, J. E. LeDoux, and H. T. Blair. 2003. Hippocampal place cells acquire location-specific responses to the conditioned stimulus during auditory fear conditioning. *Neuron* 37:485-497.
176. Moore, R. Y., A. E. Halaris, and B. E. Jones. 1978. Serotonin neurons of the midbrain raphe: ascending projections. *J. Comp Neurol.* 180:417-438.
177. Morgan, R. J., V. Santhakumar, and I. Soltesz. 2007. Modeling the dentate gyrus. *Prog. Brain Res.* 163:639-658.
178. Morris, R. G., P. Garrud, J. N. Rawlins, and J. O'Keefe. 1982. Place navigation impaired in rats with hippocampal lesions. *Nature* 297:681-683.
179. Morris, R. G., E. I. Moser, G. Riedel, S. J. Martin, J. Sandin, M. Day, and C. O'Carroll. 2003. Elements of a neurobiological theory of the hippocampus: the role of activity-dependent synaptic plasticity in memory. *Philos Trans. R. Soc. Lond B Biol. Sci.* 358:773-786.

180. Moscovitch, M., L. Nadel, G. Winocur, A. Gilboa, and R. S. Rosenbaum. 2006. The cognitive neuroscience of remote episodic, semantic and spatial memory. *Curr. Opin. Neurobiol.* 16:179-190.
181. Muller, R. U. and J. L. Kubie. 1987. The effects of changes in the environment on the spatial firing of hippocampal complex-spike cells. *J. Neurosci.* 7:1951-1968.
182. Muller, R. U., J. L. Kubie, and J. B. Ranck, Jr. 1987. Spatial firing patterns of hippocampal complex-spike cells in a fixed environment. *J. Neurosci.* 7:1935-1950.
183. Muller, R. U., J. B. Ranck, Jr., and J. S. Taube. 1996. Head direction cells: properties and functional significance. *Curr. Opin. Neurobiol.* 6:196-206.
184. Murakawa, R. and T. Kosaka. 2001. Structural features of mossy cells in the hamster dentate gyrus, with special reference to somatic thorny excrescences. *J. Comp Neurol.* 429:113-126.
185. Murray, E. A. and M. Mishkin. 1998. Object recognition and location memory in monkeys with excitotoxic lesions of the amygdala and hippocampus. *J. Neurosci.* 18:6568-6582.
186. Musen, G. and L. R. Squire. 1992. Nonverbal priming in amnesia. *Mem. Cognit.* 20:441-448.

187. Myers, C. E. and H. E. Scharfman. 2009. A role for hilar cells in pattern separation in the dentate gyrus: a computational approach. *Hippocampus* 19:321-337.
188. Nadel, L. 1995. The role of the hippocampus in declarative memory: a comment on Zola-Morgan, Squire, and Ramus (1994). *Hippocampus* 5:232-239.
189. Nadel, L., A. Samsonovich, L. Ryan, and M. Moscovitch. 2000. Multiple trace theory of human memory: computational, neuroimaging, and neuropsychological results. *Hippocampus* 10:352-368.
190. Nafstad, P. H. 1967. An electron microscope study on the termination of the perforant path fibres in the hippocampus and the fascia dentata. *Z. Zellforsch. Mikrosk. Anat.* 76:532-542.
191. Nakazawa, K., M. C. Quirk, R. A. Chitwood, M. Watanabe, M. F. Yeckel, L. D. Sun, A. Kato, C. A. Carr, D. Johnston, M. A. Wilson, and S. Tonegawa. 2002. Requirement for hippocampal CA3 NMDA receptors in associative memory recall. *Science* 297:211-218.
192. Nakazawa, K., L. D. Sun, M. C. Quirk, L. Rondi-Reig, M. A. Wilson, and S. Tonegawa. 2003. Hippocampal CA3 NMDA receptors are crucial for memory acquisition of one-time experience. *Neuron* 38:305-315.
193. Nobre, A. C., G. N. Sebestyen, D. R. Gitelman, M. M. Mesulam, R. S. Frackowiak, and C. D. Frith. 1997. Functional localization of the system for

- visuospatial attention using positron emission tomography. *Brain* 120 ( Pt 3):515-533.
194. Norman, G. and M. J. Eacott. 2005. Dissociable effects of lesions to the perirhinal cortex and the postrhinal cortex on memory for context and objects in rats. *Behav. Neurosci.* 119:557-566.
  195. O'Keefe, J. 1976. Place units in the hippocampus of the freely moving rat. *Exp. Neurol.* 51:78-109.
  196. O'Keefe, J. and N. Burgess. 1996. Geometric determinants of the place fields of hippocampal neurons. *Nature* 381:425-428.
  197. O'Keefe, J. and N. Burgess. 2005. Dual phase and rate coding in hippocampal place cells: theoretical significance and relationship to entorhinal grid cells. *Hippocampus* 15:853-866.
  198. O'Keefe, J. and D. H. Conway. 1978. Hippocampal place units in the freely moving rat: why they fire where they fire. *Exp. Brain Res.* 31:573-590.
  199. O'Keefe, J. and J. Dostrovsky. 1971. The hippocampus as a spatial map. Preliminary evidence from unit activity in the freely-moving rat. *Brain Res.* 34:171-175.
  200. O'Keefe, J. and L. Nadel. 1978. The hippocampus as a cognitive map. Clarendon Press, Oxford.

201. O'Reilly, R. C. and J. L. McClelland. 1994. Hippocampal conjunctive encoding, storage, and recall: avoiding a trade-off. *Hippocampus* 4:661-682.
202. Olson, I. R., K. Page, K. S. Moore, A. Chatterjee, and M. Verfaellie. 2006. Working memory for conjunctions relies on the medial temporal lobe. *J. Neurosci.* 26:4596-4601.
203. Ono, T., S. Eifuku, K. Nakamura, and H. Nishijo. 1993a. Monkey hippocampal neuron responses related to spatial and non-spatial influence. *Neurosci. Lett.* 159:75-78.
204. Ono, T., K. Nakamura, H. Nishijo, and S. Eifuku. 1993b. Monkey hippocampal neurons related to spatial and nonspatial functions. *J. Neurophysiol.* 70:1516-1529.
205. Overstreet-Wadiche, L. S. and G. L. Westbrook. 2006. Functional maturation of adult-generated granule cells. *Hippocampus* 16:208-215.
206. Parslow, D. M., D. Rose, B. Brooks, S. Fleminger, J. A. Gray, V. Giampietro, M. J. Brammer, S. Williams, D. Gasston, C. Andrew, G. N. Vythelingum, G. Loannou, A. Simmons, and R. G. Morris. 2004. Allocentric spatial memory activation of the hippocampal formation measured with fMRI. *Neuropsychology.* 18:450-461.

207. Paul, C. M., G. Magda, and S. Abel. 2009. Spatial memory: Theoretical basis and comparative review on experimental methods in rodents. *Behav. Brain Res.* 203:151-164.
208. Penttonen, M., A. Kamondi, A. Sik, L. Acsady, and G. Buzsaki. 1997. Feed-forward and feed-back activation of the dentate gyrus in vivo during dentate spikes and sharp wave bursts. *Hippocampus* 7:437-450.
209. Phillips, R. G. and J. E. LeDoux. 1992. Differential contribution of amygdala and hippocampus to cued and contextual fear conditioning. *Behav. Neurosci.* 106:274-285.
210. Pickel, V. M., M. Segal, and F. E. Bloom. 1974. A radioautographic study of the efferent pathways of the nucleus locus coeruleus. *J. Comp Neurol.* 155:15-42.
211. Pikkarainen, M., S. Ronkko, V. Savander, R. Insausti, and A. Pitkanen. 1999. Projections from the lateral, basal, and accessory basal nuclei of the amygdala to the hippocampal formation in rat. *J. Comp Neurol.* 403:229-260.
212. Pitkanen, A., M. Pikkarainen, N. Nurminen, and A. Ylinen. 2000. Reciprocal connections between the amygdala and the hippocampal formation, perirhinal cortex, and postrhinal cortex in rat. A review. *Ann. N. Y. Acad. Sci.* 911:369-391.

213. Raby, C. R., D. M. Alexis, A. Dickinson, and N. S. Clayton. 2007. Planning for the future by western scrub-jays. *Nature* 445:919-921.
214. Ranck, J. B., Jr. 1973. Studies on single neurons in dorsal hippocampal formation and septum in unrestrained rats. I. Behavioral correlates and firing repertoires. *Exp. Neurol* 41:461-531.
215. Rapp, P. R. and M. Gallagher. 1996. Preserved neuron number in the hippocampus of aged rats with spatial learning deficits. *Proc. Natl. Acad. Sci. U. S. A* 93:9926-9930.
216. Redish, A. D., F. P. Battaglia, M. K. Chawla, A. D. Ekstrom, J. L. Gerrard, P. Lipa, E. S. Rosenzweig, P. F. Worley, J. F. Guzowski, B. L. McNaughton, and C. A. Barnes. 2001. Independence of firing correlates of anatomically proximate hippocampal pyramidal cells. *J. Neurosci.* 21:RC134.
217. Reinvang, I., S. Magnussen, M. W. Greenlee, and P. G. Larsson. 1998. Electrophysiological localization of brain regions involved in perceptual memory. *Exp. Brain Res.* 123:481-484.
218. Rescorla, R. A. 1972. "Configural" conditioning in discrete-trial bar pressing. *J. Comp Physiol Psychol.* 79:307-317.
219. Ribot, T. 1881. Les Maladies de la Memoire [English translation: Diseases of Memory. Appleton-Century-Crofts, New York.

220. Robertson, R. G., E. T. Rolls, and o. P. Georges-Fran. 1998. Spatial view cells in the primate hippocampus: effects of removal of view details. *J. Neurophysiol.* 79:1145-1156.
221. Rolls, E. T. 1999. Spatial view cells and the representation of place in the primate hippocampus. *Hippocampus* 9:467-480.
222. Rolls, E. T. and R. P. Kesner. 2006. A computational theory of hippocampal function, and empirical tests of the theory. *Prog. Neurobiol.* 79:1-48.
223. Rolls, E. T., Y. Miyashita, P. M. Cahusac, R. P. Kesner, H. Niki, J. D. Feigenbaum, and L. Bach. 1989. Hippocampal neurons in the monkey with activity related to the place in which a stimulus is shown. *J. Neurosci.* 9:1835-1845.
224. Rolls, E. T., R. G. Robertson, and P. Georges-Francois. 1997. Spatial view cells in the primate hippocampus. *Eur. J. Neurosci.* 9:1789-1794.
225. Rolls, E. T. and A. Treves. 1994. Neural networks in the brain involved in memory and recall. *Prog. Brain Res.* 102:335-341.
226. Rolls, E. T. and A. Treves. 1998. Neural networks and brain function. Oxford University Press, Oxford.



227. Rolls, E. T., A. Treves, R. G. Robertson, P. Georges-Francois, and S. Panzeri. 1998. Information about spatial view in an ensemble of primate hippocampal cells. *J. Neurophysiol.* 79:1797-1813.
228. Ross, R. S. and H. Eichenbaum. 2006. Dynamics of hippocampal and cortical activation during consolidation of a nonspatial memory. *J. Neurosci.* 26:4852-4859.
229. Rothblat, L. A. and L. F. Kromer. 1991. Object recognition memory in the rat: the role of the hippocampus. *Behav. Brain Res.* 42:25-32.
230. Rudy, J. W. and R. J. Sutherland. 1989. The hippocampal formation is necessary for rats to learn and remember configural discriminations. *Behav. Brain Res.* 34:97-109.
231. Rudy, J. W. and R. J. Sutherland. 1995. Configural association theory and the hippocampal formation: an appraisal and reconfiguration. *Hippocampus* 5:375-389.
232. Sainsbury, R. S. 1998. Hippocampal theta: a sensory-inhibition theory of function. *Neurosci. Biobehav. Rev* 22:237-241.
233. Sandi, C., M. Loscertales, and C. Guaza. 1997. Experience-dependent facilitating effect of corticosterone on spatial memory formation in the water maze. *Eur. J. Neurosci.* 9:637-642.

234. Saunders, R. C. and L. Weiskrantz. 1989. The effects of fornix transection and combined fornix transection, mammillary body lesions and hippocampal ablations on object-pair association memory in the rhesus monkey. *Behav. Brain Res.* 35:85-94.
235. Save, E., M. C. Buhot, N. Foreman, and C. Thinus-Blanc. 1992. Exploratory activity and response to a spatial change in rats with hippocampal or posterior parietal cortical lesions. *Behav. Brain Res.* 47:113-127.
236. Savelli, F., D. Yoganarasimha, and J. J. Knierim. 2008. Influence of boundary removal on the spatial representations of the medial entorhinal cortex. *Hippocampus* 18:1270-1282.
237. Schacter, D. L. 2001. Forgotten ideas, neglected pioneers: Richard Semon and the story of memory: Richard Semon and the story of memory. Psychology Press, Philadelphia.
238. Scharfman, H. E. 1991. Dentate hilar cells with dendrites in the molecular layer have lower thresholds for synaptic activation by perforant path than granule cells. *J. Neurosci.* 11:1660-1673.
239. Scharfman, H. E. 1992. Differentiation of rat dentate neurons by morphology and electrophysiology in hippocampal slices: granule cells, spiny hilar cells and aspiny 'fast-spiking' cells. *Epilepsy Res. Suppl* 7:93-109.

240. Scharfman, H. E. 1994. Evidence from simultaneous intracellular recordings in rat hippocampal slices that area CA3 pyramidal cells innervate dentate hilar mossy cells. *J. Neurophysiol.* 72:2167-2180.
241. Scharfman, H. E., D. D. Kunkel, and P. A. Schwartzkroin. 1990. Synaptic connections of dentate granule cells and hilar neurons: results of paired intracellular recordings and intracellular horseradish peroxidase injections. *Neuroscience* 37:693-707.
242. Scharfman, H. E. and P. A. Schwartzkroin. 1988. Electrophysiology of morphologically identified mossy cells of the dentate hilus recorded in guinea pig hippocampal slices. *J. Neurosci.* 8:3812-3821.
243. Schmajuk, N. A. and E. T. Segura. 1981. [Theories and models of the function of the hippocampus]. *Acta Physiol Lat. Am.* 31:261-282.
244. Schmidt-Hieber, C., P. Jonas, and J. Bischofberger. 2004. Enhanced synaptic plasticity in newly generated granule cells of the adult hippocampus. *Nature* 429:184-187.
245. Scoville, W. B. and B. Milner. 1957. Loss of recent memory after bilateral hippocampal lesions. *J. Neurol Neurosurg. Psychiatry* 20:11-21.
246. Shapiro, M. L., H. Tanila, and H. Eichenbaum. 1997. Cues that hippocampal place cells encode: dynamic and hierarchical representation of local and distal stimuli. *Hippocampus* 7:624-642.

247. Sik, A., M. Penttonen, and G. Buzsaki. 1997. Interneurons in the hippocampal dentate gyrus: an in vivo intracellular study. *Eur. J. Neurosci.* 9:573-588.
248. Sikstrom, S. 2002. Forgetting curves: implications for connectionist models. *Cogn Psychol.* 45:95-152.
249. Skaggs, W. E., B. L. McNaughton, M. A. Wilson, and C. A. Barnes. 1996. Theta phase precession in hippocampal neuronal populations and the compression of temporal sequences. *Hippocampus* 6:149-172.
250. Solstad, T., E. I. Moser, and G. T. Einevoll. 2006. From grid cells to place cells: a mathematical model. *Hippocampus* 16:1026-1031.
251. Soltesz, I. and I. Mody. 1994. Patch-clamp recordings reveal powerful GABAergic inhibition in dentate hilar neurons. *J. Neurosci.* 14:2365-2376.
252. Sommer, W., E. Komoss, and S. R. Schweinberger. 1997. Differential localization of brain systems subserving memory for names and faces in normal subjects with event-related potentials. *Electroencephalogr. Clin. Neurophysiol.* 102:192-199.
253. Spruston, N. and D. Johnston. 1992. Perforated patch-clamp analysis of the passive membrane properties of three classes of hippocampal neurons. *J. Neurophysiol.* 67:508-529.

254. Squire, L. R. 1992. Memory and the hippocampus: a synthesis from findings with rats, monkeys, and humans. *Psychol. Rev.* 99:195-231.
255. Squire, L. R. 2004. Memory systems of the brain: a brief history and current perspective. *Neurobiol. Learn. Mem.* 82:171-177.
256. Squire, L. R., R. E. Clark, and B. J. Knowlton. 2001. Retrograde amnesia. *Hippocampus* 11:50-55.
257. Squire, L. R., C. E. Stark, and R. E. Clark. 2004. The medial temporal lobe. *Annu. Rev. Neurosci.* 27:279-306.
258. Squire, L. R. and S. Zola-Morgan. 1983. The neurology of memory: The case for correspondence between the findings for man and nonhuman primate. Academic, New York.
259. Staley, K. J., T. S. Otis, and I. Mody. 1992. Membrane properties of dentate gyrus granule cells: comparison of sharp microelectrode and whole-cell recordings. *J. Neurophysiol.* 67:1346-1358.
260. Steward, O. 1976. Topographic organization of the projections from the entorhinal area to the hippocampal formation of the rat. *J. Comp Neurol.* 167:285-314.
261. Steward, O. and S. A. Scoville. 1976. Cells of origin of entorhinal cortical afferents to the hippocampus and fascia dentata of the rat. *J. Comp Neurol.* 169:347-370.

262. Strowbridge, B. W., P. S. Buckmaster, and P. A. Schwartzkroin. 1992. Potentiation of spontaneous synaptic activity in rat mossy cells. *Neurosci. Lett.* 142:205-210.
263. Struble, R. G., N. L. Desmond, and W. B. Levy. 1978. Anatomical evidence for interlamellar inhibition in the fascia dentata. *Brain Res.* 152:580-585.
264. Sutherland, R. J. and R. J. McDonald. 1990. Hippocampus, amygdala, and memory deficits in rats. *Behav. Brain Res.* 37:57-79.
265. Sutherland, R. J., R. J. McDonald, C. R. Hill, and J. W. Rudy. 1989. Damage to the hippocampal formation in rats selectively impairs the ability to learn cue relationships. *Behav. Neural Biol.* 52:331-356.
266. Swanson, L. W., J. M. Wyss, and W. M. Cowan. 1978. An autoradiographic study of the organization of intrahippocampal association pathways in the rat. *J. Comp Neurol.* 181:681-715.
267. Tamamaki, N. and Y. Nojyo. 1993. Projection of the entorhinal layer II neurons in the rat as revealed by intracellular pressure-injection of neurobiotin. *Hippocampus* 3:471-480.
268. Tamura, R., T. Ono, M. Fukuda, and K. Nakamura. 1992. Spatial responsiveness of monkey hippocampal neurons to various visual and auditory stimuli. *Hippocampus* 2:307-322.

269. Taube, J. S. 1995. Head direction cells recorded in the anterior thalamic nuclei of freely moving rats. *J. Neurosci.* 15:70-86.
270. Taube, J. S. and H. L. Burton. 1995. Head direction cell activity monitored in a novel environment and during a cue conflict situation. *J. Neurophysiol.* 74:1953-1971.
271. Taube, J. S., R. U. Muller, and J. B. Ranck, Jr. 1990a. Head-direction cells recorded from the postsubiculum in freely moving rats. I. Description and quantitative analysis. *J. Neurosci.* 10:420-435.
272. Taube, J. S., R. U. Muller, and J. B. Ranck, Jr. 1990b. Head-direction cells recorded from the postsubiculum in freely moving rats. II. Effects of environmental manipulations. *J. Neurosci.* 10:436-447.
273. Terrazas, A., M. Krause, P. Lipa, K. M. Gothard, C. A. Barnes, and B. L. McNaughton. 2005. Self-motion and the hippocampal spatial metric. *J. Neurosci.* 25:8085-8096.
274. Thomas, K. G., M. Hsu, H. E. Lurance, L. Nadel, and W. J. Jacobs. 2001. Place learning in virtual space. III: Investigation of spatial navigation training procedures and their application to fMRI and clinical neuropsychology. *Behav. Res. Methods Instrum. Comput.* 33:21-37.
275. Thompson, L. T. and P. J. Best. 1989. Place cells and silent cells in the hippocampus of freely-behaving rats. *J. Neurosci.* 9:2382-2390.

276. Thompson, L. T. and P. J. Best. 1990. Long-term stability of the place-field activity of single units recorded from the dorsal hippocampus of freely behaving rats. *Brain Res.* 509:299-308.
277. Thompson, R. F. 2005. In search of memory traces. *Annu. Rev. Psychol.* 56:1-23.
278. Thompson, R. F. and J. J. Kim. 1996. Memory systems in the brain and localization of a memory. *Proc. Natl. Acad. Sci. U. S. A* 93:13438-13444.
279. Thomson, A. D., C. C. Cook, I. Guerrini, D. Sheedy, C. Harper, and E. J. Marshall. 2008. Wernicke's encephalopathy revisited. Translation of the case history section of the original manuscript by Carl Wernicke 'Lehrbuch der Gehirnerkrankheiten für Aerzte und Studierende' (1881) with a commentary. *Alcohol Alcohol* 43:174-179.
280. Tolman, E. C. 1948. Cognitive maps in rats and men. *Psychol. Rev* 55:189-208.
281. Tolman, E. C., B. F. Ritchie, and D. Kalish. 1946a. Studies in spatial learning: Orientation and the short-cut. *J. Exp. Psychol.* 36:13-24.
282. Tolman, E. C., B. F. Ritchie, and D. Kalish. 1946b. Studies in spatial learning; place learning versus response learning. *J. Exp. Psychol.* 36:221-229.



283. Treves, A. and E. T. Rolls. 1992. Computational constraints suggest the need for two distinct input systems to the hippocampal CA3 network. *Hippocampus* 2:189-199.
284. Treves, A. and E. T. Rolls. 1994. Computational analysis of the role of the hippocampus in memory. *Hippocampus* 4:374-391.
285. Tsodyks, M. 1999. Attractor neural network models of spatial maps in hippocampus. *Hippocampus* 9:481-489.
286. Tsodyks, M. 2005. Attractor neural networks and spatial maps in hippocampus. *Neuron* 48:168-169.
287. Tulving, E. 1972. Episodic and semantic memory. *In* Organization of memory. E. Tulving and W. Donaldson, editors. Academic Press, New York. 381-403.
288. Tulving, E. 1983. Elements of Episodic Memory. Oxford University Press, New York.
289. Tulving, E. 2001. Episodic memory and common sense: how far apart? *Philos Trans. R. Soc. Lond B Biol. Sci.* 356:1505-1515.
290. Tulving, E. 2002. Episodic memory: from mind to brain. *Annu. Rev Psychol.* 53:1-25.
291. Tulving, E. and H. J. Markowitsch. 1998. Episodic and declarative memory: role of the hippocampus. *Hippocampus* 8:198-204.

292. van der Meer, M. A., A. Johnson, N. C. Schmitzer-Torbert, and A. D. Redish. 2010. Triple dissociation of information processing in dorsal striatum, ventral striatum, and hippocampus on a learned spatial decision task. *Neuron* 67:25-32.
293. Vargha-Khadem, F., D. G. Gadian, K. E. Watkins, A. Connelly, P. W. Van, and M. Mishkin. 1997. Differential effects of early hippocampal pathology on episodic and semantic memory. *Science* 277:376-380.
294. Vazdarjanova, A. and J. F. Guzowski. 2004. Differences in hippocampal neuronal population responses to modifications of an environmental context: evidence for distinct, yet complementary, functions of CA3 and CA1 ensembles. *J. Neurosci.* 24:6489-6496.
295. Von Gudden JBA. 1896. Klinische und anatomische Beitrage zur Kenntniss der multiplen Alcoholneuritis nebst Bemerkungen uber die Regenerationsvorgange in peripheren Nervensystem. *Arch Psychiatr Nervenkr* 28:643-741.
296. Voytko, M. L. 1996. Cognitive functions of the basal forebrain cholinergic system in monkeys: memory or attention? *Behav. Brain Res.* 75:13-25.
297. Wang, S., B. W. Scott, and J. M. Wojtowicz. 2000. Heterogenous properties of dentate granule neurons in the adult rat. *J. Neurobiol.* 42:248-257.

298. Weiler, J. A., B. Suchan, and I. Daum. 2010. When the future becomes the past: Differences in brain activation patterns for episodic memory and episodic future thinking. *Behav. Brain Res.* 212:196-203.
299. Wenzel, H. J., P. S. Buckmaster, N. L. Anderson, M. E. Wenzel, and P. A. Schwartzkroin. 1997. Ultrastructural localization of neurotransmitter immunoreactivity in mossy cell axons and their synaptic targets in the rat dentate gyrus. *Hippocampus* 7:559-570.
300. Wernicke, C. 1881. Lehrbuch der Gehirnkrankheiten für Aerzte and Studierende. Theodore Fischer, Berlin.
301. West, M. J., L. Slomianka, and H. J. Gundersen. 1991. Unbiased stereological estimation of the total number of neurons in the subdivisions of the rat hippocampus using the optical fractionator. *Anat. Rec.* 231:482-497.
302. Wishaw, I. Q. 1998. Place learning in hippocampal rats and the path integration hypothesis. *Neurosci. Biobehav. Rev.* 22:209-220.
303. Wishaw, I. Q. and L. E. Jarrard. 1996. Evidence for extrahippocampal involvement in place learning and hippocampal involvement in path integration. *Hippocampus* 6:513-524.
304. Wishaw, I. Q. and H. Maaswinkel. 1998. Rats with fimbria-fornix lesions are impaired in path integration: a role for the hippocampus in "sense of direction". *J. Neurosci.* 18:3050-3058.

305. Whishaw, I. Q., J. E. McKenna, and H. Maaswinkel. 1997. Hippocampal lesions and path integration. *Curr. Opin. Neurobiol.* 7:228-234.
306. Whitlow, J. W. and A. D. Wagner. 1972. Negative patterning in classical conditioning: summation of response tendencies to isolable and configural components. *Psychon. Sci.* 27:299-301.
307. Wible, C. G., R. L. Findling, M. Shapiro, E. J. Lang, S. Crane, and D. S. Olton. 1986. Mnemonic correlates of unit activity in the hippocampus. *Brain Res.* 399:97-110.
308. William, J. 1890. The principles of psychology. Holt, New York.
309. Wills, T. J., C. Lever, F. Cacucci, N. Burgess, and J. O'Keefe. 2005. Attractor dynamics in the hippocampal representation of the local environment. *Science* 308:873-876.
310. Wilson, M. A. and B. L. McNaughton. 1993. Dynamics of the hippocampal ensemble code for space. *Science* 261:1055-1058.
311. Wirth, S., E. Avsar, C. C. Chiu, V. Sharma, A. C. Smith, E. Brown, and W. A. Suzuki. 2009. Trial outcome and associative learning signals in the monkey hippocampus. *Neuron* 61:930-940.
312. Wirth, S., M. Yanike, L. M. Frank, A. C. Smith, E. N. Brown, and W. A. Suzuki. 2003. Single neurons in the monkey hippocampus and learning of new associations. *Science* 300:1578-1581.

313. Witter, M. and D. G. Amaral. 2004. Hippocampal Formation. *In* The Rat Nervous System. G. Paxinos, editor. Elsevier Academic Press, 635-704.
314. Witter, M. P. 1993. Organization of the entorhinal-hippocampal system: a review of current anatomical data. *Hippocampus* 3 Spec No:33-44.
315. Witter, M. P., H. E. Daelmans, B. Jorritsma-Byham, J. F. Staiger, and F. G. Wouterlood. 1992. Restricted origin and distribution of projections from the lateral to the medial septal complex in rat and guinea pig. *Neurosci. Lett.* 148:164-168.
316. Witter, M. P., G. W. Van Hoesen, and D. G. Amaral. 1989. Topographical organization of the entorhinal projection to the dentate gyrus of the monkey. *J. Neurosci.* 9:216-228.
317. Wood, E. R., P. A. Dudchenko, and H. Eichenbaum. 1999. The global record of memory in hippocampal neuronal activity. *Nature* 397:613-616.
318. Wood, E. R., P. A. Dudchenko, R. J. Robitsek, and H. Eichenbaum. 2000. Hippocampal neurons encode information about different types of memory episodes occurring in the same location. *Neuron* 27:623-633.
319. Woodberry. 1943. The learning of stimulus patterns by dogs. *Journal of Comparative Psychology* 35:29-40.
320. Wyss, J. M. 1981. An autoradiographic study of the efferent connections of the entorhinal cortex in the rat. *J. Comp Neurol.* 199:495-512.

321. Ylinen, A., I. Soltesz, A. Bragin, M. Penttonen, A. Sik, and G. Buzsaki. 1995. Intracellular correlates of hippocampal theta rhythm in identified pyramidal cells, granule cells, and basket cells. *Hippocampus* 5:78-90.
322. Yoganarasimha, D. and J. J. Knierim. 2005. Coupling between place cells and head direction cells during relative translations and rotations of distal landmarks. *Exp. Brain Res.* 160:344-359.
323. Yoganarasimha, D., G. Rao, and J. J. Knierim. 2010. Lateral entorhinal neurons are not spatially selective in cue-rich environments. *Hippocampus*.
324. Yoganarasimha, D., X. Yu, and J. J. Knierim. 2006. Head direction cell representations maintain internal coherence during conflicting proximal and distal cue rotations: comparison with hippocampal place cells. *J. Neurosci.* 26:622-631.
325. Young, B. J., G. D. Fox, and H. Eichenbaum. 1994. Correlates of hippocampal complex-spike cell activity in rats performing a nonspatial radial maze task. *J. Neurosci.* 14:6553-6563.
326. Zalutsky, R. A. and R. A. Nicoll. 1990. Comparison of two forms of long-term potentiation in single hippocampal neurons. *Science* 248:1619-1624.
327. Zhao, C. S. and L. Overstreet-Wadiche. 2008. Integration of adult generated neurons during epileptogenesis. *Epilepsia* 49 Suppl 5:3-12.

328. Zola-Morgan, S. and L. R. Squire. 1985. Medial temporal lesions in monkeys impair memory on a variety of tasks sensitive to human amnesia. *Behav. Neurosci.* 99:22-34.
329. Zola-Morgan, S., L. R. Squire, and S. J. Ramus. 1994. Severity of memory impairment in monkeys as a function of locus and extent of damage within the medial temporal lobe memory system. *Hippocampus* 4:483-495.

## VITA

Joshua Paul Neunuebel was born in Columbia, Missouri on September 14, 1977, the son of Paul Michael Neunuebel and Carolyn Sue Neunuebel. After completing his work at Huntsville High School, Huntsville, Texas in 1996, he entered Texas A&M University in College Station, Texas. He received the degree of Bachelor of Science with a major in cell and molecular biology from Texas A&M in May, 2001.

In September of 2001, he started graduate school for his Master's at Texas A&M University. In the lab of Mark J. Zoran, he studied synaptogenesis in cultured invertebrate neurons extracted from snails (*Helisoma trivolvis*) using dual intracellular recordings, calcium imaging, and synaptic vesicle imaging. During synaptogenesis, these cultured cells exhibited an inverse temporal relationship between electrical and chemical neurotransmission. The results showed that transient electrical coupling between paired neurons disrupted calcium-dependent exocytosis, but not vesicle mobilization. These observations indicate that the presence of gap junction coupling delays the onset of chemical neurotransmission by disrupting the chemical transmission at a step occurring between calcium influx and transmitter release.

After graduating with his Master's, he entered the University of Texas Health Science Center at Houston in 2004 and joined the lab of James J. Knierim. For his dissertation research, he studied the flow of information through the hippocampal formation in freely moving rats. Subfields of the hippocampal formation (i.e., CA1, CA3, and DG) are thought to differentially contribute to the formation, storage, and recollection of episodic-like memories. The dentate gyrus has been suggested by many computational models to use a mechanism of pattern separation, which decreases similarity among incoming information by producing output patterns that overlap less than the inputs, for the storage of new



memories. CA3 has been suggested to use a mechanism of pattern completion, which reproduces a previously stored output pattern from a partial or degraded input pattern, in order to recall memories. Simultaneous recordings from the dentate gyrus and CA3 were performed and analyzed in combination with recordings from the medial and lateral entorhinal cortex (primary input to hippocampus) in the same conditions. The results show that the dentate gyrus representation dramatically changes compared to its input representations, whereas the CA3 representation changes less than its input representations. These findings are consistent with the theories that CA3 performs pattern completion and that DG performs pattern separation.

Current address:

43825 Thornberry Square #401  
Lansdowne, VA 20176

Email:

[jneunuebel@mail.mb.jhu.edu](mailto:jneunuebel@mail.mb.jhu.edu)